



CHORUS

This is the accepted manuscript made available via CHORUS. The article has been published as:

Dirac spectrum of the Wilson-Dirac operator for QCD with two colors

Mario Kieburg, Jacobus J. M. Verbaarschot, and Savvas Zafeiropoulos

Phys. Rev. D **92**, 045026 — Published 21 August 2015

DOI: [10.1103/PhysRevD.92.045026](https://doi.org/10.1103/PhysRevD.92.045026)

Dirac Spectrum of the Wilson Dirac Operator for QCD with Two Colors

Mario Kieburg^{1,2,*}, Jacobus J. M. Verbaarschot^{1,†} and Savvas Zafeiropoulos^{1,3‡}

¹ *Department of Physics and Astronomy, Stony Brook University, Stony Brook, NY 11794-3800, USA*

² *Fakultät für Physik, Universität Bielefeld, Postfach 100131, 33501 Bielefeld, Germany and*

³ *Institut für Theoretische Physik, Goethe-Universität Frankfurt,
Max-von-Laue-Str. 1, 60438 Frankfurt am Main, Germany*

We study the lattice artefacts of the Wilson Dirac operator for QCD with two colors and fermions in the fundamental representation from the viewpoint of chiral perturbation theory. These effects are studied with the help of the following spectral observables: the level density of the Hermitian Wilson Dirac operator, the distribution of chirality over the real eigenvalues, and the chiral condensate for the quenched as well as for the unquenched theory. We provide analytical expressions for all these quantities. Moreover we derive constraints for the level density of the real eigenvalues of the non-Hermitian Wilson Dirac operator and the number of additional real modes. The latter is a good measure for the strength of lattice artefacts. All computations are confirmed by Monte Carlo simulations of the corresponding random matrix theory which agrees with chiral perturbation theory of two color QCD with Wilson fermions.

PACS numbers: 12.38.Gc, 05.50.+q, 02.10.Yn, 11.15.Ha

Keywords: Wilson Dirac operator, lattice QCD, infra-red limit of QCD, random matrix theory

* mkieburg@physik.uni-bielefeld.de

† jacobus.verbaarschot@stonybrook.edu

‡ zafeiro@th.physik.uni-frankfurt.de

I. INTRODUCTION

The breaking of chiral symmetry is an essential feature of the vacuum structure of QCD. It is a non-perturbative phenomenon that can only be studied from first principles by means of lattice QCD simulations. Because of the Nielsen-Ninomya theorem, exact continuum type chiral symmetry on the lattice necessarily implies the presence of doublers which have to be eliminated. Two widely used methods to do so are staggered fermions, which break the flavor symmetry but preserve a “chiral” symmetry, and Wilson fermions which preserve the flavor symmetry but explicitly break the chiral symmetry.

An important ingredient of the vacuum structure is the topology of the gauge field configurations and its relation to the zero modes of the Dirac operator according to the Atiyah-Singer index theorem. Strictly speaking there is no topology at non-zero lattice spacing. For the Wilson Dirac operator one can obtain the topological charge by the spectral flow in the quark mass [1]. Other ways to define the topological charge on the lattice are through the index of the overlap operator [2] as well as through spectral projectors [3, 4]. One can equivalently employ purely gluonic methods where one measures a lattice discretized version of the volume integral of the topological charge density. The most common methods involve the gradient flow [5], cooling [6–9] and APE/HYP smearing [10, 11]. Of course all these methods agree up to cut-off effects but it is only the spectral flow and the index of the overlap operator that give an integer result. We refer the reader to [12] for a critical comparison of all methods.

The order parameter for chiral symmetry breaking is the chiral condensate which, according to the Banks-Casher formula, is directly related to the spectral density of the smallest Dirac eigenvalues. It is therefore important to have a detailed understanding of discretization effects on the Dirac spectrum and in particular on the topological zero modes. This problem was studied by means of chiral Lagrangians for the Wilson Dirac operator for QCD with three or more colors in the fundamental representation [13, 14]. Using mean field theory it was shown that the gap of the Hermitian Wilson Dirac operator closes when entering the Aoki phase. The microscopic Dirac spectrum was evaluated in great detail by means of a supersymmetric extension of the chiral Lagrangian and exploiting its equivalence with chiral random matrix theory [15, 16]. One of the main results is that the Gaussian broadening of the topological zero modes scales as $\sqrt{V}\tilde{a} = a$ for small values of the lattice spacing a which was first observed by lattice simulations [17]. In the thermodynamic limit the real eigenvalues develop a band with a width proportional to $VW_8\tilde{a}^2 = a^2$. A second important result is that the first order scenario [18] can only occur in the presence of dynamical quarks while in the quenched case at non-zero lattice spacing we necessarily have a transition to the Aoki phase when approaching the chiral limit [19]. We have also shown that the low-energy constants can be determined in a simple way by the properties of the Dirac spectrum [20].

In the present article we consider the spectrum of the Wilson Dirac operator for QCD with quarks in the fundamental representation of $SU(2)$. This theory reaches the conformal window for a smaller number of flavors as compared to three color QCD [21, 22] and is of interest for modeling physics beyond the standard model, see for example two interesting reviews by Rummukainen and Kuti [23, 24]. What distinguishes this theory from QCD with three or more colors is that $SU(2)$ is pseudo-real, and so it is possible to construct a gauge field independent basis for which the Dirac operator becomes real. For QCD at non-zero chemical potential this gives rise to a fermion determinant that is real so that the theory can be simulated for an even number of pairwise degenerate quark flavors, and is frequently studied as a model for QCD at non-zero chemical potential [25–28]. More physically, this implies that quarks and conjugate quarks are in the same flavor multiplet resulting in a doubling of the flavor symmetry group. We expect that the discretization effects for two colors are qualitatively the same as for QCD with three or more colors. The main difference is the repulsion between the eigenvalues of the Dirac operator which is linear for small spacings.

We compute the microscopic spectral density ρ_5 of the Hermitian Wilson Dirac operator starting from a supersymmetric extension of the chiral Lagrangian for two color Wilson fermions [29] in the epsilon regime. The calculation is much more complicated than for QCD with three colors, and it is not clear whether the density of the complex and real eigenvalues of the Wilson Dirac operator can be obtained analytically. Moreover we compute the distribution ρ_χ of chirality over the real spectrum of the non-Hermitian Wilson-Dirac operator and the mass dependence of the level density ρ_5 at the origin. Both quantities provide lower and upper bounds for the level density ρ_{real} of the real eigenvalues of the non-Hermitian Wilson Dirac operator. We also consider the chiral condensate in the theory with and without dynamical quarks.

Before calculating the observables mentioned above we briefly recall the properties of the Wilson Dirac operator for two colors and the definitions of the spectral observables in Sec. II. In Sec. III we discuss the chiral Lagrangian for fermionic and bosonic quarks. The supersymmetric partition function for the quenched theory is evaluated and discussed in Sec. IV. Thereby we consider the continuum limit as well as the limit of a very coarse lattice and the related thermodynamic limit. The exact results and the detailed discussions of the single spectral observables are summarized in Sec. V. Concluding remarks are made in Sec. VI. In the appendices we briefly recall some properties of Bessel functions, present the detailed computation of the quenched partition function, and briefly rederive some spectral observables of continuum QCD with two colors and the Gaussian orthogonal ensemble.

Some of the results that appear in this article were first presented at the conference LATTICE 2012 [30].

II. QCD WITH TWO COLORS

In subsection II A we briefly recall the properties of the four dimensional QCD Dirac operator for the two color theory and fermions in the fundamental representation. Additionally we explain how chiral perturbation theory and the corresponding symmetry breaking pattern result from these properties. The variables we consider will be introduced in subsection II B.

A. Dirac Operator for QCD with Two Colors

For four dimensional QCD with two colors, the massless Dirac operator D anti-commutes with γ_5 implying chiral symmetry. Moreover, D commutes with an anti-unitary operator, [31]

$$[D, K\tau_2 C] = 0, \quad (1)$$

where K is the complex conjugation operator, $C \equiv \gamma_2\gamma_4$ the charge conjugation matrix, and τ_2 the second Pauli matrix acting in color space. Because $(K\tau_2 C)^2 = 1$ it can be shown that there exists a gauge independent basis for which the matrix elements of D are real. In the Dyson classification of random matrix ensembles this symmetry corresponds to $\beta_D = 1$.

Let us consider N_f quarks with a diagonal mass matrix $\tilde{m} = \text{diag}(\tilde{m}_1, \dots, \tilde{m}_{N_f})$. Then the fermionic part of the Euclidean Lagrangian is given by

$$\mathcal{L} = \begin{pmatrix} \psi_1^* \\ \psi_2^* \end{pmatrix}^T \begin{pmatrix} \mathbf{1} \otimes \tilde{m} & i\sigma_\mu d_\mu \otimes \mathbf{1}_{N_f} \\ i(\sigma_\mu d_\mu)^\dagger \otimes \mathbf{1}_{N_f} & \mathbf{1} \otimes \tilde{m} \end{pmatrix} \begin{pmatrix} \psi_1 \\ \psi_2 \end{pmatrix}, \quad (2)$$

where

$$d_\mu = \partial_\mu + iA_\mu \quad (3)$$

is the covariant derivative, $\sigma_4 = -i\mathbf{1}_2$ and σ_a are the two-dimensional unit matrix and the three Pauli matrices, respectively, acting in Dirac space. The transformation property of the vector field under complex conjugation, $A_\mu^* = -\tau_2 A_\mu \tau_2$ is the reason for the anti-unitary symmetry (1). It also implies $(\sigma_\mu d_\mu)^* = -\sigma_2 \tau_2 \sigma_\mu d_\mu \sigma_2 \tau_2$. This symmetry can be used to rewrite the two terms of the Lagrangian (2), [25]

$$\mathcal{L} = \mathcal{L}_0 + \mathcal{L}_m, \quad (4)$$

as

$$\mathcal{L}_0 = \begin{pmatrix} \psi_1^* \\ \sigma_2 \tau_2 \psi_1 \end{pmatrix}^T \begin{pmatrix} 0 & i\sigma_\mu d_\mu \\ i\sigma_\mu d_\mu & 0 \end{pmatrix} \otimes \mathbf{1}_{N_f} \begin{pmatrix} \sigma_2 \tau_2 \psi_2^* \\ \psi_2 \end{pmatrix} = \begin{pmatrix} \psi_1^* \\ \sigma_2 \tau_2 \psi_1 \end{pmatrix}^T i\sigma_\mu d_\mu \otimes \mathbf{1}_{2N_f} \begin{pmatrix} \psi_2 \\ \sigma_2 \tau_2 \psi_2^* \end{pmatrix} \quad (5)$$

and

$$\mathcal{L}_m = \frac{1}{2} \begin{pmatrix} \psi_1^* \\ \sigma_2 \tau_2 \psi_1 \end{pmatrix}^T \sigma_2 \tau_2 \otimes \begin{pmatrix} 0 & \tilde{m} \\ -\tilde{m} & 0 \end{pmatrix} \begin{pmatrix} \psi_1^* \\ \sigma_2 \tau_2 \psi_1 \end{pmatrix} + \frac{1}{2} \begin{pmatrix} \psi_2 \\ \sigma_2 \tau_2 \psi_2^* \end{pmatrix}^T \sigma_2 \tau_2 \otimes \begin{pmatrix} 0 & \tilde{m} \\ -\tilde{m} & 0 \end{pmatrix} \begin{pmatrix} \psi_2 \\ \sigma_2 \tau_2 \psi_2^* \end{pmatrix}. \quad (6)$$

Equation (5) implies that the flavor symmetry group is enhanced to $U(2N_f)$ given by the transformation

$$\begin{pmatrix} \psi_1^* \\ \sigma_2 \tau_2 \psi_1 \end{pmatrix} \rightarrow \mathbf{1} \otimes U^* \begin{pmatrix} \psi_1^* \\ \sigma_2 \tau_2 \psi_1 \end{pmatrix}, \quad \begin{pmatrix} \psi_2 \\ \sigma_2 \tau_2 \psi_2^* \end{pmatrix} \rightarrow \mathbf{1} \otimes U \begin{pmatrix} \psi_2 \\ \sigma_2 \tau_2 \psi_2^* \end{pmatrix} \quad (7)$$

with $U \in U(2N_f)$. The flavor symmetry is spontaneously broken by the formation of a chiral condensate which is given by the mass derivative of the partition function. Since the flavor symmetry group does not act on σ_2 and τ_2 in Eq. (6), the symmetry is broken to $\text{Sp}(2N_f)$ ¹ resulting in the symmetry breaking pattern $U(2N_f) \rightarrow \text{Sp}(2N_f)$

¹ The unitary symplectic group $\text{Sp}(2N_f)$ is the section of the unitary group and the symplectic group which is sometimes also denoted as $\text{USp}(2N_f)$. It should not be confused with the symplectic group itself which is non-compact and is sometimes denoted by $\text{Sp}(2N_f)$, too.

[32, 33]. After taking into account the axial anomaly from configurations with a non-trivial topological charge $\nu \neq 0$, the Goldstone manifold is given by $SU(2N_f)/Sp(2N_f)$ with $2N_f^2 - N_f - 1$ Goldstone bosons.

When introducing the lattice spacing \tilde{a} in the Dirac operator $D_W = D - \tilde{a}\Delta$ one has to choose one of many fermionic discretizations. We are interested in the lattice artefacts of the Wilson Dirac operator, where the additional term in the Lagrangian (2) is given by [34]

$$\begin{aligned} \mathcal{L}_W &= -\tilde{a} \begin{pmatrix} \psi_1^* \\ \psi_2^* \end{pmatrix}^T \begin{pmatrix} \Delta & 0 \\ 0 & \Delta \end{pmatrix} \otimes \mathbf{1}_{N_f} \begin{pmatrix} \psi_1 \\ \psi_2 \end{pmatrix} \\ &= -\frac{\tilde{a}}{2} \left[\begin{pmatrix} \psi_1^* \\ \sigma_2 \tau_2 \psi_1 \end{pmatrix}^T \Delta \sigma_2 \tau_2 \otimes \begin{pmatrix} 0 & \mathbf{1}_{N_f} \\ -\mathbf{1}_{N_f} & 0 \end{pmatrix} \begin{pmatrix} \psi_1^* \\ \sigma_2 \tau_2 \psi_1 \end{pmatrix} + \begin{pmatrix} \psi_2^* \\ \sigma_2 \tau_2 \psi_2 \end{pmatrix}^T \Delta \sigma_2 \tau_2 \otimes \begin{pmatrix} 0 & \mathbf{1}_{N_f} \\ -\mathbf{1}_{N_f} & 0 \end{pmatrix} \begin{pmatrix} \psi_2 \\ \sigma_2 \tau_2 \psi_2^* \end{pmatrix} \right]. \end{aligned} \quad (8)$$

Note that the four-dimensional Laplacian $\Delta = d_\mu^2$ satisfies the symmetries $\Delta^* = \tau_2 \Delta \tau_2$ and $[\Delta, \sigma_2] = 0$. Hence the Wilson term (8) transforms in the same way as the mass term (6).

B. Spectral Observables

The central object of our studies is the partially quenched partition function

$$Z_\nu(\tilde{M}, \tilde{m}, \tilde{m}', \tilde{x}_0, \tilde{x}_1, \tilde{a}) = \left\langle \frac{\det(-\tilde{a}\Delta + \gamma_\mu d_\mu + \tilde{m}\mathbf{1} + \tilde{x}_0\gamma_5)}{\det(-\tilde{a}\Delta + \gamma_\mu d_\mu + \tilde{m}'\mathbf{1} + \tilde{x}_1\gamma_5)} \right\rangle_{N_f}, \quad (9)$$

where $\langle \cdot \rangle_{N_f}$ is the average of two-color QCD with N_f dynamical quarks. The masses of the N_f dynamical quarks are encoded in the matrix \tilde{M} which may have also non-diagonal elements. The axial mass \tilde{x}_1 has a non-vanishing imaginary part $i\varepsilon$ to guarantee convergence of the integrals.

The generating function (9) allows us to derive two Green functions depending on whether we differentiate with respect to \tilde{m}' or \tilde{x}_1 . The differentiation in \tilde{x}_1 yields the Green function corresponding to the Hermitian Wilson Dirac operator $D_5 = \gamma_5 D_W$, i.e.

$$G_5(\tilde{M}, \tilde{m}, \tilde{\lambda}, \tilde{a}) = \partial_{\tilde{x}_1} Z_\nu(\tilde{M}, \tilde{m}, \tilde{m}', \tilde{x}_0, \tilde{x}_1, \tilde{a}) \Big|_{\substack{\tilde{m}=\tilde{m}' \\ \tilde{x}_0=\tilde{x}_1=\tilde{\lambda}}} = \frac{1}{V} \left\langle \text{tr} \frac{1}{D_5 + \tilde{m}\gamma_5 + \tilde{\lambda}\mathbf{1}} \right\rangle_{N_f}. \quad (10)$$

Its discontinuity yields the level density of D_5 ,

$$\rho_5(\tilde{M}, \tilde{m}, \tilde{\lambda}, \tilde{a}) = \frac{1}{\pi} \lim_{\varepsilon \rightarrow 0} \text{Im} G_5(\tilde{M}, \tilde{m}, \tilde{\lambda} + i\varepsilon, \tilde{a}) = \frac{1}{V} \left\langle \sum_k \delta[\lambda_k^5(\tilde{m}) - \tilde{\lambda}] \right\rangle_{N_f}, \quad (11)$$

where $\lambda_k^5(\tilde{m})$ is an eigenvalue of $D_5 + \tilde{m}\gamma_5$ with respect to the eigenvector $|k\rangle$.

The level density ρ_5 satisfies an inequality with respect to the level density ρ_{real} of the real eigenvalues of the non-Hermitian Wilson Dirac operator D_W . This can be seen by considering the level density (11) at $\tilde{\lambda} = 0$,

$$\rho_5(\tilde{M}, \tilde{m}, \tilde{\lambda} = 0, \tilde{a}) = \frac{1}{V} \left\langle \sum_k \delta[\lambda_k^5(\tilde{m})] \right\rangle_{N_f}. \quad (12)$$

The corresponding eigenvalue equation reads

$$(D_5 + \tilde{m}\gamma_5)|k\rangle = \lambda_k^5(\tilde{m})|k\rangle \iff (D_W - \lambda_k^5(\tilde{m})\gamma_5)|k\rangle = -\tilde{m}|k\rangle. \quad (13)$$

Hence the value $-\tilde{m}$ is a real eigenvalue of D_W when $\lambda_k^5(\tilde{m}) = 0$ which we denote by λ_k^W . Moreover taking the scalar product with the bra vector $\langle k|$ in the first equality of Eq. (13) and differentiating with respect to the mass \tilde{m} yields

$$\partial_{\tilde{m}} \lambda_k^5(\tilde{m})|_{\lambda_k^5(\tilde{m})=0} = \partial_{\tilde{m}} \langle k|(D_5 + \tilde{m}\gamma_5)|k\rangle|_{\lambda_k^5(\tilde{m})=0} = \langle k|\gamma_5|k\rangle. \quad (14)$$

The derivative of the vectors $\langle k|$ and $|k\rangle$ drops out because of the eigenvalue equations $\langle k|(D_5 + \tilde{m}\gamma_5) = 0$ and $(D_5 + \tilde{m}\gamma_5)|k\rangle = 0$. The expectation value $\langle k|\gamma_5|k\rangle$ is the chirality of the vector $|k\rangle$. Thus the slope of the spectral flow with respect to the quark mass at its zeros gives the chiralities of the real modes [1].

Expressing the eigenvalues $\lambda_k^5(\tilde{m})$ in terms of λ_k^W and plugging Eq. (14) into Eq. (12) we find the relation

$$\rho_5(\tilde{M}, \tilde{m}, \tilde{\lambda} = 0, \tilde{a}) = \frac{1}{V} \left\langle \sum_k \delta[\lambda_k^5(\tilde{m})] \right\rangle_{N_f} = \frac{1}{V} \left\langle \sum_{\lambda_k^W \in \mathbb{R}} \frac{\delta[\lambda_k^W + \tilde{m}]}{|\partial_{\tilde{m}} \lambda_k^5(\tilde{m})|_{\lambda_k^5(\tilde{m})=0}} \right\rangle_{N_f} = \frac{1}{V} \left\langle \sum_{\lambda_k^W \in \mathbb{R}} \frac{\delta[\lambda_k^W + \tilde{m}]}{| \langle k | \gamma_5 | k \rangle |} \right\rangle_{N_f}. \quad (15)$$

Since the modulus of the chirality of a normalized vector, $\langle k | k \rangle = 1$, is always less or equal to 1 we obtain the inequality

$$\rho_5(\tilde{M}, \tilde{m}, \tilde{\lambda} = 0, \tilde{a}) = \frac{1}{V} \left\langle \sum_{\lambda_k^W \in \mathbb{R}} \frac{\delta[\lambda_k^W + \tilde{m}]}{| \langle k | \gamma_5 | k \rangle |} \right\rangle_{N_f} \geq \frac{1}{V} \left\langle \sum_{\lambda_k^W \in \mathbb{R}} \delta[\lambda_k^W + \tilde{m}] \right\rangle_{N_f} = \rho_{\text{real}}(\tilde{M}, \tilde{m}, \tilde{a}), \quad (16)$$

where the right hand side is indeed the level density of the real eigenvalues of D_W .

The derivative of the partially quenched partition function with respect to the mass \tilde{m}' yields another Green function

$$G'(\tilde{M}, \tilde{m}, \tilde{\lambda}, \tilde{a}) = \partial_{\tilde{m}'} Z_\nu(\tilde{M}, \tilde{m}, \tilde{m}', \tilde{x}_0, \tilde{x}_1, \tilde{a}) \Big|_{\substack{\tilde{m}=\tilde{m}' \\ \tilde{x}_0=\tilde{x}_1=\tilde{\lambda}}} = \frac{1}{V} \left\langle \text{tr} \frac{1}{D_W + \tilde{m} \mathbf{1} + \tilde{\lambda} \gamma_5} \right\rangle_{N_f}. \quad (17)$$

Setting $\tilde{\lambda} = i\varepsilon$ in the limit $\varepsilon \rightarrow 0$ we can take the real part and the imaginary part. The real part is equal to the mass-dependent chiral condensate

$$\Sigma(\tilde{M}, \tilde{m}, \tilde{a}) = -\frac{1}{V} \left\langle \text{tr} \frac{1}{D_W + \tilde{m} \mathbf{1}} \right\rangle_{N_f}. \quad (18)$$

In the case that \tilde{m} equals one of the eigenvalues $\tilde{m}_1, \dots, \tilde{m}_{N_f}$ of the mass matrix \tilde{M} , e.g. say $\tilde{m} = \tilde{m}_1$, one does not need the partially quenched partition function (9) but the result can be immediately derived from the partition function

$$Z_\nu^{N_f}(\tilde{M}, \tilde{a}) = \left\langle \prod_{j=1}^{N_f} \det(D_W + \tilde{m}_j \mathbf{1}) \right\rangle. \quad (19)$$

Then the chiral condensate is given by

$$\Sigma^{N_f}(\tilde{M}, \tilde{m}_1, \tilde{a}) = -\frac{1}{V} \partial_{m_1} \ln Z_\nu^{N_f}(\tilde{M}, \tilde{a}) = -\frac{1}{V} \left\langle \text{tr} \frac{1}{D_W + \tilde{m}_1 \mathbf{1}} \right\rangle_{N_f}. \quad (20)$$

The imaginary part of G' yields the distribution of chirality over the real eigenvalues

$$\begin{aligned} \rho_\chi(\tilde{M}, \tilde{m}, \tilde{a}) &= -\frac{1}{\pi} \lim_{\varepsilon \rightarrow 0} \text{Im} G'(\tilde{M}, \tilde{m}, i\varepsilon, \tilde{a}) \\ &= \frac{1}{2\pi i V} \lim_{\varepsilon \rightarrow 0} \left\langle \text{tr} \left(\frac{1}{D_W + \tilde{m} \mathbf{1} - i\varepsilon \gamma_5} - \frac{1}{D_W + \tilde{m} \mathbf{1} + i\varepsilon \gamma_5} \right) \right\rangle_{N_f} \\ &= \frac{1}{2\pi i V} \lim_{\varepsilon \rightarrow 0} \left\langle \text{tr} \gamma_5 \left(\frac{1}{D_5 + \tilde{m} \gamma_5 - i\varepsilon \mathbf{1}} - \frac{1}{D_5 + \tilde{m} \gamma_5 + i\varepsilon \mathbf{1}} \right) \right\rangle_{N_f} \\ &= \frac{1}{V} \left\langle \sum_k \delta[\lambda_k^5(\tilde{m})] | \langle k | \gamma_5 | k \rangle | \right\rangle_{N_f}. \end{aligned} \quad (21)$$

Here we employ the same relation between λ_k^5 and λ_k^W as for the level density ρ_5 such that we have

$$\rho_\chi(\tilde{M}, \tilde{m}, \tilde{a}) = \frac{1}{V} \left\langle \sum_k \delta[\lambda_k^W + \tilde{m}] \text{sign}(\langle k | \gamma_5 | k \rangle) \right\rangle_{N_f}. \quad (22)$$

This expression explains the name of this quantity since it is the average sign of chirality at a fixed real eigenvalue $\lambda_k^W = -\tilde{m}$. Understanding ρ_χ in this way has two implications. First the distribution of chirality over the real eigenvalues is normalized with the index ν ,

$$\int_{\mathbb{R}} d\tilde{m} \rho_\chi(\tilde{m}) = \sum_{\lambda_k^W \in \mathbb{R}} \text{sign}[\langle k | \gamma_5 | k \rangle] = \nu. \quad (23)$$

We recall that the index ν is a topological invariant such that also this normalization is well-defined for each single configuration. It counts the total number of spectral flow lines that start at $-\infty$ for $\tilde{m} \rightarrow -\infty$ and end at $+\infty$ for $\tilde{m} \rightarrow +\infty$. Note that $\rho_\chi(\tilde{m})$ does not have to be necessarily positive definite.

The second implication of Eq. (22) is another inequality with the level density of the real eigenvalues of D_W ,

$$|\rho_\chi(\tilde{M}, \tilde{m}, \tilde{a})| = \frac{1}{V} \left| \left\langle \sum_k \delta[\lambda_k^W + \tilde{m}] \text{sign}(\langle k | \gamma_5 | k \rangle) \right\rangle_{N_f} \right| \leq \frac{1}{V} \left\langle \sum_{\lambda_k^W \in \mathbb{R}} \delta[\lambda_k^W + \tilde{m}] \right\rangle_{N_f} = \rho_{\text{real}}(\tilde{M}, \tilde{m}, \tilde{a}). \quad (24)$$

Combining this inequality with Eq. (16) we have an upper and lower bound for the level density ρ_{real} ,

$$\rho_\chi(\tilde{M}, \tilde{m}, \tilde{a}) \leq |\rho_\chi(\tilde{M}, \tilde{m}, \tilde{a})| \leq \rho_{\text{real}}(\tilde{M}, \tilde{m}, \tilde{a}) \leq \rho_5(\tilde{M}, \tilde{m}, \tilde{\lambda} = 0, \tilde{a}). \quad (25)$$

This inequality can be integrated over \tilde{m} such that we find an estimate for the average number of additional real modes for the set of configurations with a fixed index ν which is

$$0 \leq N_{\text{add}} = N_{\text{real}} - |\nu| \leq \frac{1}{V} \left\langle \sum_{\lambda_k^W \in \mathbb{R}} \frac{1 - \langle k | \gamma_5 | k \rangle}{|\langle k | \gamma_5 | k \rangle|} \right\rangle_{N_f}. \quad (26)$$

These estimates encode the only information available about the level density ρ_{real} as long as there is no closed expression for this quantity. Such a closed expression was indeed derived for QCD with three colors in [16, 20] but seems to be much harder to obtain for the two color case.

III. CHIRAL LAGRANGIAN AND PARTITION FUNCTION

We consider the epsilon regime of lattice QCD. In this regime the quark mass \tilde{m} , the level spacing \tilde{a} , the momentum of the Goldstone bosons p , and the amplitude of the Goldstone bosons Π scale with the volume V as follows [35–37]

$$\tilde{m} \sim \tilde{a}^2 \sim p^4 \sim \Pi^4 \sim \frac{1}{V}. \quad (27)$$

In this particular scaling limit the Goldstone bosons with momentum $p \neq 0$ decouple from those with zero momentum such that it is legitimate to consider only the effective action of the latter. The corresponding chiral Lagrangian \mathcal{L}_χ is space-time independent. Hence the integral (sum) over the lattice volume V can be performed yielding a prefactor of the chiral Lagrangian.

It is clear that the epsilon regime is not the most physical regime. However, the mass scale of the epsilon domain is the one of lowest eigenvalues which are most sensitive to lattice artefacts. Using the leading order epsilon domain chiral Lagrangian one can also determine the region where the artificial phase structures like the Aoki-phase [18] manifest themselves, see also subsection IV D. Another important application is the measurement of physical parameters such as the chiral condensate, the pion decay constant as well as the electroweak effective couplings from lattice simulations in the epsilon regime [38–40].

A. Chiral Lagrangian for the Fermionic Quarks

The chiral Lagrangian for QCD with two colors follows from the requirements that the effective partition function should have the same flavor transformation properties as the QCD partition function in the full theory. Similar to three color QCD the partition function in the epsilon domain is given by an integral over the Goldstone manifold $U(2N_f)/\text{Sp}(2N_f)$. A matrix $U \in U(2N_f)/\text{Sp}(2N_f)$ is an antisymmetric unitary matrix parametrized by $U = VIV^T$ with I defined by

$$I = \begin{pmatrix} 0 & \mathbf{1}_{N_f} \\ -\mathbf{1}_{N_f} & 0 \end{pmatrix}. \quad (28)$$

The chiral partition function for a fixed topological charge ν is given by [25, 29, 42, 43],

$$Z_\nu^{N_f}(M, a) = \int_{U(2N_f)/\text{Sp}(2N_f)} d\mu(U) \det^{\nu/2} U \exp \left[\frac{1}{2} \text{tr} (MIU + (MI)^\dagger U^{-1}) - a^2 \text{tr} ((IU)^2 + (IU)^{-2}) \right]. \quad (29)$$

Since the integrand is a class function, the integration can be extended to $U(N_f)$ with the integration measure given by the Haar measure. Without restriction of generality we can assume that $\nu \geq 0$ is non-negative. To keep the notation simple we have introduced the dimensionless quantities,

$$M = V\Sigma\widetilde{M} \text{ and } a^2 = VW_8\widetilde{a}^2. \quad (30)$$

Thus the low energy constants Σ (chiral condensate) and W_8 are absorbed in these new quantities. Moreover we wish to recall that the low energy constant W_8 can be *a priori* positive or negative such that the effective lattice spacing a may also appear as an imaginary number even though the physical lattice spacing \widetilde{a} is always real and positive. However, as is the case for fundamental Wilson quarks for QCD with three or more colors, we find that $W_8 > 0$ in the case of two colors. This is discussed in subsections III B and V A. The general mass matrix MI is antisymmetric, but we restrict ourselves to a mass matrix such that $M = (m + ix_0)\mathbf{1}_{2N_f}$ proportional to the identity matrix. Here we have to distinguish between the real quark mass m and the real axial mass x_0 . The latter is introduced as a source for generating particular observables, see subsection II B.

The chiral Lagrangian in Eq. (29) is not the most general lowest order Lagrangian in the epsilon regime. We can add the terms $VW_6\widetilde{a}^2\text{tr}^2 I(U - U^{-1})$ and $VW_7\widetilde{a}^2\text{tr}^2 I(U + U^{-1})$, which are of the same order as the other terms. As in the case of three color QCD these two terms have the same symmetry properties as the W_8 term, and they have to be included *a priori*. However, based on large N_c arguments [41], we expect that the strongest effect results from the W_8 term. Moreover the W_6 and W_7 term can be easily introduced by a convolution with a Gaussian in the quark mass m and in the axial mass x_0 , respectively, see [20]. Therefore we stick to the partition function $Z_\nu^{N_f}(M, a)$.

The coset of antisymmetric unitary matrices is equivalent to the circular symplectic ensemble $\text{CSE}(2N_f)$ which is the ensemble of self-dual unitary matrices. Matrices in this ensemble satisfy the relation $U^T = -IUI$ and are related to antisymmetric unitary matrices via the scaling $U \rightarrow IU$. This set of matrices was first studied by Dyson [44]. Thus the eigenvalues of U are pure phases and are Kramers degenerate. In terms of the $\text{CSE}(2N_f)$ the chiral partition function (29) reads

$$Z_\nu^{N_f}(M, a) = \int_{\text{CSE}(2N_f)} d\mu(U) \det^{\nu/2} U \exp \left[\frac{1}{2} \text{tr} (MU + M^\dagger U^{-1}) - a^2 \text{tr} (U^2 + U^{-2}) \right], \quad (31)$$

which may be more familiar to some readers. The measure $d\mu(U)$ on the Goldstone manifold $\text{CSE}(2N_f)$ is the normalized Haar measure induced from the Haar measure on $U(2N_f)$ and can be extended to an integration over $U(2N_f)$ as in case of the representation (29). The measure can also be expressed in terms of the flat measure dU which is the product of differentials of all independent matrix entries, i.e. the measure is [45]

$$d\mu(U) \propto \frac{dU}{\det^{N_f-1/2} U}. \quad (32)$$

It is invariant under the group action $U \rightarrow IV^T IUV$ for any $V \in U(2N_f)$ because the Jacobian of this transformation is $d(IV^T IUV) = \det^{2N_f-1} V dU$. When diagonalizing $U = S \text{diag}(e^{i\varphi_1}, \dots, e^{i\varphi_{N_f}}) \otimes \mathbf{1}_2 S^\dagger$ with $S \in \text{Sp}(2N_f)$ the flat measure reads

$$dU \propto \prod_{1 \leq k < l \leq N_f} (e^{i\varphi_k} - e^{i\varphi_l})^4 d\mu(S) \prod_{k=1}^{N_f} de^{i\varphi_k} \quad (33)$$

with $d\mu(S)$ the normalized Haar measure of the coset $\text{Sp}(2N_f)/\text{Sp}^{N_f}(2)$.

To interpret the a^2 term in Eq. (31) as a diffusive process, see [46] for three color QCD, it is quite convenient to express also this term as a mass term convoluted with a Gaussian,

$$\begin{aligned} \exp[-a^2 \text{tr}(U^2 + U^{-2})] &= \exp[-a^2 \text{tr}(U - U^{-1})^2 - 4N_f a^2] \\ &= C_{N_f} e^{-4N_f a^2} \int_{\text{Self}(2N_f)} d\sigma \exp \left[-\frac{1}{16a^2} \text{tr} \sigma^2 + \frac{i}{2} \text{tr} \sigma (U - U^{-1}) \right] \end{aligned} \quad (34)$$

with the constant $C_{N_f} = 2^{N_f/2} (8a^2 \pi)^{-N_f(2N_f-1)/2}$. The matrix σ is self-dual and Hermitian $\sigma = \sigma^\dagger = -I\sigma^T I$ and the set of those matrices is denoted by $\text{Self}(2N_f)$. Thus the partition function (31) simplifies to

$$\begin{aligned} Z_\nu^{N_f}(M, a) &= C_{N_f} e^{-4N_f a^2} \int_{\text{Self}(2N_f)} d\sigma \int_{\text{CSE}(2N_f)} d\mu(U) \det^{\nu/2} U \exp \left[\frac{1}{2} \text{tr} ((M + i\sigma)U + (M + i\sigma)^\dagger U^{-1}) - \frac{1}{16a^2} \text{tr} \sigma^2 \right] \\ &= C_{N_f} e^{-4N_f a^2} \int_{\text{Self}(2N_f)} d\sigma \exp \left[-\frac{1}{16a^2} \text{tr} \sigma^2 \right] Z_\nu^{N_f}(M + i\sigma, a = 0), \end{aligned} \quad (35)$$

which is expressed in terms of the partition function at $a = 0$, see [42, 46]. This expression has some interesting relations to the microscopic partition function of the chiral Gaussian orthogonal random matrix ensemble (chGOE) which is up to a factor the same as the partition function $Z_\nu^{N_f}(M + i\sigma, a = 0)$,

$$Z_{\text{chGOE}}^{(\nu)}([M + i\sigma][M^\dagger - i\sigma]) = \det^{-\nu/2}(M^\dagger - i\sigma) Z_\nu(M + i\sigma, a = 0), \quad (36)$$

and of the Gaussian orthogonal random matrix ensemble (GOE) of finite matrix dimension $\nu \times \nu$,

$$Z_{\text{GOE}}^{(\nu)}\left(\frac{M^\dagger}{4a}\right) = C_{N_f} e^{-4N_f a^2} \int_{\text{Self}(2N_f)} d\sigma \det^{\nu/2}(M^\dagger - i\sigma) \exp\left[-\frac{1}{16a^2} \text{tr} \sigma^2\right]. \quad (37)$$

In subsection IV B we will argue that in the continuum limit the partition function (35) factorizes into these two partition functions, i.e.

$$Z_\nu^{N_f}(M, a) \stackrel{|a| \ll 1}{=} Z_{\text{GOE}}^{(\nu)}\left(\frac{M^\dagger}{4a}\right) Z_{\text{chGOE}}^{(\nu)}(MM^\dagger). \quad (38)$$

Thus the ν eigenvalues of the finite dimensional GOE lie on the scale a and shrink to a single Dirac delta function at the origin showing that they are the former ν zero modes of continuum QCD with two colors.

Since the matrix σ is self-dual its eigenvalues are Kramers degenerate. The flat measure $d\sigma$ can be rephrased in terms of these eigenvalues via a diagonalization $\sigma = SsS^\dagger = S \text{diag}(s_1, \dots, s_{N_f}) \otimes \mathbf{1}_2 S^\dagger$ with $S \in \text{Sp}(2N_f)$ yielding

$$d\sigma \propto \prod_{1 \leq k < l \leq N_f} (s_k - s_l)^4 d\mu(S) \prod_{k=1}^{N_f} ds_k. \quad (39)$$

When additionally assuming that the mass matrix $M = (m + ix_0)\mathbf{1}_{2N_f}$ is proportional to the identity matrix the diagonalizing matrix S drops out in Eq. (35). Note that S can be absorbed by U because U is Haar distributed. Then the partition function (35) reduces to

$$Z_\nu^{N_f}(M, a) \propto \prod_{k=1}^{N_f} \left(\int_{-\infty}^{\infty} ds_k (m + ix_0 + is_k)^\nu \exp\left[-\frac{s_k^2}{8a^2}\right] \right) \prod_{1 \leq k < l \leq N_f} (s_k - s_l)^4 Z_{\text{chGOE}}^{(\nu)}([m + ix_0]\mathbf{1}_{2N_f} + is). \quad (40)$$

Therefore the chiral partition function at finite lattice spacing can be understood as a convolution of each single quark mass with a Gaussian. Since these Gaussians are not completely statistical independent we can understand such a convolution as collective fluctuations as we have already seen those for three color QCD, cf. [19, 20].

B. Chiral Lagrangian for Bosonic Quarks

To find the bosonic chiral Lagrangian, we start from the observation that it is possible to find a gauge independent basis in which the massive Hermitian Wilson Dirac operator of N_b bosonic flavors, $D_5 = \gamma_5 D_W = \gamma_5 \gamma_\mu d_\mu \otimes \mathbf{1}_{N_b} + \gamma_5 \otimes \tilde{m} + \mathbf{1} \otimes \tilde{x} - \tilde{a} \gamma_5 \Delta \otimes \mathbf{1}_{N_b}$, is real and symmetric because of the anti-unitary symmetry. We need to generate its inverse and, hence, its matrix Green function such that the axial mass \tilde{x} must have a non-vanishing imaginary part which we assume to have the signature $L = \text{diag}(+\mathbf{1}_p, -\mathbf{1}_{N_b-p})$ with $0 \leq p \leq N_b$ positive signs. Then the inverse square root of the determinant of D_5 can be represented as an integral over real bosonic fields (ϕ_1^T, ϕ_2^T) ,

$$\frac{1}{\sqrt{\det D_5}} = C \int d\phi_1 d\phi_2 \exp \left[i \int_V d^4x \begin{pmatrix} \phi_1 \\ \phi_2 \end{pmatrix}^T \begin{pmatrix} \mathbf{1} \otimes L\tilde{x} + \mathbf{1} \otimes L\tilde{m} - \tilde{a}\Delta \otimes L & i\sigma_\mu d_\mu \otimes L \\ -i(\sigma_\mu d_\mu)^\dagger \otimes L & \mathbf{1} \otimes L\tilde{\lambda} - \mathbf{1} \otimes L\tilde{m} + \tilde{a}\Delta \otimes L \end{pmatrix} \begin{pmatrix} \phi_1 \\ \phi_2 \end{pmatrix} \right] \quad (41)$$

with C a normalization constant. The multiplication of the matrix iL guarantees the existence of the integral.

To eliminate the square root we have to double the number of flavors $N_b \rightarrow 2N_b$. The Dirac term of the Lagrangian then reads

$$L_0 = \phi_1^T (i\sigma_\mu d_\mu - i(\sigma_\mu d_\mu)^*) \otimes \tilde{L} \phi_2, \quad (42)$$

with $\tilde{L} = L \otimes \mathbf{1}_2$ where the two-dimensional unit matrix reflects the doubling of the number of flavors. This term is invariant under

$$\phi_1 \rightarrow \mathbf{1} \otimes U \phi_1, \quad \phi_2 \rightarrow \mathbf{1} \otimes [\tilde{L}(U^{-1})^T] \phi_2 \quad (43)$$

with $U \in \text{Gl}(2N_b, \mathbb{R})$ because the bosonic fields are real. With maximum breaking of chiral symmetry [32, 33], the set of transformations that leaves the ‘‘bosonic’’ chiral condensate,

$$\Sigma \propto \left\langle \int_V d^4x \begin{pmatrix} \phi_1 \\ \phi_2 \end{pmatrix}^T \begin{pmatrix} \mathbf{1} \otimes \tilde{L} & 0 \\ 0 & -\mathbf{1} \otimes \tilde{L} \end{pmatrix} \begin{pmatrix} \phi_1 \\ \phi_2 \end{pmatrix} \right\rangle \neq 0, \quad (44)$$

invariant reduces to the set of matrices satisfying $U^T \tilde{L} U = \tilde{L}$ and $U \in \text{Gl}(2N_b, \mathbb{R})$. This set is known as the non-compact orthogonal group $\text{O}(2p, 2N_b - 2p)$. The Lorentz group $\text{O}(3, 1)$ is a particular example of this kind of non-compact groups.

The pattern of spontaneous symmetry breaking is given by $\text{Gl}(2N_b, \mathbb{R}) \rightarrow \text{O}(2p, 2N_b - 2p)$ and the resulting Goldstone manifold $\text{Sym}_+(2p, 2N_b - 2p) = \text{Gl}(2N_b, \mathbb{R})/\text{O}(2p, 2N_b - 2p)$ is the set of real matrices $U \in \mathbb{R}^{2N_b \times 2N_b}$ with the symmetry $U^T = \tilde{L} U \tilde{L}$ and $2p$ positive real eigenvalues and $2N_b - 2p$ negative real eigenvalues. Such matrices can be parametrized by $U = L W W^T$ with $W \in \text{Gl}(2N_b, \mathbb{R})$. Another parametrization is via a diagonalization $U = O \text{diag}(e^{s_1}, \dots, e^{s_{2p}}, -e^{s_{2p+1}}, \dots, -e^{s_{2N_b}}) O^{-1}$ with $O \in \text{O}(2p, 2N_b - 2p)$ and $s_j \in \mathbb{R}$. The corresponding invariant measure $d\mu(U)$ is given by

$$d\mu(U) \propto \frac{dU}{\det^{N_b+1/2} U}, \quad \text{with } dU \propto \prod_{1 \leq k < l \leq 2p} |e^{s_k} - e^{s_l}| \prod_{\substack{1 \leq k \leq 2p \\ 2p+1 \leq l \leq 2N_b}} (e^{s_k} + e^{s_l}) \prod_{2p+1 \leq k < l \leq 2N_b} |e^{s_k} - e^{s_l}| d\mu(O) \prod_{k=1}^{2N_b} d e^{s_k} \quad (45)$$

and $d\mu(O)$ the invariant measure on $\text{O}(2p, 2N_b - 2p)$. Hence $d\mu(U)$ is indeed invariant under the group action $U \rightarrow L V^T L U V$ with $V \in \text{Gl}(2N_b, \mathbb{R})$ because the flat measure (product of the differentials of all independent matrix entries) transforms as $d(L V^T L U V) = \det^{2N_b+1} V dU$.

Let us first discuss the bosonic partition function for $p = 0$ or $p = 2N_b$. In these cases the imaginary part of x has only positive or negative entries, i.e. $L \rightarrow L \mathbf{1}_{N_b}$ with $L = \pm 1$. Then the non-compact orthogonal group reduces to the compact $\text{O}(2N_b)$ and the coset is equal to the set of all real symmetric positive definite matrices $\text{Sym}_+(2N_b)$. There are no integrability issues, even for $a = 0$, since the convergence of the integrals is assured by the imaginary part of \tilde{x} . For $a \neq 0$, the convergence of the integral is already guaranteed by the a^2 term if $p = 0, 2N_b$.

For $p = 0, 2N_b$ the chiral partition function is given by

$$Z_\nu(m, x, a) = \int_{\text{Sym}_+(2N_b)} d\mu(U) \det^{-\nu/2} U \exp \left[\frac{iL}{2} \text{tr} m (U - U^{-1}) + \frac{iL}{2} \text{tr} x (U + U^{-1}) - a^2 \text{tr} (U^2 + U^{-2}) \right]. \quad (46)$$

The sign $L = \pm 1$ does not drop out although the imaginary part of x can be dropped for finite a . Because the eigenvalues of U are positive definite, the transformation $U \rightarrow -U$ is not allowed. However we can absorb the sign in front of the mass by changing $U \rightarrow U^{-1}$ which yields a change of the topological charge $\nu \rightarrow -\nu$. There is some freedom in the choice of the signs and phase factors of the terms in the action, but the sign of the a^2 term is fixed by the physics of the problem. To have convergent integrals for $a^2 \neq 0$ we necessarily need that the sign of this term is negative. We also require that the bosonic and fermionic terms in the action can be combined into a supertrace. This is achieved by rotating the fermionic and bosonic variables by a factor i and including an overall minus sign in the bosonic action which gives the representation of Eq. (46), cf. the fermionic partition function (31).

For $p \neq 0, 2N_b$ the integral over $\text{O}(2p, 2N_b - 2p)$ is non-compact such that the measure (45) cannot be normalized even by group invariant potentials. We always have to include an infinitesimal increment in x , even for $a^2 \neq 0$, in order to get a convergent integral. The bosonic partition function is then given by

$$Z_\nu(m, x, a) = \int_{\text{Sym}_+(2p, 2N_b - 2p)} d\mu(U) \det^{-\nu/2} U \exp \left[\frac{i}{2} \text{tr} m L (U - U^{-1}) + \frac{i}{2} \text{tr} (xL + i\epsilon) (U + U^{-1}) - a^2 \text{tr} (U^2 + U^{-2}) \right]. \quad (47)$$

C. Supersymmetric Partition Function and Quenched Theory

Having discussed the bosonic and fermionic partition function we are now ready to formulate the supersymmetric partition function that generates the microscopic Dirac spectrum. Especially we focus on the average of the Green function which can be traced back to derivatives of the partially quenched partition function (9). Hence we put

$N_f \rightarrow N_f + 1$ in Eq. (31) and set $N_b = 1$ in Eq. (46). Then the combined chiral partition function reads

$$Z_\nu(\widehat{M}, \widehat{X}, a) = C^{-1} \int_{\Sigma(2N_f+2|2)} d\mu(U) \text{Sdet}^{\nu/2} U \exp \left[-\frac{iL}{2} \text{Str}(\widehat{M}U - \widehat{M}^\dagger U^{-1}) - \frac{iL}{2} \text{Str} \widehat{X}(U + U^{-1}) + a^2 \text{Str}(U^2 + U^{-2}) \right] \quad (48)$$

with

$$\widehat{M} = \begin{pmatrix} M & 0 & 0 \\ 0 & m\mathbf{1}_2 & 0 \\ 0 & 0 & m'\mathbf{1}_2 \end{pmatrix}, \quad \widehat{X} = \begin{pmatrix} 0 & 0 & 0 \\ 0 & x_0\mathbf{1}_2 & 0 \\ 0 & 0 & x_1\mathbf{1}_2 \end{pmatrix}, \quad (49)$$

and

$$C = \int_{\Sigma(2N_f+2|2)} d\mu(U) \text{Sdet}^{\nu/2} U \exp \left[-\frac{iL}{2} \text{Str}(\widehat{M}U - \widehat{M}^\dagger U^{-1}) - \frac{iL}{2} \text{Str} \widehat{X}(U + U^{-1}) + a^2 \text{Str}(U^2 + U^{-2}) \right] \Bigg|_{\substack{m=m' \\ x_0=x_1}}. \quad (50)$$

The mass matrix of the dynamical quarks again satisfies $M = -IM^T I$. The normalization constant guarantees that the partition function is equal to 1 if $m = m'$ and $x_0 = x_1$ because the determinants in Eq. (9) cancel. A supermatrix U in the Goldstone manifold $\Sigma(2N_f + 2|2) = \text{U}(2N_f + 2|2)/\text{UOSP}(2N_f + 2|2)$ has the block structure

$$U = \begin{pmatrix} U_f & -Ig^T \\ g & U_b \end{pmatrix}, \quad (51)$$

where $U_f \in \text{CSE}(2N_f + 2)$, $U_b \in \text{Sym}_+(2)$, and g is a $2 \times (2N_f + 2)$ matrix whose matrix entries are independent Grassmann (anti-commuting) variables. The whole matrix fulfills the symmetry

$$U^T = \begin{pmatrix} U_f^T & -g^T \\ gI & U_b^T \end{pmatrix} = \begin{pmatrix} -I\mathbf{1}_{2N_f+2} & 0 \\ 0 & \mathbf{1}_2 \end{pmatrix} \begin{pmatrix} U_f & -Ig^T \\ g & U_b \end{pmatrix} \begin{pmatrix} I\mathbf{1}_{2N_f+2} & 0 \\ 0 & \mathbf{1}_2 \end{pmatrix} = \begin{pmatrix} -I\mathbf{1}_{2N_f+2} & 0 \\ 0 & \mathbf{1}_2 \end{pmatrix} U \begin{pmatrix} I\mathbf{1}_{2N_f+2} & 0 \\ 0 & \mathbf{1}_2 \end{pmatrix}. \quad (52)$$

We recall that “ T ” acts on a supermatrix as the supertransposition which has a slightly different action on the off-diagonal blocks (the sign of the upper right block changes). Moreover, we choose the following notation of the supertrace and the superdeterminant

$$\text{Str} U = \text{tr} U_f - \text{tr} U_b, \quad \text{Sdet} U = \frac{\det(U_f + iIg^T U_b^{-1}g)}{\det U_b}. \quad (53)$$

This choice differs with respect to some other works [47, 48] where the sign of the supertrace is reversed and the superdeterminant is the inverse of the definition here. The invariant measure $d\mu(U)$ is given by

$$d\mu(U) = \frac{dU_f dU_b dg}{\text{Sdet}^{N_f-1/2} U}, \quad (54)$$

where dU_f , dU_b , and dg are the flat measures meaning the product of the differentials of all independent matrix entries. It naturally appears in superbosonization [49–51] which can be used to directly map random matrix theory to a finite dimensional version of the chiral partition function [52].

For the quenched theory where $N_f = 0$, the partition function drastically simplifies

$$Z_\nu(\widehat{M}, \widehat{X}, a) = C^{-1} \int_{\Sigma(2|2)} dU_f dU_b dg \text{Sdet}^{(\nu+1)/2} U \exp \left[-\frac{iL}{2} \text{Str} \widehat{M}(U - U^{-1}) - \frac{iL}{2} \text{Str} \widehat{X}(U + U^{-1}) + a^2 \text{Str}(U^2 + U^{-2}) \right], \quad (55)$$

where we already wrote the measure in terms of the flat one. The matrices in this expression are

$$\widehat{M} = \begin{pmatrix} m\mathbf{1}_2 & 0 \\ 0 & m'\mathbf{1}_2 \end{pmatrix}, \quad \widehat{X} = \begin{pmatrix} x_0\mathbf{1}_2 & 0 \\ 0 & x_1\mathbf{1}_2 \end{pmatrix}, \quad U = \text{diag}(\mathbf{1}_2, O) \begin{pmatrix} e^{i\varphi} & 0 & \alpha^* & \beta^* \\ 0 & e^{i\varphi} & -\alpha & -\beta \\ \alpha & \alpha^* & e^{s_1} & 0 \\ \beta & \beta^* & 0 & e^{s_2} \end{pmatrix} \text{diag}(\mathbf{1}_2, O^T) \quad (56)$$

with $O \in \text{O}(2)$. The orthogonal matrix O drops out and yields a constant. Thus the remaining integration is over a phase $e^{i\varphi}$ with $\varphi \in [-\pi, \pi]$, two positive variables e^{s_1} and e^{s_2} with $s_1, s_2 \in \mathbb{R}$, and four Grassmann variables $\alpha, \alpha^*, \beta, \beta^*$. The measure becomes

$$dU_f dU_b dg \rightarrow de^{i\varphi} |e^{s_1} - e^{s_2}| de^{s_1} de^{s_2} d\alpha d\alpha^* d\beta d\beta^* = ie^{i\varphi+s_1+s_2} |e^{s_1} - e^{s_2}| d\varphi ds_1 ds_2 d\alpha d\alpha^* d\beta d\beta^*. \quad (57)$$

We recall that the integration over Grassmann variables is defined as $\int d\alpha = 0$ and $\int \alpha d\alpha = 1$ and similar for the other Grassmann variables. Integrations of higher orders are not needed to be defined since Grassmann variables are nilpotent because of their anti-commuting nature.

As for the partition function of fermionic quarks (31) we can linearize the term in a^2 by introducing an auxiliary supermatrix σ ,

$$Z_\nu(\widehat{M}, \widehat{X}, a) = C^{-1} \int_{\widetilde{\Sigma}(2|2)} d\sigma \int_{\Sigma(2|2)} d\mu(U) \text{Sdet}^{\nu/2} U \exp \left[\frac{1}{16a^2} \text{Str} \sigma^2 - \frac{iL}{2} \text{Str} (\widehat{M} - \sigma)(U - U^{-1}) \right] \\ \times \exp \left[-\frac{iL}{2} \text{Str} \widehat{X} (U + U^{-1}) \right] / \int_{\widetilde{\Sigma}(2|2)} d[\sigma] \exp \left[\frac{1}{16a^2} \text{Str} \sigma^2 \right]. \quad (58)$$

The set $\widetilde{\Sigma}(2|2)$ consists of $(2|2) \times (2|2)$ supermatrices which can be parametrized as follows

$$\sigma = \text{diag}(\mathbf{1}_2, \widetilde{O}) \begin{pmatrix} iu & 0 & \eta^* & \chi^* \\ 0 & iu & -\eta & -\chi \\ \eta & \eta^* & v_1 & 0 \\ \chi & \chi^* & 0 & v_2 \end{pmatrix} \text{diag}(\mathbf{1}_2, \widetilde{O}^T) \quad (59)$$

with $\widetilde{O} \in \text{O}(2)$, $u, v_1, v_2 \in \mathbb{R}$ and $\eta, \eta^*, \chi, \chi^*$ four independent Grassmann variables. Additionally, the supermatrix σ fulfills the symmetry (52). With the help of the partition function of the chiral Gaussian orthogonal ensemble,

$$Z_{\text{chGOE}}^{(\nu)}([\widehat{M} + \widehat{X} - \sigma][\widehat{M} - \widehat{X} - \sigma]) = \text{Sdet}^{-\nu/2}(\widehat{M} - \widehat{X} - \sigma) Z_\nu(\widehat{M} - \sigma, \widehat{X}, a = 0), \quad (60)$$

we can rewrite the quenched partition function as a convolution of the $Z_{\text{chGOE}}^{(\nu)}$ with a Gaussian

$$Z_\nu(\widehat{M}, \widehat{X}, a) = \frac{C(a=0)}{C(a \neq 0)} \int_{\widetilde{\Sigma}(2|2)} d\sigma \exp \left[\frac{1}{16a^2} \text{Str} \sigma^2 \right] \text{Sdet}^{\nu/2}(\widehat{M} - \widehat{X} - \sigma) \\ Z_{\text{chGOE}}^{(\nu)}([\widehat{M} + \widehat{X} - \sigma][\widehat{M} - \widehat{X} - \sigma]) / \int_{\widetilde{\Sigma}(2|2)} d[\sigma] \exp \left[\frac{1}{16a^2} \text{Str} \sigma^2 \right]. \quad (61)$$

This representation shows the diffusive character of the effect of a finite lattice spacing a on the spectrum of the Dirac operator, see [53] for the diffusive approach in supersymmetric spaces. Thus it exhibits a similar effect as already found for lattice QCD with three colors of the Wilson Dirac operator [20, 46]. Interestingly, when omitting the term $Z_{\text{chGOE}}^{(\nu)}$ in the integral (61) we obtain the finite dimensional quenched partition function of an orthogonal Gaussian random matrix ensemble,

$$Z_{\text{GOE}}^{(\nu)} \left(\frac{\widehat{M} - \widehat{X}}{4a} \right) = \int_{\widetilde{\Sigma}(2|2)} d\sigma \exp \left[\frac{1}{16a^2} \text{Str} \sigma^2 \right] \text{Sdet}^{\nu/2}(\widehat{M} - \widehat{X} - \sigma) / \int_{\widetilde{\Sigma}(2|2)} d[\sigma] \exp \left[\frac{1}{16a^2} \text{Str} \sigma^2 \right]. \quad (62)$$

We recall that the real eigenvalues of this ensemble scale with the lattice spacing a which can be also seen in this expression. The normalization constant C is independent of a because the partition function should be normalized for any choice of $\widehat{M} = m\mathbf{1}_4$ and $\widehat{X} = x\mathbf{1}_4$, cf. Eq. (9) where we started from. Thus the ratio is $C(a=0)/C(a \neq 0) = 1$.

Now we have all ingredients to calculate and discuss the quenched partition function.

IV. QUENCHED PARTITION FUNCTION

In subsection IV A we present the result for the quenched partition function at finite lattice spacing, quark mass and axial mass. We reduce this result to a compact integral which represents the fermionic valence quark and a non-compact two-fold integral which reflects the nature of the bosonic valence quark. The continuum limit $a \rightarrow 0$ is derived in subsection IV B. The limit of a very coarse lattice $|a| \gg 1$ and the related thermodynamic limit are discussed in subsections IV C and IV D, respectively.

A. Discussion of the Partition Function at finite a

The evaluation of the partition function (55) is straightforward but tedious. Since we have only four different Grassmann variables, the Grassmann integrals can be evaluated by a brute force expansion. This is worked out in

appendix B 1. The final result for the generating function is given by

$$\begin{aligned}
Z_\nu(\widehat{M}, \widehat{X}, a) &= \frac{1}{4} \int_{-\pi}^{\pi} \frac{d\varphi}{2\pi} \int_{-\infty}^{\infty} ds_1 \int_{-\infty}^{\infty} ds_2 \left| \sinh \frac{s_1 - s_2}{2} \right| e^{\nu(2i\varphi - s_1 - s_2)/2} \exp [2Lm \sin \varphi + iLm'(\sinh s_1 + \sinh s_2)] \\
&\times \exp [-2iLx_0 \cos \varphi + iLx_1(\cosh s_1 + \cosh s_2) + 4a^2 \cos 2\varphi - 2a^2(\cosh 2s_1 + \cosh 2s_2)] \\
&\times [(4a^2(e^{-2i\varphi} + e^{-2s_1} + e^{i\varphi+s_1} + e^{-i\varphi-s_1}) + iL(m-x_0)e^{-i\varphi} + iL(m'-x_1)e^{-s_1} - \nu - 1) \\
&\quad \times (4a^2(e^{-2i\varphi} + e^{-2s_2} + e^{i\varphi+s_2} + e^{-i\varphi-s_2}) + iL(m-x_0)e^{-i\varphi} + iL(m'-x_1)e^{-s_2} - \nu - 1) \\
&\quad + 4a^2(3e^{-2i\varphi} + e^{-s_1-s_2} + e^{-2s_1} + e^{-2s_2} + 2e^{-i\varphi-s_1} + 2e^{-i\varphi-s_2}) \\
&\quad + iL(2(m-x_0)e^{-i\varphi} + (m'-x_1)(e^{-s_1} + e^{-s_2})) - \nu - 1] \\
&= 16a^4(\Phi_{\nu-4}S_{\nu,0} + \Phi_\nu S_{\nu+4,0} + \Phi_{\nu+2}S_{\nu-2,0} - \Phi_{\nu-2}S_{\nu+2,0} + 4\Phi_{\nu-2}S_{\nu+2,2} + 2\Phi_{\nu-1}S_{\nu-1,1} \\
&\quad + 2\Phi_{\nu-3}S_{\nu+1,1} + 8\Phi_{\nu+1}S_{\nu+1,3} - 6\Phi_{\nu+1}S_{\nu+1,1} + 2\Phi_{\nu-1}S_{\nu+3,1} + 4\Phi_\nu S_{\nu,2} - 2\Phi_\nu S_{\nu,0}) \\
&\quad + 4a^2((2\nu-1)\Phi_{\nu-2}S_{\nu,0} - (2\nu+1)\Phi_\nu S_{\nu+2,0} + 4\nu\Phi_\nu S_{\nu+2,2} + 2(\nu+1)\Phi_{\nu+1}S_{\nu-1,1} + 2(\nu-1)\Phi_{\nu-1}S_{\nu+1,1}) \\
&\quad - 8a^2(m-x_0)(\Phi_{\nu-3}S_{\nu,0} + 2\Phi_{\nu-1}S_{\nu+2,2} - \Phi_{\nu-1}S_{\nu+2,0} + \Phi_\nu S_{\nu-1,1} + \Phi_{\nu-2}S_{\nu+1,1}) \\
&\quad - 8a^2(m'-x_1)(\Phi_{\nu-2}S_{\nu+1,1} + \Phi_\nu S_{\nu+3,1} + 2\Phi_{\nu+1}S_{\nu,2} - \Phi_{\nu+1}S_{\nu,0} + \Phi_{\nu-1}S_{\nu+2,0}) \\
&\quad + (m-x_0)^2\Phi_{\nu-2}S_{\nu,0} + 2(m-x_0)(m'-x_1)\Phi_{\nu-1}S_{\nu+1,1} - 2\nu(m-x_0)\Phi_{\nu-1}S_{\nu,0} \\
&\quad + (m'-x_1)^2\Phi_\nu S_{\nu+2,0} - 2\nu(m'-x_1)\Phi_\nu S_{\nu+1,1} + (\nu+1)\nu\Phi_\nu S_{\nu,0}. \tag{63}
\end{aligned}$$

Each term factorizes into a non-compact two-dimensional integral $S_{\mu,\alpha}$ and a compact one-dimensional integral Φ_μ which are defined by

$$\begin{aligned}
\Phi_\mu(m, x_0, a) &= (-iL)^\mu \int_{-\pi}^{\pi} \frac{d\varphi}{2\pi} e^{i\mu\varphi} \exp [2Lm \sin \varphi - 2iLx_0 \cos \varphi + 4a^2 \cos 2\varphi] \\
&= (-i)^\mu \int_{-\pi}^{\pi} \frac{d\varphi}{2\pi} e^{i\mu\varphi} \exp [2m \sin \varphi - 2ix_0 \cos \varphi + 4a^2 \cos 2\varphi] \\
&= \frac{(m^2 - x_0^2)^{\mu/2}}{(m+x_0)^\mu} \sum_{l=-\infty}^{\infty} \left(\frac{x_0 - m}{x_0 + m} \right)^l I_l(4a^2) I_{\mu+2l} \left(2\sqrt{m^2 - x_0^2} \right) \tag{64}
\end{aligned}$$

and

$$\begin{aligned}
S_{\mu,\alpha}(m', x_1, a) &= \frac{(iL)^\mu}{4} \int_{-\infty}^{\infty} ds_1 \int_{-\infty}^{\infty} ds_2 \left| \sinh \frac{s_1 - s_2}{2} \right| e^{-\mu(s_1+s_2)/2} \cosh^\alpha \frac{s_1 - s_2}{2} \\
&\times \exp [iLm'(\sinh s_1 + \sinh s_2) + iLx_1(\cosh s_1 + \cosh s_2) - 2a^2(\cosh 2s_1 + \cosh 2s_2)] \\
&\times \exp [im'(\sinh s_1 + \sinh s_2) + ix_1(\cosh s_1 + \cosh s_2) - 2a^2(\cosh 2s_1 + \cosh 2s_2)] \\
&= (iL)^\mu \int_{-\infty}^{\infty} ds \int_1^{\infty} dy e^{-\mu s} y^\alpha \exp [2iLm'y \sinh s + 2iLx_1y \cosh s - 4a^2(2y^2 - 1) \cosh 2s], \tag{65}
\end{aligned}$$

where we have performed the substitution $y = \cosh(s_1 - s_2)/2$ and $s = (s_1 + s_2)/2$ in the second line of Eq. (65). The function I_l is the modified Bessel function of the first kind.

The partition function is correctly normalized which can be readily checked either by setting $a^2 = m = m' = 0$ and $x_0 = x_1 = iL\varepsilon$ with $\varepsilon \rightarrow \infty$ or by setting $m = m' = x_0 = x_1 = 0$ and $a^2 \rightarrow \infty$. In the latter case where we take $a \rightarrow \infty$ we have to distinguish between even and odd ν because of the following asymptotics,

$$\begin{aligned}
\Phi_\mu(m=0, x_0 = i\varepsilon \rightarrow \infty, a=0) &\rightarrow \frac{(-iL)^\mu e^{2\varepsilon}}{2\sqrt{\pi\varepsilon}}, & \Phi_\mu(m=0, x_0=0, a \rightarrow \infty) &\rightarrow \frac{(iL)^\mu e^{2a^2}}{\sqrt{8\pi} a} \delta_{\text{mod}_2(\nu),0}, \\
S_{\mu,\alpha}(m=0, x_0 = i\varepsilon \rightarrow \infty, a=0) &\rightarrow \frac{\sqrt{\pi}(iL)^\mu e^{-2\varepsilon}}{2\varepsilon^{3/2}}, & S_{\mu,\alpha}(m=0, x_0=0, a \rightarrow \infty) &\rightarrow \frac{\sqrt{\pi}(-iL)^\mu e^{-2a^2}}{2^{11/2} a^3}. \tag{66}
\end{aligned}$$

The partition function should be also unity when $m = m'$, $x_0 = x_1$, and a finite. However this general situation is quite non-trivial to verify. It goes back to Cauchy-like integrals of superfunctions invariant under supersymmetric groups [48, 54–58] which were first derived in a general form by Wegner [59]. Indeed the integrand in Eq. (55) is invariant under the supergroup $\text{UOSp}(2|2)$ when $m = m'$ and $x_0 = x_1$.

We emphasize that the representation of the compact integral (64) as a sum is highly convergent for m, x_0, a^2 small enough since the Bessel function behaves as $I_l \propto 1/l!$ for large order. This cannot be said about the non-compact twofold integral (65) which causes some trouble if the lattice spacing a is too large or too small or when the quark mass

m' or the axial mass x_1 are too large. Then we have large cancellations which challenge the numerical integration. Hence it is advantageous to improve this integral. Luckily we are either interested in its value for $x_1 = 0$ or in its imaginary part. In appendix B 3 we calculate both expressions and find

$$S_{\mu,\alpha}(m', x_1 = 0, a) = \frac{[\text{sign}(\mu)]^\mu}{\sqrt{2\pi a^2}(|\mu| - 1)!} \int_1^\infty dy \int_0^\infty dt \frac{y^{\alpha+1}}{\sqrt{2y^2 - 1}} \exp[-4a^2(2y^2 - 1)] \quad (67)$$

$$\times \frac{1}{t} \partial_{t'}^{|\mu|-1} \left[|t' + t|^{|\mu|} \exp\left[-\frac{y^2}{8a^2(2y^2 - 1)}(t' + t - m')^2\right] K_\mu(2y|t' + t|) - \{t \rightarrow -t\} \right]_{t'=0}$$

and

$$S_{\mu,\alpha}(m', x_1, a) = \frac{1}{\pi} \lim_{\varepsilon \rightarrow 0} \text{Im} S_{\mu,\alpha}(m', x_1 + i\varepsilon, a) \quad (68)$$

$$= -(-\text{sign } \mu)^\mu \sqrt{\frac{\pi}{8a^2}} \int_1^\infty dy \int_{-\infty}^\infty dt \frac{y^{\alpha-|\mu|+1}}{\sqrt{2y^2 - 1}} \exp\left[-\frac{y^2}{8a^2(2y^2 - 1)}(t - \text{sign}(\mu)m')^2 - 4a^2(2y^2 - 1)\right]$$

$$\times \sum_{k=0}^{|\mu|-1} \frac{(|\mu| - k - 1)!}{(|\mu| - 1)!k!} [y^2(x_1^2 - t^2)]^k \delta^{(|\mu|-1)}(t - x_1)$$

$$+ (-1)^\mu \text{sign } x_1 \sqrt{\frac{\pi}{8a^2}} \int_1^\infty dy \int_{-\infty}^\infty dt \frac{y^{\alpha+1}}{\sqrt{2y^2 - 1}} \exp\left[-\frac{y^2}{8a^2(2y^2 - 1)}(t - m')^2 - 4a^2(2y^2 - 1)\right]$$

$$\times J_\mu\left(2y\sqrt{x_1^2 - t^2}\right) \left(\frac{x_1 + t}{x_1 - t}\right)^{\mu/2} \Theta(x_1^2 - t^2).$$

The Heaviside step function $\Theta(x_1^2 - t^2)$ restricts the integral over t to a compact interval in the second term while in the first term the integral can be simply evaluated by a Taylor expansion in t and has to be skipped for $\mu = 0$. For $\mu = 0$ the term $1/t$ and the derivative have to be omitted and the minus sign in front of $\{t \rightarrow -t\}$ becomes a plus sign in Eq. (67). The functions J_μ and K_μ are the Bessel function of the first kind and the modified Bessel function of the second kind.

B. Continuum Limit ($|a| \ll 1$)

To understand what happens when taking the continuum limit $|a| \rightarrow 0$ it is useful to consider a random matrix theory which is equivalent to the same chiral partition function as two color QCD with Wilson fermions. This random matrix ensemble consists of random matrices of the form

$$D_W = \begin{pmatrix} aA & W \\ -W^T & aB \end{pmatrix} \quad (69)$$

with $A = A^T$ and $B = B^T$ real symmetric matrices of size $n \times n$ and $(n+\nu) \times (n+\nu)$, respectively, and W an $n \times (n+\nu)$ real rectangular matrix. The random matrix (69) belongs to the symmetry class 19QC_+^* in the classification scheme of non-Hermitian matrices by Magnea [60]. When we choose the Gaussian

$$P(D_W) = \exp\left[-\frac{1}{16}(\text{tr } A^2 + \text{tr } B^2) - \frac{1}{2n} \text{tr } WW^T\right] \quad (70)$$

as the distribution of D_W , we do not have to unfold its spectrum, i.e. in the limit of large matrix dimension $n \rightarrow \infty$ the smallest eigenvalues of D_W and $D_5 = \gamma_5 D_W$ (with $\gamma_5 = \text{diag}(\mathbf{1}_n, -\mathbf{1}_{n+\nu})$ in its matrix form) around the origin are of order $\mathcal{O}(1)$. We have chosen the Gaussian distribution for simplicity. Due to universality other probability distributions give rise to the same chiral Lagrangian.

The random matrix (69) can be brought into the form

$$D'_W = \begin{pmatrix} O_1^T & 0 \\ 0 & O_2^T \end{pmatrix} \begin{pmatrix} A & C & 0 \\ C^T & B' & f \\ 0 & f^T & b \end{pmatrix} \begin{pmatrix} O_1 & 0 \\ 0 & O_2 \end{pmatrix}, \quad (71)$$

where A, B', f and b are of $\mathcal{O}(a)$, $O_1 \in \text{O}(n)$, and $O_2 \in \text{O}(n+\nu)$. At vanishing lattice spacing a the matrix D'_W has ν zero modes and n pairs of imaginary eigenvalues $\pm iy$. This ensemble is known as the chiral Gaussian orthogonal

ensemble [42, 43, 61]. For small lattice spacing $|a| \ll 1$ we can apply first order perturbation theory. To lowest order in a , the secular equation factorizes as

$$\det(D_W - \lambda \mathbf{1}_{2n+\nu}) = \det \left[\begin{pmatrix} -\lambda \mathbf{1}_n & C \\ C^T & -\lambda \mathbf{1}_n \end{pmatrix} \right] \det(b - \lambda \mathbf{1}_\nu). \quad (72)$$

Therefore to leading order the effect of a non-zero lattice spacing is the broadening of the zero modes to the spectral density of the ensemble the matrix b is drawn from. By the central limit theorem, the distributions of the matrix elements of b are Gaussian even if the matrix elements of B do not have a Gaussian distribution. Hence the distribution of b is a ν dimensional GOE. The variance of b is equal to the one of B so that the distribution of b is given by

$$p(b) \propto \exp \left[-\frac{N}{4\tilde{a}^2} \text{tr} b^2 \right] = \exp \left[-\frac{V}{32a^2 W_8} \text{tr} b^2 \right], \quad (73)$$

where we used the relation between the dimensionless lattice spacing a and the physical one when identifying $N \sim V$, i.e.

$$a^2 V W_8 = N \tilde{a}^2 / 8. \quad (74)$$

For $\nu = 1$ the distribution is a simple Gaussian

$$p(b) = \exp \left[-\frac{V}{32a^2 W_8} b^2 \right]. \quad (75)$$

In applying the central limit theorem, we have assumed that the average of the matrix elements of $O_2 B O_2^T$ vanishes. This is not the case if the average $\langle A_{kl} \rangle, \langle B_{kl} \rangle \sim a \delta_{kl}$ which indeed is the situation in lattice simulations, e.g. see [62]. However, such term is exactly of the form of a mass term and can be eliminated by a redefinition of the mass justifying that the central limit theorem gives a centered Gaussian (73).

Indeed the splitting of the spectrum into to one of chGOE and one of GOE can be also seen at the level of chiral perturbation theory which also applies to the epsilon domain of QCD.

Considering the quenched partition function (55) we have shown that it can be rewritten as the convolution of the partition function of continuum QCD without zero modes and a Gaussian function of the supermatrix σ , see Eq. (61). Rescaling $\sigma \rightarrow a\sigma$ we can drop the σ dependence in the partition function $Z_{\text{chGOE}}^{(\nu)}([\widehat{M} + \widehat{X} - a\sigma][\widehat{M} - \widehat{X} - a\sigma])$ since the function remains finite at $a = 0$. Hence the quenched partition function factorizes for $|a| \ll 1$,

$$Z_\nu(\widehat{M}, \widehat{X}, a) \stackrel{a \ll 1}{\approx} Z_{\text{chGOE}}^{(\nu)}(\widehat{M}^2 - \widehat{X}^2) Z_{\text{GOE}}^{(\nu)}\left(\frac{\widehat{M} - \widehat{X}}{4a}\right). \quad (76)$$

Both partition functions and their resulting spectral observables are summarized in appendix C. This factorization is also shown in Fig. 1. The comparison of the approximation (76) with Monte Carlo simulations of the random matrix model (69) and the full analytical result (63) confirms that this factorization applies quite well for $|a| < 0.1$. Only for small indices, namely $\nu = 0, 1, 2$, the deviations are persistent. The reason is the non-analytic nature of the spectrum of the continuum QCD Dirac operator at the spectral edge $\lambda = \pm m \neq 0$. The first derivative of the level density of the Hermitian Dirac operator D_5 diverges at the edge for $\nu = 0, 1, 2$. Thus the limit $a \rightarrow 0$ cannot be interchanged with the integral over the eigenvalues when averaging over the spectrum implying that the continuum limit is not uniform in these cases. If the quark mass vanishes, only the case $\nu = 0$ is non-uniform. We return to this point in subsection VB.

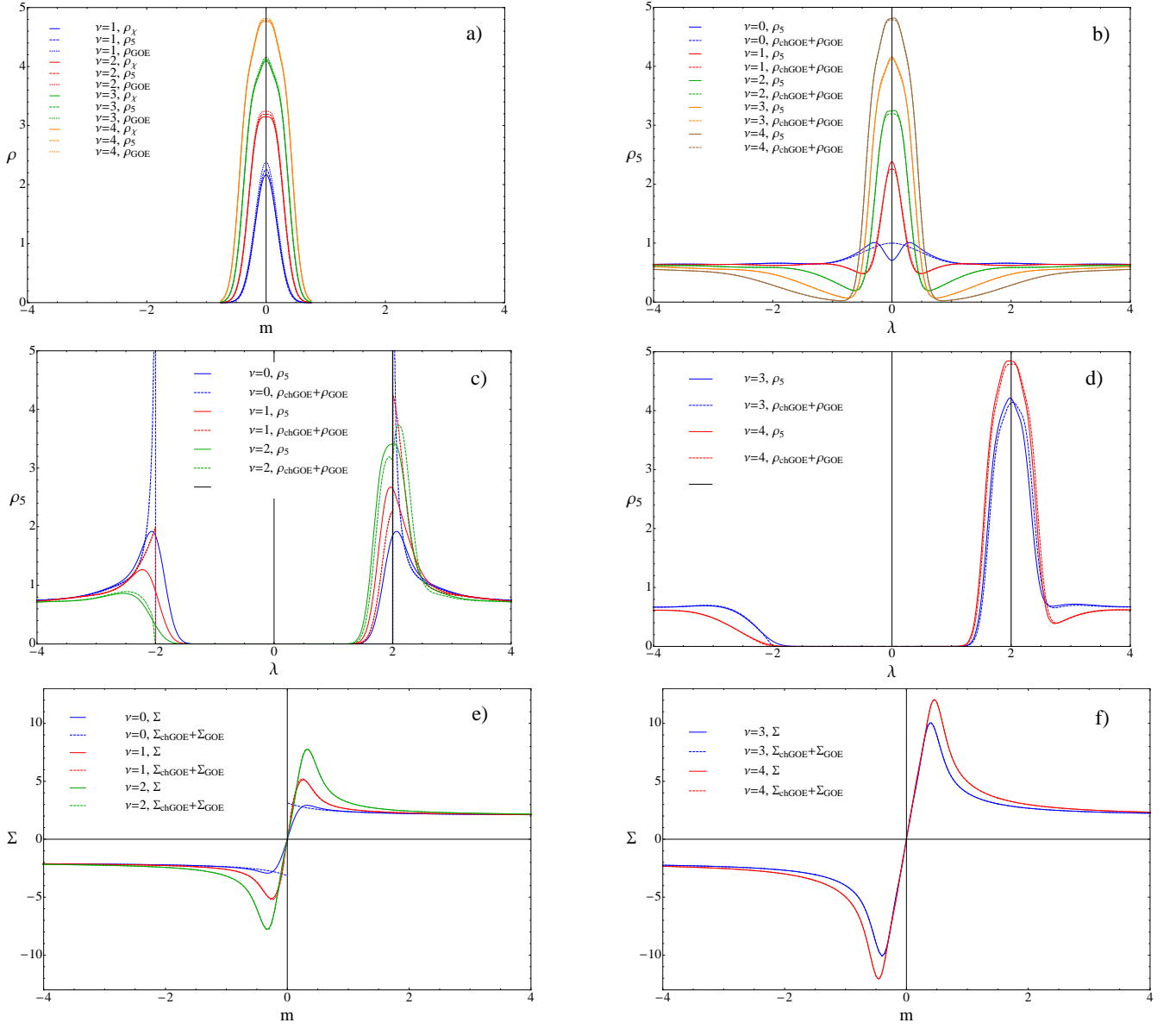


FIG. 1. Comparison of some spectral observables of the Wilson Dirac operator with lattice spacing $\sqrt{W_8 V \tilde{a}} = |a| = 0.0625$ and of the spectrum consisting of the sum of continuum QCD without zero modes and a $\nu \times \nu$ dimensional GOE for indices ($\nu = 0, 1, 2, 3, 4$). Figure a) emphasizes that the distribution of chirality $\rho_\chi(m)$ over the real eigenvalues (solid curves), see Eq. (B19), and the level density $\rho_5(m, \lambda = 0)$ of the Hermitian Wilson Dirac operator at the origin as a function of the quark mass (dashed curves), see Eq. (B17), become the level density of a GOE. In subsection VE we argue that then also the level density of the real eigenvalues of the non-Hermitian Wilson Dirac operator D_W shares this distribution. The splitting of the spectrum of D_5 into the superposition of a chGOE and a GOE is shown in figure b) where the quark mass is set to $m = 0$. The level density ρ_5 (solid curves) perfectly agrees with the sum $\rho_{\text{chGOE}} + \rho_{\text{GOE}}$ (dashed curves) when the eigenvalue λ stays away from the origin while the deviations remain close to the origin. Especially the case of vanishing index $\nu = 0$ shows obvious deviations which are discussed in subsection VB. These deviations are particularly large for small index $\nu = 0, 1, 2$ and become more prominent when the quark mass m becomes non-zero, see figure c) for $m = 2$ (black vertical line). The spectral discontinuities of the continuum Dirac operator are hardly suppressed by the GOE level density ρ_{GOE} shifted by the quark mass (dashed curves). However the level densities $\rho_5(m = 2, \lambda)$ (solid curves) are smooth at any finite values of the lattice spacing. Only for larger indices, here $\nu = 3, 4$, the agreement with a splitting into the two sub-spectra is almost striking, cf. figure d). The bad, see figure e), or good, see figure f), agreement carries over to the mass dependent chiral condensate $\Sigma(m)$, see Eq. (18). Also in these two plots the solid curves are the exact results (B18) at finite lattice spacing while the dashed curves are the approximation of the chiral condensate as the sum of the chiral condensate of continuum QCD without the contribution from the zero modes, Σ_{chGOE} , and of the “chiral condensate” resulting from a finite dimensional GOE, Σ_{GOE} , see Eqs. (C7) and (C30).

C. Limit to a very Coarse Lattice ($|a| \gg 1$)

We also consider the limit of a coarse lattice $|a| \gg 1$ to get a full understanding of lattice artefacts in the spectrum of the Wilson Dirac operator. Especially this limit shows the change of scales in the spectrum when increasing the lattice spacing. It may help to estimate the strength of the lattice artefacts.

In the limit of a very coarse lattice the quark mass m and the axial mass x are an order smaller than a^2 . Then the compact integral (64) is dominated by the term $4a^2 \cos 2\phi$. Expanding around the two saddle points $\varphi = \delta\varphi/a$ and $\varphi = \pi + \delta\varphi/a$ the function Φ_μ becomes

$$\begin{aligned} \Phi_\mu(m, x_0, a) &\stackrel{|a| \gg 1}{\approx} \frac{(-iL)^\mu e^{4a^2}}{2\pi a} \int_{-\infty}^{\infty} d\delta\varphi e^{-8\delta\varphi^2} \left(\exp\left[\frac{2Lm}{a}\delta\varphi - 2iLx_0\right] + (-1)^\mu \exp\left[-\frac{2Lm}{a}\delta\varphi + 2iLx_0\right] \right) \\ &= \frac{(-iL)^\mu}{\sqrt{8\pi a}} \exp\left[4a^2 + \frac{m^2}{16a^2}\right] \frac{e^{-2iLx_0} + (-1)^\mu e^{-2iLx_0}}{2}. \end{aligned} \quad (77)$$

A similar expansion can be done for the non-compact double integral (65). However this time we have only one saddle point namely $s_{1/2} = \delta s_{1/2}/a$,

$$\begin{aligned} S_{\mu,\alpha}(m', x_1, a) &\stackrel{|a| \gg 1}{\approx} \frac{(iL)^\mu}{8a^3} \exp[2iLx_1 - 4a^2] \int_{-\infty}^{\infty} d\delta s_1 \int_{-\infty}^{\infty} d\delta s_2 |\delta s_1 - \delta s_2| \exp\left[\frac{iLm'}{a}(\delta s_1 + \delta s_2) - 4(\delta s_1^2 + \delta s_2^2)\right] \\ &= \frac{(iL)^\mu \sqrt{\pi}}{2^{11/2} a^3} \exp\left[2iLx_1 - 4a^2 - \frac{m'^2}{16a^2}\right]. \end{aligned} \quad (78)$$

Since $m, x \ll a^2$ we can omit all terms in the sum (63) which do not come with an a^4 factor. Using the approximations (77) and (78) the quenched partition function becomes

$$Z_\nu(\widehat{M}, \widehat{X}, a) \stackrel{a \gg 1}{\approx} \exp\left[2iL(x_1 - x_0) + \frac{m^2 - m'^2}{16a^2}\right]. \quad (79)$$

The second term in Eq. (77) depending on the sign $(-1)^\mu$ cancels in the sum. Therefore the dependence on the topological charge is completely lost.

We wish to emphasize that this scaling is only valid around the origin and applies for the eigenvalues which are of order $\mathcal{O}(a)$, cf. Figs. 2. A more physical scale for the level density of the real eigenvalues and the ‘‘mesoscopic’’ spectrum around the origin of the Hermitian Wilson Dirac operator is discussed in the next subsection.

D. Thermodynamic Limit

In this section we discuss the thermodynamic limit sometimes also referred to as the mean field limit where the quark mass m , the axial mass λ , and the squared lattice spacing are of the same order, and satisfy $m = \Sigma V \widetilde{m}$, $\lambda = \Sigma V \widetilde{\lambda}$, $a^2 = W_8 V \widetilde{a}^2 \gg 1$. This limit is best performed in an eigenvalues representation of the supersymmetric integral (55). Choosing $V = -iLU$ as a new variable, the exponent in the partition function (55) is given by

$$\exp\left[-\frac{1}{2}\text{Str}\widehat{M}(V + V^{-1}) - \frac{1}{2}\text{Str}\widehat{X}(V - V^{-1}) - a^2\text{Str}(V^2 + V^{-2})\right]. \quad (80)$$

The corresponding saddle point equation reads

$$p(V) = \frac{m}{2}(V - V^{-1}) + \frac{\lambda}{2}(V + V^{-1}) - 2a^2(V^2 - V^{-2}) = 0. \quad (81)$$

The solution of this equation is computed in appendix D. For $\lambda = 0$ it is

$$V = \begin{cases} \left(\frac{m}{8a^2} - iL\sqrt{1 - \left(\frac{m}{8a^2}\right)^2}\right) \mathbf{1}_4, & |m| < 8a^2, \\ \text{sign } m \mathbf{1}_4, & |m| > 8a^2. \end{cases} \quad (82)$$

while for $\lambda \neq 0$ it takes the quite complicated form

$$V = e^{\vartheta + Li\varphi} \mathbf{1}_4 \text{ with } \varphi = \arccos\left[\frac{m \cosh \vartheta + \lambda \sinh \vartheta}{8a^2 \cosh 2\vartheta}\right] \quad (83)$$

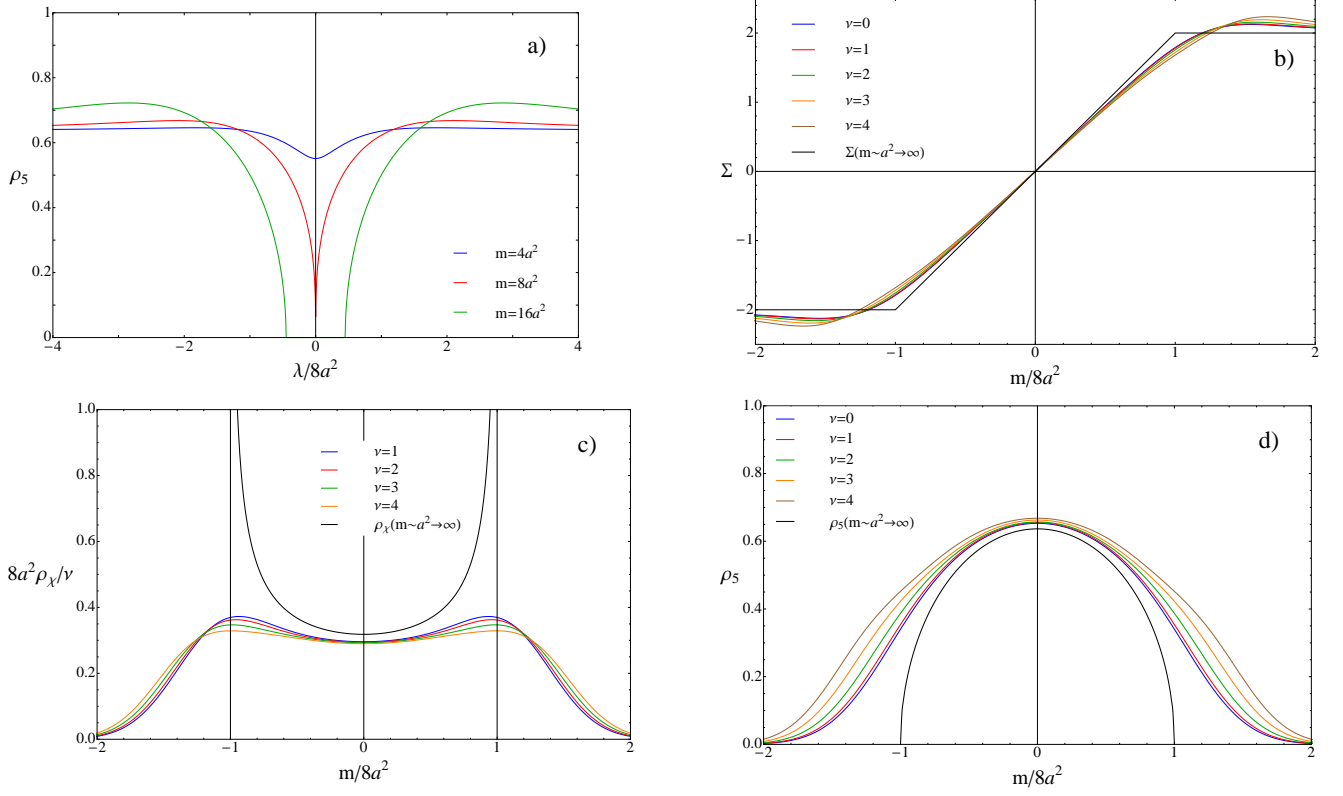


FIG. 2. In plot a) we show three different cases for the thermodynamic limit of the level density ρ_5 . The Hermitian Wilson Dirac operator D_5 exhibits a spectral gap around the origin when the quark mass $|m|$ is larger than $8a^2$. This gap closes at $m = 8a^2$ and the system enters the Aoki phase. Hence the value of the level density ρ_5 at the origin is an order parameter for the Aoki phase. In plots b), c) and d) we compare the thermodynamic limit (black curves) of the chiral condensate, the distribution of the chiralities over the real eigenvalues, and the mass dependence of the level density ρ_5 at the origin $\lambda = 0$, respectively, with the behavior at finite lattice spacing $\sqrt{V}W_8\tilde{a} = a = 1$. Although the finite a result has still large deviations from the thermodynamic limit, the phase transition building up at $m = \pm 8a^2$ is clearly visible. Also the dependence of the observables on the index ν has almost disappeared.

and

$$\sinh 2\vartheta = - \left(\frac{m\lambda}{(8a^2)^2} + \sqrt{\frac{m^2\lambda^2}{(8a^2)^4} - \frac{1}{27} \left(\frac{m^2 - \lambda^2}{(8a^2)^2} - 1 \right)^3} \right)^{1/3} - \left(\frac{m\lambda}{(8a^2)^2} - \sqrt{\frac{m^2\lambda^2}{(8a^2)^4} - \frac{1}{27} \left(\frac{m^2 - \lambda^2}{(8a^2)^2} - 1 \right)^3} \right)^{1/3}. \quad (84)$$

The level density of the Hermitian Wilson Dirac operator can be calculated from these saddlepoint solutions via

$$\rho_5(m, \lambda, a) = \left[\frac{\nu}{2\pi} \text{Im Str } V^{-1} \partial_{x_1} V + \frac{L}{2} \text{Str diag}(0, 0, 1, 1) \text{Im}(V - V^{-1}) \right]_{\substack{m=m' \\ x_1=x_2=\lambda}}. \quad (85)$$

The first term is sub-leading such that it can be omitted in the discussion. The density ρ_5 is plotted in Fig. 2.a) and d). It exhibits two different scenarios, either ρ_5 has a spectral gap at the origin or the gap is closed. The critical points in the case of a gap can be read off the solution (84) which are

$$\lambda = \pm m \left(1 - \left(\frac{8a^2}{m} \right)^{2/3} \right)^{3/2}. \quad (86)$$

Instead of the involved derivation of these critical points via the saddle point solution presented in appendix D one can also simply find them by a substitution $W = \text{sign } m(V - V^{-1})/2$ in Eq. (80) such that we have to minimize the function

$$q(W) = |m| \sqrt{\mathbf{1}_4 + W^2} + \lambda W - 4a^2 W^2. \quad (87)$$

At the critical points the first two derivatives of $q(W)$ vanish, i.e.

$$q'(W) = \frac{mW}{\sqrt{\mathbf{1}_4 + W^2}} + \lambda - 8a^2W = 0 \text{ and } q''(W) = \frac{m}{(\mathbf{1}_4 + W^2)^{3/2}} - 8a^2 = 0. \quad (88)$$

This yields $W = \pm\sqrt{(m/8a^2)^{2/3} - 1}$ implying the critical point (86) from the first derivative. Hence the spectrum of D_5 has a gap for $m > 8a^2$ in the interval

$$\lambda \in \left[-|m| \left(1 - \left(\frac{8a^2}{m} \right)^{2/3} \right)^{3/2}, |m| \left(1 - \left(\frac{8a^2}{m} \right)^{2/3} \right)^{3/2} \right]. \quad (89)$$

For $m < 8a^2$ and $\lambda = 0$ the gap is closed and the system is in the Aoki phase.

The distribution of chirality over the real eigenvalues and the mass dependent chiral condensate are given by the saddlepoints solution V via the relations

$$\begin{aligned} \rho_\chi(m, a) &= \left[-\frac{\nu}{2\pi} \text{Im Str } V^{-1} \partial_{m'} V - \frac{1}{2} \text{Str diag}(0, 0, 1, 1) \text{Im}(V + V^{-1}) \right]_{\substack{m=m' \\ x_1=x_2=0}}, \\ \Sigma(m, a) &= \left[-\frac{\nu}{2\pi} \text{Re Str } V^{-1} \partial_{m'} V - \frac{1}{2} \text{Str diag}(0, 0, 1, 1) \text{Re}(V + V^{-1}) \right]_{\substack{m=m' \\ x_1=x_2=0}}. \end{aligned} \quad (90)$$

Since the axial mass is set to zero we only need to consider the solution (82). The first term is again sub-leading for $\Sigma(m, a)$ while it is leading for $\rho_\chi(m, a)$. This different behaviour hints to a separation of scales which indeed happens, see Fig. 2.

We discuss the thermodynamic limit of the spectral observables in more detail in the next section.

V. SPECTRAL STATISTICS OF THE WILSON DIRAC OPERATOR OF TWO COLOR QCD

In this section we discuss the spectral observables in more detail and derive their analytical expressions. In particular, we summarize the continuum and thermodynamic limit. We study the following spectral observables: The unquenched partition function $Z_\nu^{N_f}$ and its chiral condensate Σ^{N_f} in subsection V A, the level density ρ_5 of the Hermitian Wilson Dirac operator D_5 in subsection V B, the chiral condensate $\Sigma(m)$ of the quenched theory in subsection V C, the distribution of chirality ρ_χ over the real eigenvalues of the non-Hermitian Wilson Dirac operator D_W in subsection V D, and the level density of the real eigenvalues and the number of the additional real eigenvalues in subsection V E.

A. Partition Function of Dynamical Quarks

For $N_f = 1$ there is no spontaneous symmetry breaking and the QCD partition function for QCD with two colors is the same as for QCD with three or more colors. Indeed for $N_f = 1$ the partition function (29) can be written as

$$Z_\nu^{N_f=1}(m, a) = \int_{-\pi}^{\pi} \frac{d\varphi}{2\pi} e^{i\nu\varphi} \exp[2m \cos \varphi - 4a^2 \cos 2\varphi], \quad (91)$$

which coincides with the one-flavor partition function for $\beta = 2$, see [14].

For two or more flavors the partition function is the $N_f(2N_f - 1)$ dimensional integral (29). For simplicity we assume that all quark masses are equal to m . Then the partition function

$$Z_\nu^{N_f}(m, a) = \int_{\text{CSE}(2N_f)} d\mu(U) \det^{\nu/2} U \exp \left[\frac{m}{2} \text{tr}(U + U^{-1}) - a^2 \text{tr}(U^2 + U^{-2}) \right] \quad (92)$$

can be calculated by diagonalizing U and applying de Bruijn's integration theorem [63]. Then we end up with a Pfaffian (essentially an exact square root of a determinant of an antisymmetric matrix) [64]

$$Z_\nu^{N_f}(m, a) \propto \text{Pf}[A] \quad \text{with} \quad A_{kl} = (k - l) \Phi_{\nu-2N_f+k+l-1}^0(m, x_0 = 0, a), \quad 1 \leq k, l \leq 2N_f. \quad (93)$$

where Φ_0^μ is the integral given in Eq. (64) evaluated of $x_0 = 0$,

$$\Phi_0^\mu(m, x_0 = 0, a) = (-i)^\mu \int_{-\pi}^{\pi} \frac{d\varphi}{2\pi} e^{i\mu\varphi} \exp[2m \sin \varphi + 4a^2 \cos 2\varphi]. \quad (94)$$

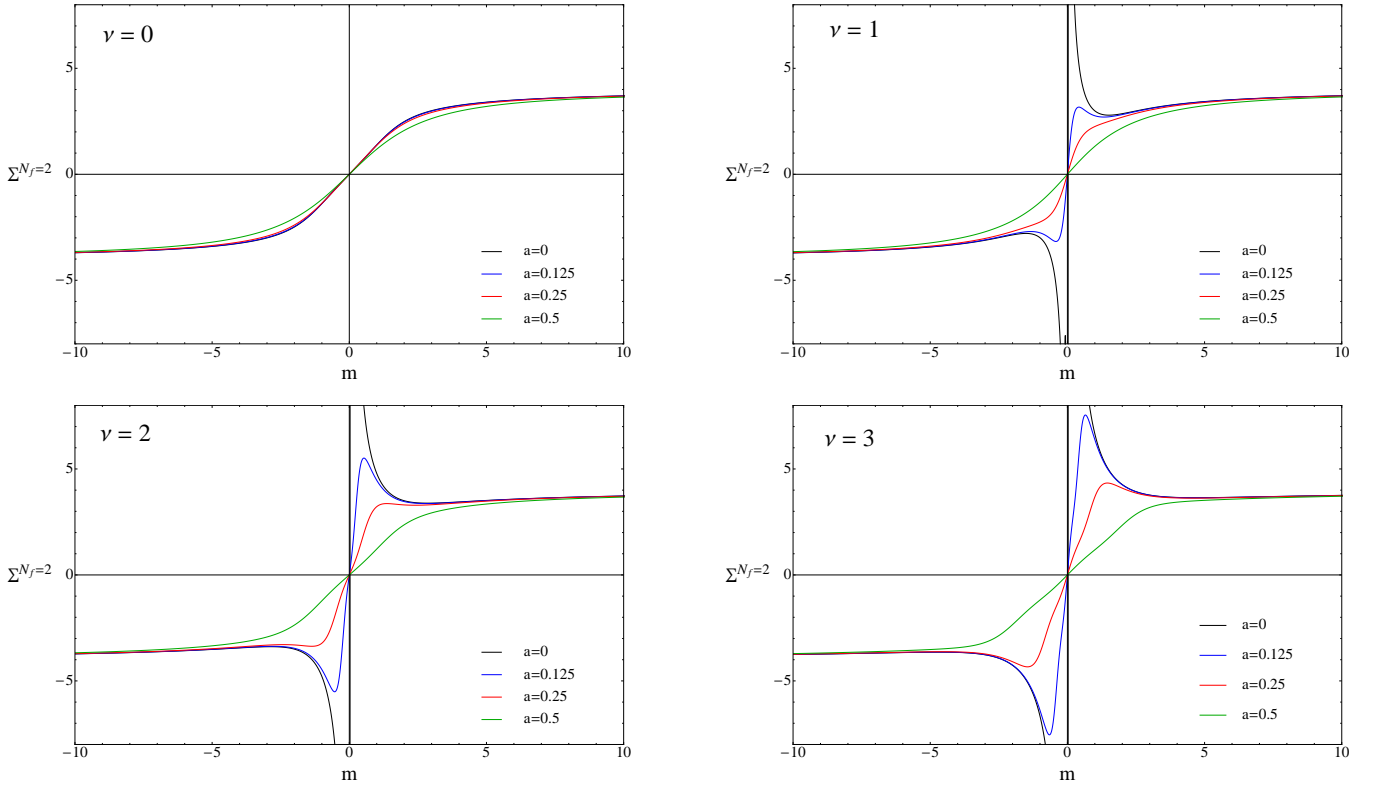


FIG. 3. Chiral condensate for two dynamical quarks for index $\nu = 0, 1, 2, 3$ and lattice spacing $\sqrt{VW_8\tilde{a}} = a = 0, 0.125, 0.25, 0.5$. The continuum limit (black curves) diverges as ν/m for $m \rightarrow 0$ due to the zero modes. For larger index ν , the peaks reminiscent of this singularity are more persistent at finite lattice spacing. The reason is the localization of real eigenvalues around the origin which are smoothed out only very slowly.

The chiral condensate is easily calculated by taking the derivative of the free energy $\ln Z_\nu^{N_f}(m, a)$ with respect to the quark mass resulting in

$$\Sigma_\nu^{N_f}(m, a) = \frac{1}{2} \partial_m \ln Z_\nu^{N_f}(m, a) = \frac{1}{4} \text{tr} A^{-1} \partial_m A. \quad (95)$$

The derivative of A is given by

$$\partial_m A_{kl} = (k-l) [\Phi_{\nu-2N_f+k+l}^0(m, x_0=0, a) + \Phi_{\nu-2N_f+k+l-2}^0(m, x_0=0, a)]. \quad (96)$$

The chiral condensate is normalized to the asymptotics $\lim_{m \rightarrow +\infty} \Sigma_\nu^{N_f}(m, a) = N_f$. In Fig. 3 we illustrate the behavior for particular indices $\nu = 0, 1, 2, 3$.

As already mentioned in subsection III A, the unquenched partition function (92) factorizes in the partition function of continuum QCD without the zero modes and in the partition function of a $\nu \times \nu$ dimensional GOE in the continuum limit $|a| \ll 1$. The spectrum of the finite dimensional GOE is of the order a which shrinks to the origin in the continuum limit. This creates a singularity of the chiral condensate at $a = 0$ for configurations with $\nu \neq 0$, cf. Fig. 3.

In the thermodynamic limit the partition function is either dominated by the saddlepoint $U_0 = \text{sign } m$ for $|m| \geq 8a^2$ or by the saddlepoints satisfying $U_0 + U_0^{-1} = m/4a^2$ for $|m| \leq 8a^2$. Then the resulting chiral condensate is given by

$$\langle \bar{\psi} \psi \rangle_{N_f} = \frac{1}{N_f} \Sigma_\nu^{N_f}(m, a) \approx \begin{cases} \frac{m}{4a^2}, & |m| < 8a^2, \\ \text{sign } m, & |m| > 8a^2. \end{cases} \quad (97)$$

This result does not depend on N_f and we will show in subsection VC that it is also valid for the quenched theory. The thermodynamic limit is already well approximated for a lattice spacing $\sqrt{VW_8\tilde{a}} = a \approx 2$, see Fig. 4.

Finally, let us show that the sign of W_8 has to be positive. We start from the observation that the partition

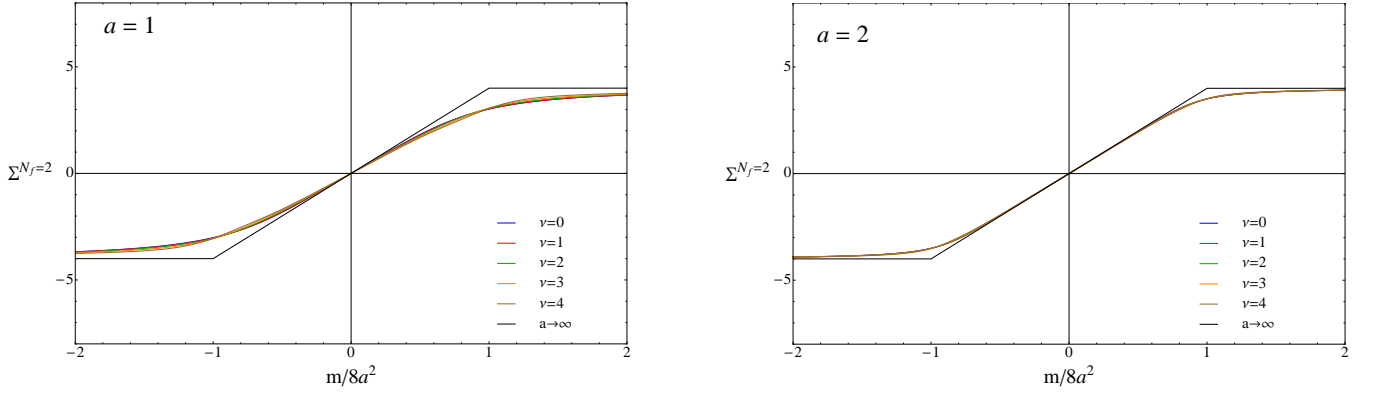


FIG. 4. Comparison of the chiral condensate with two dynamical quarks for index $\nu = 0, 1, 2, 3, 4$ with the thermodynamic limit (black curve). Although around the origin the thermodynamic limit is a good approximation for lattice spacing $\sqrt{VW_8}\tilde{a} = a = 1$, we have still large deviations in the phase transition region around the quark mass $m = 8a^2$. At $\sqrt{VW_8}\tilde{a} = a = 2$ the thermodynamic limit is almost approached. Nonetheless the ν dependence is barely visible already at smaller lattice spacings.

function (92) has to be the same as the average over the eigenvalues over $D_5 + m\gamma_5$ which are real,

$$Z_\nu^{N_f}(m, a) = (-1)^{\nu N_f} \left\langle \prod_j (\lambda_j^5(m))^{N_f} \right\rangle_{D_5}, \quad (98)$$

Hence the partition function has to be positive definite for N_f even. The sign $(-1)^{\nu N_f}$ in front of the average results from multiplying γ_5 with the non-Hermitian Wilson Dirac operator D_W . As is the case for $\beta = 2$ the partition function satisfies the general relation (see Eq. (29))

$$Z_\nu^{N_f}(m = 0, a^2) = (i)^{N_f \nu} Z_\nu^{N_f}(m = 0, -a^2). \quad (99)$$

Therefore, the partition function for $N_f \in 4\mathbb{N}_0 + 2$ cannot be positive definite for both values of the sign of W_8 . This can also be seen from the explicit expression for the two-flavor partition function, which, at $m = 0$ is given by the two dimensional integral

$$Z_\nu^{N_f=2}(m = 0, a) = \frac{1}{2} \int_{-\pi}^{\pi} \frac{d\varphi_1}{2\pi} \int_{-\pi}^{\pi} \frac{d\varphi_2}{2\pi} |e^{i\varphi_1} - e^{i\varphi_2}|^4 e^{i\nu(\varphi_1 + \varphi_2)} \exp[-4a^2 \cos 2\varphi_1 - 4a^2 \cos 2\varphi_2]. \quad (100)$$

All odd powers of the phases $e^{i\varphi_1}$ and $e^{i\varphi_2}$ vanish since the a dependent term has double the frequency. Therefore, for odd ν , only two terms remain in the expansion of the Vandermonde determinant. They can be combined as

$$Z_\nu^{N_f=2}(m = 0, a) = -4I_{(\nu-1)/2}(-4a^2)I_{(\nu+1)/2}(-4a^2) = 4I_{(\nu-1)/2}(4a^2)I_{(\nu+1)/2}(4a^2). \quad (101)$$

This term is always positive definite if a is real and thus W_8 is positive while it is negative when $VW_8\tilde{a}^2 = a^2 < 0$. Hence a negative value of W_8 contradicts the positivity of the partition function.

The unquenched partition function (101) is shown in Fig. 5 for $\nu = 1$ and $N_f = 2, 4$. Indeed the partition function for $N_f = 4$ does not depend on the sign of a^2 at $m = 0$ (see Eq. (99)), but the figure shows that the partition function is not positive definite for a negative value of W_8 .

B. Level Density of D_5

The level density ρ_5 given by

$$\rho_5(m, \lambda, a) = \partial_{x_1} \text{Im} Z_\nu(\widehat{M}, \widehat{X}, a) \Big|_{\substack{\widehat{M}=m\mathbf{1}_4 \\ \widehat{X}=(\lambda+i\varepsilon)\mathbf{1}_4 \rightarrow \lambda\mathbf{1}_4}}$$

immediately results from combining Eqs. (10), (11), (63), and (B10). We obtain a quite complicated expression (see Eq. (B17) of appendix B 4) which can be evaluated numerically. In Fig. 6 we compare this result with Monte Carlo simulations of the random matrix theory (69).

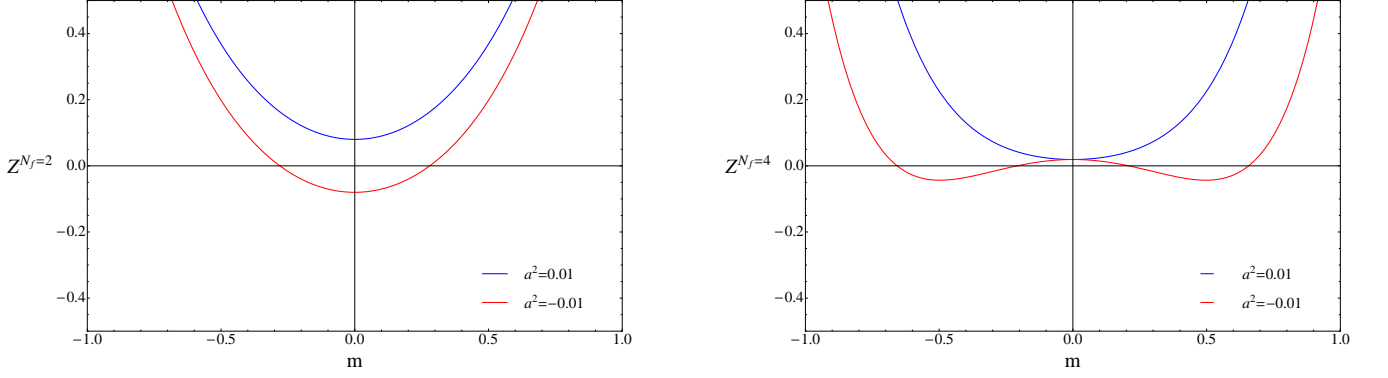


FIG. 5. The mass dependence of the two flavor (left) and the four flavor partition function (right) for $VW_8 \tilde{a}^2 = a^2 = \pm 0.01$ and $\nu = 1$. In the case where the low energy constant is negative we have always regions where the chiral partition function is negative although it is positive when considering the full theory.

When taking the continuum limit $a \rightarrow 0$ the peak around the quark mass m shrinks to a single Dirac delta function with area ν . At non-zero a , the peaks are no longer degenerate and broaden to a width $\sim a$. Due to the weak level repulsion which is linear for real matrices we do not observe separate peaks for $\nu > 1$.

In the limit $a \rightarrow 0$ the density of the cluster of ν peaks around m combine into the level density ρ_{GOE} , see Eq. (C33), of a $\nu \times \nu$ dimensional Gaussian, cf. Figs. 1 b), c) and d). In this limit we expect that ρ_5 can be approximated by

$$\rho_5(m, \lambda, a) \stackrel{|a| \ll 1}{\approx} \frac{|\lambda|}{\sqrt{\lambda^2 - m^2}} \rho_{\text{chGOE}}^{(\nu)}(\sqrt{\lambda^2 - m^2}) \Theta(\lambda^2 - m^2) + \rho_{\text{GOE}}^{(\nu)}\left(\frac{m - \lambda}{4a}\right) \quad (102)$$

with $\rho_{\text{GOE}}^{(\nu)}$ the level densities (C34), (C35), and (C33) depending on ν and

$$\rho_{\text{chGOE}}^{(\nu)}(x) = J_\nu(2|x|) \left(1 - \int_0^{2|x|} dy J_\nu(y)\right) + 2|x| (J_\nu^2(2|x|) - J_{\nu-1}(2|x|)J_{\nu+1}(2|x|)) \quad (103)$$

the microscopic level density of continuum QCD and, thus, of chiral GOE without zero modes [65]. This approximation is shown in Figs. 1.b), c) and d).

As we already pointed out in subsection IV B the continuum limit via the approximation (102) is not uniform at $\lambda = m$ for small values of ν . In particular, as can be seen by a brief computation (see appendix E), for $m = \lambda = 0$ and $\nu = 0$ we never reach the correct value at the origin in the continuum limit, see Fig. 7. Thus we obtain the limit

$$\lim_{a \rightarrow 0} \rho_5(m = 0, \lambda = 0, a) = \frac{1}{\sqrt{2}} \neq 1 = \lim_{\lambda \rightarrow 0} \rho_5(m = 0, \lambda, a = 0). \quad (104)$$

The non-commutativity of the two limits has also been confirmed by Monte Carlo simulations, see Fig. 7. Therefore the continuum limit is not uniform in m so that one has to be careful with quantities which depend essentially on eigenvalues close to the origin.

As was discussed in Eq. (15), the mass dependence of $\rho_5(m, \lambda = 0, a)$ is given by the density of the real eigenvalues of D_W weighted by the absolute value of the inverse chirality of the states. In the continuum limit the density of the real eigenvalues is well approximated by the level density ρ_{GOE} , see Eq. (C33), of exactly the same finite dimensional GOE which also describes the former zero modes, cf. Fig. 9 with height that is of order $1/a$ and a width that is of order a . Since the chirality of the states with real eigenvalues is $|\langle k | \gamma_5 | k \rangle| \approx 1$, in the continuum limit, we also find that the mass dependence of $\rho_5(m, \lambda = 0, a)$ is given by a GOE in this limit.

In the thermodynamic limit the level density ρ_5 takes the form

$$\rho_5\left(\frac{m}{8a^2}, \frac{\lambda}{8a^2}\right) \approx \frac{2}{\pi} \cosh\left[\vartheta\left(\frac{m}{8a^2}, \frac{\lambda}{8a^2}\right)\right] \sin\left[\varphi\left(\frac{m}{8a^2}, \frac{\lambda}{8a^2}\right)\right] \Theta\left[\lambda^2 - (|m|^{2/3} - (8a^2)^{2/3})^3\right] \quad (105)$$

where φ and ϑ are given by Eqs. (83) and (84). The Heaviside theta function implies a spectral gap if $|m| > 8a^2$. If the gap is closed the system is in the Aoki phase. The order parameter is the pion condensate which is proportional to $\partial_x \log Z|_{x=0}$ and, hence, to $\rho_5(m, \lambda = 0, a)$. In the thermodynamic limit this quantity becomes a semi-circle

$$\langle \bar{\psi} \gamma \tau_3 \psi \rangle_{N_f=0} \propto \rho_5\left(\frac{m}{8a^2}, \frac{\lambda}{8a^2} = 0\right) \approx \frac{2}{\pi} \sqrt{1 - \frac{m^2}{(8a^2)^2}} \Theta[8a^2 - |m|], \quad (106)$$

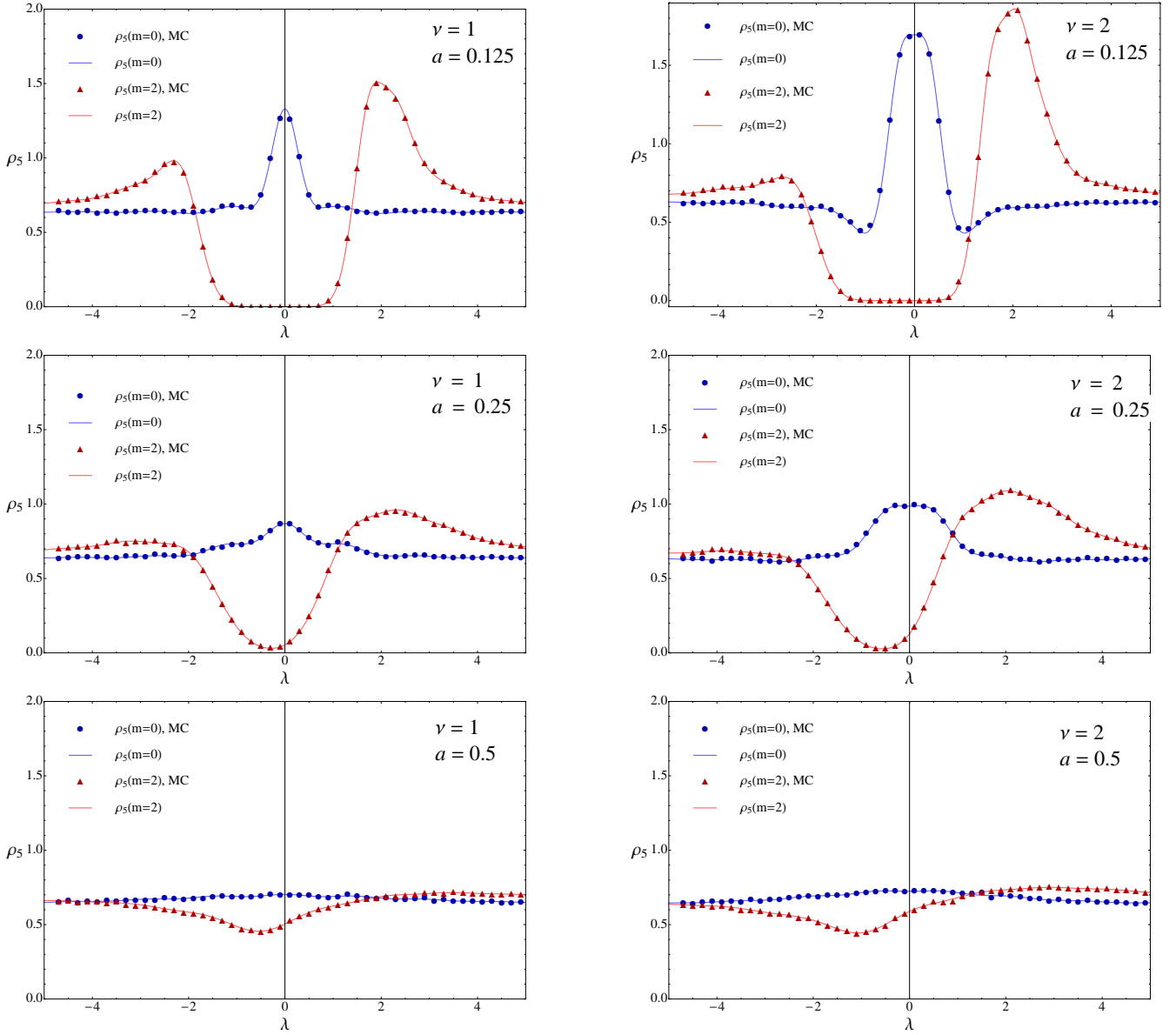


FIG. 6. Comparison of the analytical result (B17) for the level density ρ_5 (solid curves) with Monte Carlo simulations (MC, symbols). We have simulated for two different values for the valence quark mass, $m = 0$ (blue curves) and $V\Sigma\tilde{m} = m = 2$ (red curves). The index has been chosen $\nu = 1$ (left plots) and $\nu = 2$ (right plots) and the lattice spacing is $\sqrt{V}W_8\tilde{a} = a = 0.125, 0.25, 0.5$. For each plot we have generated 10^5 matrices distributed according to Eq. (70). The prominent peaks at $m = 0$ and $m = 2$ result from the broadened former zero modes. They will become Dirac delta functions in the continuum limit.

(see Fig. 2.d). It immediately shows that the phase transition at $|m| = 8a^2$ is of second order as in the case of three color QCD with Wilson fermions. Furthermore we can say that the height of the limit (106) is of order $\mathcal{O}(1)$ and its integral is of order $\mathcal{O}(a^2)$. These two pieces of information become important in the discussion of the real eigenvalues in subsection V E.

C. The Chiral Condensate

The analytical result for the chiral condensate

$$\Sigma(m, a) = \partial_{m'} \text{Re} Z_\nu(\widehat{M}, \widehat{X}, a) \Big|_{\substack{\widehat{M}=m\mathbf{1}_4 \\ \widehat{X}=i\varepsilon\mathbf{1}_4 \rightarrow 0}} \quad (107)$$

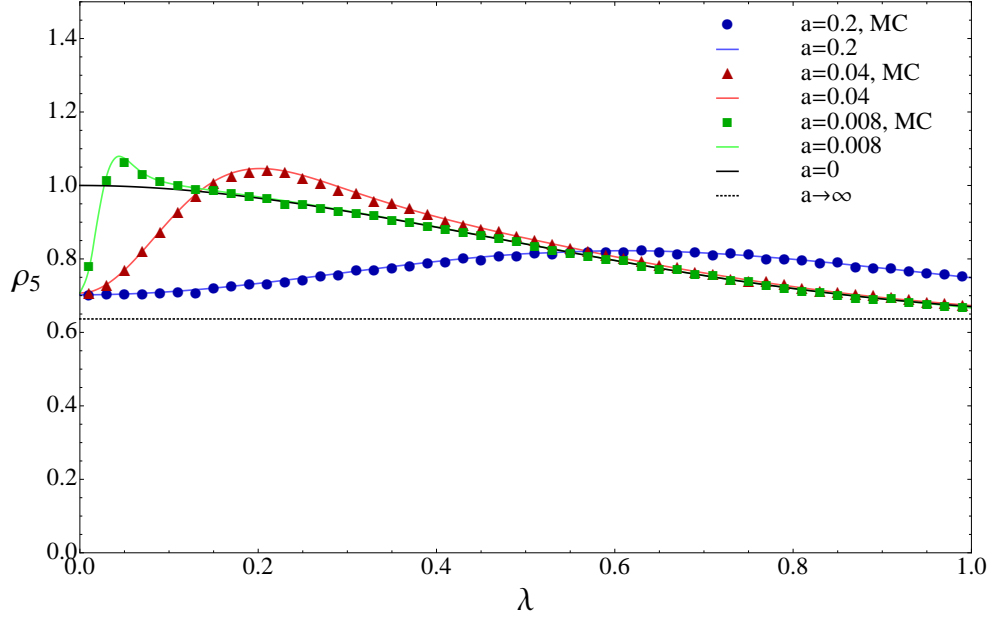


FIG. 7. Continuum limit of the level density ρ_5 of the Hermitian Wilson Dirac operator. The index and the quark mass are set to zero, $\nu = m = 0$. The continuum limit (black solid curve) is not uniformly approached by the analytical result (B17). We have confirmed our analytical result by Monte Carlo simulations of the random matrix model (69) and (70). The ensemble of 2.5×10^6 matrices gives an accuracy of about 1%. The dotted black curve is the limit for a very coarse lattice where $\rho_5 = 2/\pi$ is a constant.

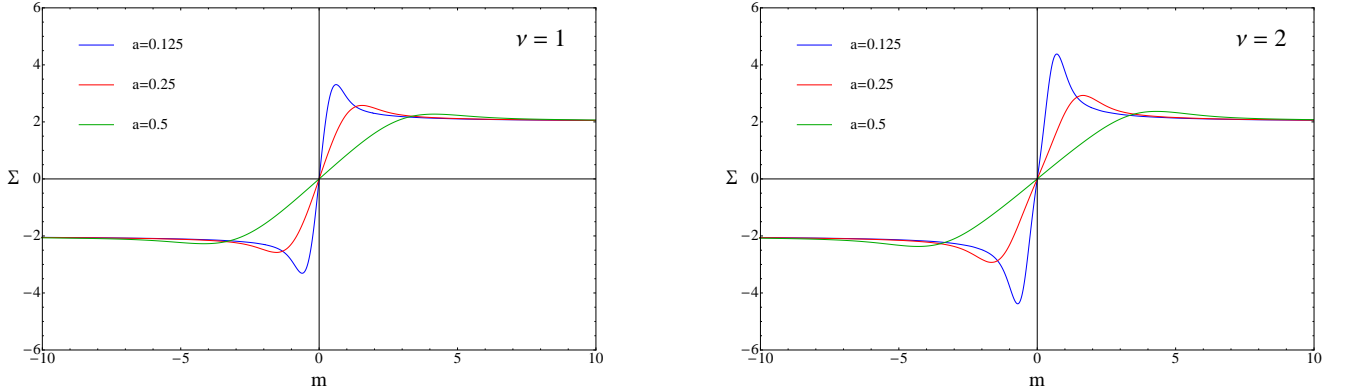


FIG. 8. The chiral condensate for parameters used for the simulation in Figs. 6 and 9. We underline that the chiral condensate is for the quenched theory while the one shown in Fig. 3 is for the theory with dynamical quarks. Interestingly, the chiral condensate in the quenched theory approaches the asymptotic value 2 from above while it is approached from below for the theory with dynamical quarks.

for the quenched theory is explicitly shown in Eq. (B18) of appendix B4. Its behavior is shown in Fig. 8.

As in the theory with dynamical quarks we have a $1/m$ singularity for $m \rightarrow 0$ due to the zero modes at non-zero index $\nu \neq 0$ in the continuum theory. These singularities are washed out by the finite dimensional GOE according to the approximation

$$\Sigma(m, a) \stackrel{|a| \ll 1}{\approx} \Sigma_{\text{chGOE}}^{(\nu)}(m) + \Sigma_{\text{GOE}}^{(\nu)}(m), \quad (108)$$

where the continuum limit of the chiral condensate without the contribution of the zero modes, $\Sigma_{\text{chGOE}}^{(\nu)}(m)$, is given in Eq. (C9). The continuum result is in agreement with earlier work by Damgaard et al. [66]. Indeed the contribution of $\Sigma_{\text{GOE}}^{(\nu)}$, see Eq. (C30), works quite well for small but finite lattice spacing and $|\nu| > 2$, cf. Figs. 1 e) and f). The large deviations for smaller indices result from the non-uniform continuum limit of the smallest eigenvalues. The

former zero modes help to push the spectrum away from the origin. This is the reason why the approximation by the GOE and continuum QCD without zero modes is very accurate for larger indices.

The thermodynamic limit of the chiral condensate (B18) can be easily taken via the Eqs. (90) and (82) yielding

$$\langle \bar{\psi}\psi \rangle_{N_f=0} = \Sigma \left(\frac{m}{8a^2} \right) \approx \begin{cases} \frac{m}{4a^2}, & |m| < 8a^2 \\ 2\text{sign } m \mathbf{1}_4, & |m| > 8a^2. \end{cases} \quad (109)$$

This limit is already visible for a lattice spacing $\sqrt{VW_8}\tilde{a} = a \approx 1$. Moreover, it is exactly the same result (97) as obtained for dynamical quarks.

D. The Distribution of Chirality over the Real Eigenvalues

Also the distribution of the chiralities over the real eigenvalues

$$\rho_\chi(m, a) = - \frac{1}{\pi} \partial_m \text{Im} Z_\nu(\widehat{M}, \widehat{X}, a) \Big|_{\substack{\widehat{M}=m\mathbf{1}_4 \\ \widehat{X}=(\lambda+i\varepsilon)\mathbf{1}_4 \rightarrow \lambda\mathbf{1}_4}} \quad (110)$$

can be written as a sum of products of a compact integral and a non-compact twofold integral (see Eq. (B19) of B4). Comparisons with Monte Carlo simulations of the random matrix model (69) are shown in Fig. 9.

In the limit $a \rightarrow 0$ the chirality distribution, $\rho_\chi(\lambda)$ becomes the level density ρ_{GOE} of a ν -dimensional GOE which, for $\nu = 1$, is a Gaussian, see Eqs. (C33), (C34) and (C35). We compared this behavior of ρ_χ with ρ_{GOE} and $\rho_5(\lambda = 0)$ in Fig. 1.a) at a lattice spacing $\sqrt{VW_8}\tilde{a} = a = 0.0625$. The agreement is almost perfect. An interesting distinction from the case of three color QCD, where the distribution of the chiralities over the Dirac spectrum in the continuum limit also agrees with a finite dimensional Gaussian random matrix model, is that the peaks corresponding to the zero modes are only barely visible humps. As in the case of three color QCD the number of these humps is equal to ν . However they merge with the main peak at the origin due to the very weak level repulsion. This becomes apparent when comparing Figs. 1.a) and 9 with Fig. 1 of [14].

The thermodynamic limit of ρ_χ follows from the first equality of Eq. (90). The supermatrix $V + V^{-1}$ is real at the saddle point (82) such that the second term in Eq. (90) vanishes. Hence the first term is the leading one. The derivative in the mass yields an inverse square root behavior,

$$\rho_\chi(m) \approx \frac{\nu}{\pi} \frac{\Theta(8a^2 - |m|)}{\sqrt{(8a^2)^2 - m^2}}. \quad (111)$$

Therefore, ρ_χ of two color QCD exhibits the same square root singularities at the boundary of the support as in the case of three color QCD, see [20]. We observe this asymptotic behavior in Monte Carlo simulations where it is starting to build up, cf. Fig. 9, and in the numerical evaluation for even larger lattice spacings $a = 1$ shown in Fig. 2.c).

E. Level Density of the Real Modes of D_W

Since the analytical derivation of ρ_{real} for $\beta = 2$ was a *tour de force* [16, 20], it is not surprising that we did not succeed to find an analytical result for the density of the real eigenvalues of the non-Hermitian Wilson Dirac operator D_W for two color QCD with $\beta = 1$. Nonetheless we can extract some information via the inequality (25) and thus via the distributions $\rho_5(m, \lambda = 0)$ and $\rho_\chi(\lambda)$.

For small level spacing $|a| \ll 1$ the distributions $\rho_5(m, \lambda = 0)$ and $\rho_\chi(\lambda)$ are well approximated by the density ρ_{GOE} of the finite dimensional GOE, see Fig. 1.a). Therefore also the level density of the real eigenvalues has to be $\rho_{\text{real}} \approx \rho_{\text{GOE}}$ for $|a| \ll 1$. This is indeed the case already for the lattice spacing $\sqrt{VW_8}\tilde{a} = a \approx 0.1$, see Fig. 9. Surprisingly the distribution of the chiralities over the Dirac spectrum agrees quite well with ρ_{real} even for $\sqrt{VW_8}\tilde{a} = a \approx 0.25$ when the index is $\nu > 2$. Since the integral of the difference $\rho_{\text{real}} - \rho_\chi$ is equal to the average number of additional real modes N_{add} we deduce that this number is highly suppressed for configurations with a larger index ν at small lattice spacing. For the Wilson Dirac operator of three color QCD the average number N_{add} is of order $\mathcal{O}(a^{2\nu+1})$, see [20]. The reason is that the probability of finding an additional real eigenvalue is proportional to

$$\prod_{\lambda \in \mathbb{R}} (\lambda - \lambda_k)^{\beta_D}, \quad (112)$$

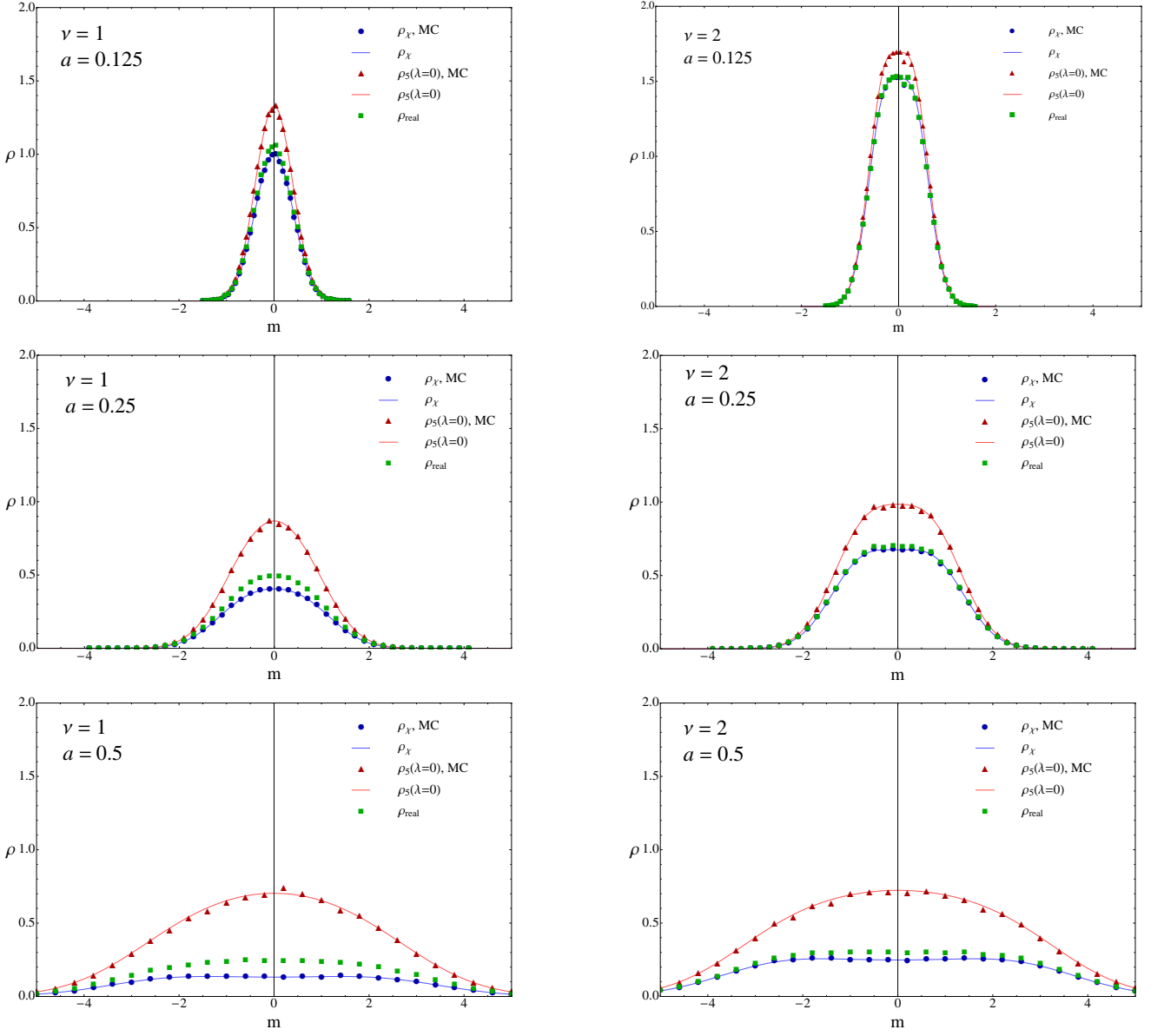


FIG. 9. Comparison of the analytical results (B17) (red solid curves) and (B19) (blue solid curves) of the mass dependence of the level density $\rho_5(\lambda = 0)$ at the origin and the distribution of chirality over the real eigenvalues, respectively, with Monte Carlo simulations of the random matrix model (69) (MC, symbols). We have generated an ensemble of 10^5 matrices both for index $\nu = 1$ (left plots) and index $\nu = 2$ (right plots) at lattice spacings $\sqrt{V}\overline{W}_3\tilde{a} = a = 0.125, 0.25, 0.5$. We have also calculated the distribution of the real eigenvalues ρ_{real} of the non-Hermitian Wilson Dirac operator D_W (green symbols). As correctly predicted by the inequality (25) the level density ρ_{real} lies always in between ρ_χ and $\rho_5(\lambda = 0)$. Interestingly, for small lattice spacings, the level density is better approximated by ρ_χ than by $\rho_5(\lambda = 0)$ for small lattice spacings. Moreover, we notice a significant difference between the integral of the three distributions for large lattice spacings while their support remains the same.

where the real eigenvalues λ_k are of order a . In the present two color case we expect that N_{add} is of order $\mathcal{O}(a^{\nu+1})$ because of the smaller level repulsion. Our expectation is confirmed by Monte-Carlo simulations of the random matrix model (69), see Fig. 10.

In the thermodynamic limit the height of ρ_{real} has to lie between the square root singularity of ρ_χ on the scale $\mathcal{O}(a^{-2})$ and the semi-circle of $\rho_5(\lambda = 0)$ on the scale $\mathcal{O}(1)$. From the simulations shown in Fig. 9 we notice some kind of flattening of ρ_{real} and a departure from ρ_χ for larger values of a . Moreover, the average number of additional real modes extracted from Monte Carlo simulations, see Fig. 10, suggest a ν independent behavior where $N_{\text{add}} \propto a$. Since also the distribution of the real eigenvalues lives on the support $[-8a^2, 8a^2]$, we conjecture that ρ_{real} becomes a

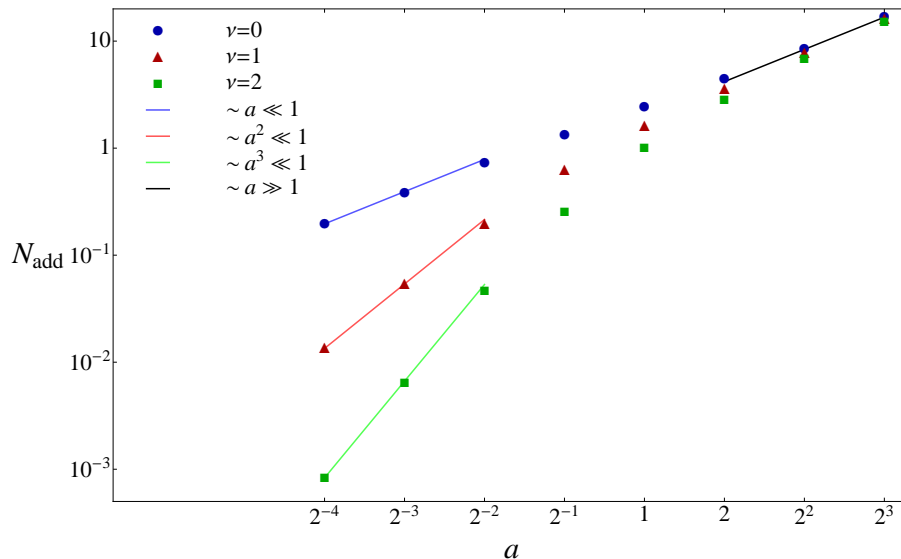


FIG. 10. Log-log plot of the dependence of the average number of additional real modes on the lattice spacing a . The Monte Carlo simulations (symbols) of the random matrix model (69) for index $\nu = 0, 1, 2$ were fitted by the behavior $\propto a^\nu$ for small lattice spacing (colored lines) and $\propto a$ for large lattice spacing (black line), separately. We generated random matrices for various matrix dimensions and ensemble sizes to keep the statistical and systematic error below 2%. The transition region, $\sqrt{VW_8}\tilde{a} = a = 0.25 - 2$, for the scaling behavior is excluded from the fits.

constant flat plateau on this interval with a height of order $\mathcal{O}(a^{-1})$ in the thermodynamic limit. Interestingly this is exactly same behavior as in three color QCD, cf. [20].

VI. CONCLUSIONS

We have computed and analyzed the microscopic spectrum of the Wilson Dirac operator for QCD with two colors and the quarks in the fundamental representation. The discretization effects are very similar to the three color case. Especially in the thermodynamic limit, $|VW_8\tilde{a}^2| = |a|^2 \propto |V\Sigma\tilde{m}| = |m| \propto |V\Sigma\lambda| \gg 1$, they are essentially the same. When the quark mass is large enough, $|m| > 8a^2$, the microscopic spectrum of the Hermitian Wilson Dirac operator D_5 develops a symmetric gap around the origin of a width $[|m|^{2/3} - (8a^2)^{2/3}]^{3/2}$. The system enters the Aoki phase when the gap closes, or in terms of the eigenvalues of the non-Hermitian Dirac operator D_W , when the mass $|m|$ hits the strip of eigenvalues. In this phase, parity is broken spontaneously with a non-vanishing pion condensate that is proportional to the eigenvalue density of D_5 at the origin. In the thermodynamic limit, the support of the distribution of chirality over the real eigenvalues of D_W as well as the support of the level density of the real eigenvalues is of the order a^2 while the number of the additional real modes increases linearly in a .

In the continuum limit $|a| \ll 1$ the scaling behavior is crucially different. Then the spectrum can be approximated by the microscopic spectrum of the continuum Dirac operator without zero modes plus the spectrum of a finite dimensional GOE. The GOE describes the broadening of the former zero modes which scale like a in the continuum limit and stands in contrast to the thermodynamic limit. Moreover, we have on average $a^{\nu+1}$ additional real modes. Hence additional real modes are strongly suppressed for larger topological indices ν as is the case for QCD with three colors. However the suppression is much weaker than for three color QCD. The reason is the weaker level repulsion which is linear for the two color case. This repulsion is also the reason why no separate peaks are visible.

Surprisingly the continuum limit is not uniform for the microscopic level density ρ_5 of D_5 at the origin. In the continuum we would expect $\rho_5(m=0, \lambda \rightarrow 0, a=0) = 1$. However the continuum limit yields $\rho_5(m=0, \lambda=0, a \rightarrow 0) = 1/\sqrt{2}$. This shows that one has to be careful when considering observables which essentially depend on the eigenvalue nearest to the origin for configurations with $\nu = 0$ and also $\nu = 1, 2$ if the quark mass is non-zero. The mass dependent chiral condensate of the quenched theory confirms this statement. It can be quite accurately approximated with continuum QCD without zero modes and the finite dimensional GOE for larger values of the index, while it has the strongest deviations for small topological indices. The ν zero modes broadened along the real axis push the spectrum away from the quark mass m which is the point where the limit is non-uniform.

As is the case for QCD with three colors, we have also found that the low energy constant W_8 has to be positive. The reason is that the chiral partition function with an even number of dynamical quarks is not positive definite if $W_8 < 0$. Effects from the low energy constants W_6 and W_7 were not considered in the present work. They may weaken this conclusion, though we would not expect this due to the analogy with the case of three color QCD.

Technically the two color case is much more complicated than the three color QCD. Particularly, there are no analytical results for the spectral density of D_W . At least for small lattice spacings the density of the real eigenvalues is tightly constrained by the distribution of the chirality over the real eigenvalues of D_W and by the mass dependence of ρ_5 at the origin. It is not clear if it is at all possible to derive analytical expressions for the microscopic spectral density of D_W . For the three color case our derivation relied heavily on the existence of an Itzykson-Zuber integral over a non-compact group. Such an integral is not available for two color QCD. But there is another way to deduce some results for the real eigenvalues of D_W in two color QCD. We expect that the results of three color QCD should also apply to the two color case. Mean field results generally do not depend on the Dyson index β_D . Indeed we have seen that apart from factors of 2 for continuum QCD. This is sometimes referred to as orbifolding [67].

Let us summarize. Our results provide an analytical control of the smallest eigenvalues of the Dirac operator which can potentially compromise numerical simulations. It is noteworthy that the absence of level repulsion from the origin for the case of $N_c = 2$ QCD makes this effect much more pronounced than in the case of $N_c = 3$ QCD.

ACKNOWLEDGMENTS

We thank Gernot Akemann and Kim Splittorff for helpful comments. MK and SZ are financially supported by the Alexander-von-Humboldt Foundation. JV and SZ are supported by U.S. DOE Grant No. DE-FG-88ER40388 and MK is also partially financially supported by the CRC 701: *Spectral Structures and Topological Methods in Mathematics* of the Deutsche Forschungsgemeinschaft.

Appendix A: Some Properties of Bessel Functions

In this section we recall some properties of Bessel functions which play a crucial role in the spectral statistics of chiral perturbation theory of QCD. More information on Bessel functions can be found in [68].

Especially, we need the Bessel function of the first kind,

$$J_\mu(x) = \int_{-\pi}^{\pi} \frac{d\varphi}{2\pi} \exp[-ix \sin \varphi] e^{i\mu\varphi}, \text{ for } \mu \in \mathbb{Z} \text{ and } x \in \mathbb{C}, \quad (\text{A1})$$

the modified Bessel function of the first kind

$$I_\mu(x) = \int_{-\pi}^{\pi} \frac{d\varphi}{2\pi} \exp[x \cos \varphi] e^{i\mu\varphi}, \text{ for } \mu \in \mathbb{Z} \text{ and } x \in \mathbb{C}, \quad (\text{A2})$$

and the modified Bessel function of the second kind

$$K_\mu(x) = \frac{1}{2} \int_{-\infty}^{\infty} dt \exp[-x \cosh t] e^{-\mu t}, \text{ for } \mu, x \in \mathbb{C} \text{ and } \text{Re } x > 0. \quad (\text{A3})$$

The Bessel function K_μ is particularly important because of the integral

$$\frac{1}{2} \int_{-\infty}^{\infty} dt \exp[-2(\varepsilon - iLx) \cosh t + 2iLy \sinh t] e^{-\mu t} = \left| \frac{x+y}{x-y} \right|^{\mu/2} e^{i\mu\phi_-} K_\mu(\sqrt{|y^2 - x^2|} e^{i\phi_+}) \quad (\text{A4})$$

with the two angles

$$\phi_{\pm} = -L \frac{\pi}{4} (\text{sign}(x+y) \pm \text{sign}(x-y)). \quad (\text{A5})$$

We have assumed that $\varepsilon > 0$ is infinitesimally small, $L = \pm 1$ and x and y are real. The right hand side of Eq. (A4) can be obtained by the complex shift $t \rightarrow t + \ln|(x-t)/(x+t)|/2 - i\phi_-$. The angles satisfy the relations

$$\phi_+ = -L \frac{\pi}{2} \text{sign}(x) \Theta(x^2 - y^2) \quad \text{and} \quad e^{i(\phi_- - \phi_+)} = iL \text{sign}(x-y). \quad (\text{A6})$$

This results in the very useful identity

$$\frac{(iL)^\mu}{2} \int_{-\infty}^{\infty} dt \exp[-2(\varepsilon - iLx) \cosh t + 2iLy \sinh t] e^{-\mu t} = \frac{1}{(y-x-iL\varepsilon)^\mu} \left(\sqrt{|y^2-x^2|} e^{i\phi_+} \right)^\mu K_\mu(\sqrt{|y^2-x^2|} e^{i\phi_+}). \quad (\text{A7})$$

All Bessel functions satisfy a symmetry regarding the transformation $\mu \rightarrow -\mu$,

$$J_{-\mu}(x) = J_\mu(-x) = (-1)^\mu J_\mu(x), \quad I_{-\mu}(x) = I_\mu(x), \quad \text{and} \quad K_\mu(x) = K_{-\mu}(x). \quad (\text{A8})$$

Except for the Bessel function K_μ this relation is only valid for integer μ .

The functions J_μ and I_μ have a particular simple representation as an absolutely convergent series which extends its index to general $\mu \in \mathbb{C}$,

$$J_\mu(x) = \sum_{j=0}^{\infty} \frac{(-1)^j}{j! \Gamma(\mu + j + 1)} \left(\frac{x}{2}\right)^{2j+\mu} \quad \text{and} \quad I_\mu(x) = \sum_{j=0}^{\infty} \frac{1}{j! \Gamma(\mu + j + 1)} \left(\frac{x}{2}\right)^{2j+\mu}. \quad (\text{A9})$$

These series representations make it obvious that the two Bessel functions J_μ and I_μ are related by

$$J_\mu(x) = e^{-i\mu\pi/2} I_\mu(e^{i\pi/2}x). \quad (\text{A10})$$

Also the Bessel function K_μ is related to the other two Bessel functions. This relation is based on a representation of the Bessel functions as Meijer G-functions [68] which are given by contour integrals,

$$x^\mu J_\mu(2x) = \int_{\mathcal{C}} \frac{ds}{2\pi i} \frac{\Gamma[\mu-s]}{\Gamma[1+s]} x^{2s} \quad (\text{A11})$$

and

$$x^\mu K_\mu(2x) = \frac{1}{2} \int_{\mathcal{C}} \frac{ds}{2\pi i} \Gamma[\mu-s] \Gamma[-s] x^{2s}. \quad (\text{A12})$$

The contour \mathcal{C} encircles the positive real axis clockwise and thus all poles of the Gamma functions. When choosing $x = e^{i\pi n/2} x'$ imaginary ($n = \pm 1$ and $x' > 0$, cf. Eq. (A7)) we can take the imaginary part of Eq. (A12) and obtain

$$\begin{aligned} \text{Im} \left[e^{i\pi n\mu/2} x'^\mu K_\mu(2e^{i\pi n/2} x') \right] &= \frac{1}{2} \text{Im} \int_{\mathcal{C}} \frac{ds}{2\pi i} \Gamma[\mu-s] \Gamma[-s] e^{i\pi n s} x'^{2s} \\ &= \frac{1}{2} \text{Im} \int_{\mathcal{C}} \frac{ds}{2\pi i} \frac{\Gamma[\mu-s]}{\Gamma[1+s]} \frac{\pi}{\sin(-\pi s)} e^{i\pi n s} x'^{2s} \\ &= -n \frac{\pi}{2} \int_{\mathcal{C}} \frac{ds}{2\pi i} \frac{\Gamma[\mu-s]}{\Gamma[1+s]} x'^{2s} \\ &= -n \frac{\pi}{2} x'^\mu J_\mu(2x'). \end{aligned} \quad (\text{A13})$$

We have used the reflection formula of the Gamma function $\Gamma[z]\Gamma[1-z] = \pi/\sin \pi z$. Since the integral is equal to a sum over the residues at the poles of the Gamma functions which are real, the imaginary part is obtained by replacing $\exp[i\pi n s] \rightarrow \sin \pi n s = n \sin \pi s$.

One can also understand the relation (A13) from the logarithmic cut along the imaginary axis of K_μ which follows from the series expansion

$$\begin{aligned} K_\mu(z) &= \frac{1}{2} \left(\frac{2}{z}\right)^\mu \sum_{k=0}^{\mu-1} \frac{(\mu-k-1)!}{k!} \left(-\frac{z^2}{4}\right)^k + (-1)^{\mu+1} \ln\left(\frac{z}{2}\right) I_\mu(z) \\ &\quad + \frac{(-1)^\mu}{2} \left(\frac{z}{2}\right)^\mu \sum_{k=0}^{\infty} \frac{\psi(k+1) + \psi(\mu+k+1)}{k!(\mu+k)!} \left(\frac{z^2}{4}\right)^k, \end{aligned} \quad (\text{A14})$$

where $\psi(k) = \partial_k \ln \Gamma(k)$ is the Digamma function, meaning the logarithmic derivative of the Gamma function. This series can indeed be calculated by taking the residues of the contour integral (A12).

Another relation which is less known but essential to derive results for two color QCD is based on an integral over the Bessel functions K_μ and J_μ . In particular we consider the imaginary part of the integral

$$S'_{\mu,\alpha}(x) = x^\mu \int_1^\infty dy y^\alpha K_\mu(2xy) \quad (\text{A15})$$

with $\mu, \alpha \in \mathbb{R}_+$, $x \in \mathbb{C}$, and $\text{Re } x > 0$. By introducing an auxiliary Gaussian $e^{-\epsilon y^2}$ in the integrand we can extend the definition to purely imaginary $x = e^{i\pi n/2} x'$ ($n = \pm 1$ and $x' > 0$) and ensure that the integral over y is always absolutely convergent. Then we can perform the following calculation

$$\begin{aligned} \text{Im } S'_{\mu, \alpha} \left(e^{i\pi n/2} x' \right) &= \lim_{\epsilon \rightarrow 0} \int_1^\infty dy y^{\alpha - \mu} e^{-\epsilon y^2} \text{Im} \left[\left(e^{i\pi n/2} x' y \right)^\mu K_\mu \left(2e^{i\pi n/2} x' y \right) \right] \\ &\stackrel{\text{Eq. (A13)}}{=} -n \frac{\pi}{2} x'^\mu \lim_{\epsilon \rightarrow 0} \left(\int_0^\infty - \int_0^1 \right) dy y^\alpha e^{-\epsilon y^2} J_\mu (2x' y) \\ &= n \frac{\pi}{2} x'^\mu \int_0^1 dy y^\alpha J_\mu (2x' y) - n \frac{\pi}{4} \frac{\Gamma[(\mu + \alpha + 1)/2]}{\Gamma[\mu + 1]} \lim_{\epsilon \rightarrow 0} \frac{x'^{2\mu}}{\epsilon^{(\mu + \alpha + 1)/2}} {}_1F_1 \left(\frac{\mu + \alpha + 1}{2}; \mu + 1; -\frac{x'^2}{\epsilon} \right). \end{aligned} \quad (\text{A16})$$

The function ${}_1F_1$ is the hypergeometric function,

$${}_1F_1 \left(\frac{\mu + \alpha + 1}{2}; \mu + 1; -\frac{x'^2}{\epsilon} \right) = \sum_{j=0}^{\infty} \frac{\Gamma[j + (\mu + \alpha + 1)/2] \Gamma[\mu + 1]}{j! \Gamma[(\mu + \alpha + 1)/2] \Gamma[\mu + j + 1]} \left(-\frac{x'^2}{\epsilon} \right)^j. \quad (\text{A17})$$

The limit $\epsilon \rightarrow 0$ can be performed by rewriting the Gamma functions as an integral where the limit is trivial,

$$\begin{aligned} &\frac{\pi}{4} \frac{\Gamma[(\mu + \alpha + 1)/2]}{\Gamma[\mu + 1]} \lim_{\epsilon \rightarrow 0} \frac{x'^{2\mu}}{\epsilon^{(\mu + \alpha + 1)/2}} {}_1F_1 \left(\frac{\mu + \alpha + 1}{2}; \mu + 1; -\frac{x'^2}{\epsilon} \right) \\ &= \frac{\pi}{4} \frac{1}{\Gamma[(\mu - \alpha + 1)/2]} \lim_{\epsilon \rightarrow 0} \frac{x'^{2\mu}}{\epsilon^{(\mu + \alpha + 1)/2}} \int_0^1 dt t^{(\mu + \alpha - 1)/2} (1 - t)^{(\mu - \alpha - 1)/2} \exp \left[-\frac{x'^2}{\epsilon} t \right] \\ &= \frac{\pi}{4} \frac{\Gamma[(\mu + \alpha + 1)/2]}{\Gamma[(\mu - \alpha + 1)/2]} x'^{\mu - \alpha - 1}. \end{aligned} \quad (\text{A18})$$

The intermediate step is only true for $\mu - \alpha > -1$. However one can analytically extend this identity to arbitrary μ and α since both expressions are analytical in the combination $\mu - \alpha$. They are also bounded by the analytic function $x'^{\mu - \alpha} / \Gamma[(\mu - \alpha)/2]$ on the positive complex half-plane $\text{Re}(\mu - \alpha) > 1$. Hence Carlson's theorem, see [61], can be applied which allows such a unique analytic continuation.

Summarizing this calculation we have

$$\text{Im} \left[\left(e^{i\pi n/2} x' \right)^\mu \int_1^\infty dy y^\alpha K_\mu \left(2e^{i\pi n/2} x' y \right) \right] = n \frac{\pi}{2} x'^\mu \int_0^1 dy y^\alpha J_\mu (2x' y) - n \frac{\pi}{4} \frac{\Gamma[(\mu + \alpha + 1)/2]}{\Gamma[(\mu - \alpha + 1)/2]} x'^{\mu - \alpha - 1}. \quad (\text{A19})$$

It becomes important to find the well-known results of continuum QCD from our calculations.

Appendix B: Evaluation of the Partition Function

The quenched partition function (55), in particular its imaginary part, plays a crucial role in the spectral statistics of the Wilson Dirac operator. Since its evaluation is cumbersome we split the calculation in the integration over the four Grassmann variables ($\alpha, \alpha^*, \beta, \beta^*$), see subsection B1, and in the explicit calculation of the imaginary part in subsection B3. In subsection B2 we present some properties of the integrals involved. The explicit expressions for the spectral observables are summarized in subsection B4.

1. Integration over the Grassmann Variables

We evaluate the Grassmann integrals of the supersymmetric partition function (55) using the representation of U given in Eq. (56). To calculate the inverse of U and its traces thereof we split U into a numerical part U_0 which is a diagonal matrix and a nilpotent part G ,

$$U = \begin{pmatrix} e^{i\varphi} & 0 & \alpha^* & \beta^* \\ 0 & e^{i\varphi} & -\alpha & -\beta \\ \alpha & \alpha^* & e^{s_1} & 0 \\ \beta & \beta^* & 0 & e^{s_2} \end{pmatrix} = U_0 + G. \quad (\text{B1})$$

For this purpose it is suitable to know what the square of G is,

$$G^2 = \begin{pmatrix} (\alpha^* \alpha + \beta^* \beta) \mathbf{1}_2 & 0 & 0 \\ 0 & 2\alpha\alpha^* & \alpha\beta^* + \beta\alpha^* \\ 0 & \alpha\beta^* + \beta\alpha^* & 2\beta\beta^* \end{pmatrix}. \quad (\text{B2})$$

Additionally we need

$$\begin{aligned} (U_0^{-1}G)^2 &= \begin{pmatrix} (e^{-i\varphi-s_1}\alpha^*\alpha + e^{-i\varphi-s_2}\beta^*\beta)\mathbf{1}_2 & 0 & 0 \\ 0 & 2e^{-i\varphi-s_1}\alpha\alpha^* & e^{-i\varphi-s_1}(\alpha\beta^* + \beta\alpha^*) \\ 0 & e^{-i\varphi-s_2}(\alpha\beta^* + \beta\alpha^*) & 2e^{-i\varphi-s_2}\beta\beta^* \end{pmatrix}, \\ (U_0^{-1}GU_0^{-1})^2 &= \begin{pmatrix} (e^{-2i\varphi-2s_1}\alpha^*\alpha + e^{-2i\varphi-2s_2}\beta^*\beta)\mathbf{1}_2 & 0 & 0 \\ 0 & 2e^{-2i\varphi-2s_1}\alpha\alpha^* & e^{-2i\varphi-s_1-s_2}(\alpha\beta^* + \beta\alpha^*) \\ 0 & e^{-2i\varphi-s_1-s_2}(\alpha\beta^* + \beta\alpha^*) & 2e^{-2i\varphi-2s_2}\beta\beta^* \end{pmatrix}, \\ (U_0^{-1}G)^4 &= 2e^{-2i\varphi-s_1-s_2} \text{diag}(\mathbf{1}_2, -\mathbf{1}_2)\alpha^*\alpha\beta^*\beta, \\ (U_0^{-1}GU_0^{-1})^2(U_0^{-1}G)^2 &= e^{-3i\varphi-s_1-s_2} \text{diag}([e^{-s_1} + e^{-s_2}]\mathbf{1}_2, -2e^{-s_1}, -2e^{-s_2})\alpha^*\alpha\beta^*\beta, \\ [(U_0^{-1}G)^2U_0^{-1}]^2 &= 2e^{-2i\varphi-s_1-s_2} \text{diag}(e^{-2i\varphi}\mathbf{1}_2, -e^{-s_1-s_2}\mathbf{1}_2)\alpha^*\alpha\beta^*\beta. \end{aligned} \quad (\text{B3})$$

The inverse of U is given by a finite geometric sum

$$U^{-1} = [1 - U_0^{-1}G + (U_0^{-1}G)^2 - (U_0^{-1}G)^3 + (U_0^{-1}G)^4] U_0^{-1}. \quad (\text{B4})$$

Now we are ready to compute the traces.

Only even powers of the Grassmann variables and, thus, even powers of G contribute to the traces,

$$\begin{aligned} \text{Str}(\widehat{M} + \widehat{X})U &= \text{Str}(\widehat{M} + \widehat{X})U_0 \\ &= 2(m + x_0)e^{i\varphi} - (m' + x_1)(e^{s_1} + e^{s_2}), \\ \text{Str}(\widehat{M} - \widehat{X})U^{-1} &= \text{Str}(\widehat{M} - \widehat{X})(U_0^{-1} + (U_0^{-1}G)^2U_0^{-1} + (U_0^{-1}G)^4U_0^{-1}) \\ &= 2(m - x_0)e^{-i\varphi} - (m' - x_1)(e^{-s_1} + e^{-s_2}) + 2[(m - x_0)e^{-2i\varphi-s_1} + (m - x_1)e^{-i\varphi-2s_1}]\alpha^*\alpha \\ &\quad + 2[(m - x_0)e^{-2i\varphi-s_2} + (m - x_1)e^{-i\varphi-2s_2}]\beta^*\beta \\ &\quad + 2[2(m - x_0)e^{-i\varphi} + (m' - x_1)(e^{-s_1} + e^{-s_2})]e^{-2i\varphi-s_1-s_2}\alpha^*\alpha\beta^*\beta, \\ \text{Str}U^2 &= \text{Str}(U_0^2 + G^2) \\ &= 2e^{2i\varphi} - e^{2s_1} - e^{2s_2} + 4(\alpha^*\alpha + \beta^*\beta), \\ \text{Str}U^{-2} &= \text{Str}U_0^{-2} + \text{Str}(U_0^{-1}GU_0^{-1})^2 + 2\text{Str}U_0^{-2}(U_0^{-1}G)^2 + \text{Str}[(U_0^{-1}G)^2U_0^{-1}]^2 \\ &\quad + 2\text{Str}(U_0^{-1}GU_0^{-1})^2(U_0^{-1}G)^2 + 2\text{Str}U_0^{-2}(U_0^{-1}G)^4 \\ &= 2e^{-2i\varphi} - e^{-2s_1} - e^{-2s_2} \\ &\quad + 4(e^{-2i\varphi} + e^{-i\varphi-s_1} + e^{-2s_1})^2e^{-i\varphi-s_1}\alpha^*\alpha + 4(e^{-2i\varphi} + e^{-i\varphi-s_2} + e^{-2s_2})e^{-i\varphi-s_2}\beta^*\beta \\ &\quad + 4[3 + e^{-2i\varphi} + e^{-s_1-s_2} + 2e^{-i\varphi-s_1} + 2e^{-i\varphi-s_2} + e^{-2s_1} + e^{-2s_2}]e^{-2i\varphi-s_1-s_2}\alpha^*\alpha\beta^*\beta. \end{aligned} \quad (\text{B5})$$

We also need the $\text{Sdet}^{(\nu+1)/2}U$ which can be expanded as

$$\text{Sdet}^{(\nu+1)/2}U = e^{(\nu+1)(i\varphi-(s_1+s_2)/2)} [1 - (\nu+1)(e^{-i\varphi-s_1}\alpha^*\alpha + e^{-i\varphi-s_2}\beta^*\beta) + \nu(\nu+1)e^{-2i\varphi-s_1-s_2}\alpha^*\alpha\beta^*\beta]. \quad (\text{B6})$$

Collecting everything we can integrate over the Grassmann variables which only selects the highest order polynomial in those. To keep the notation simple we define the following abbreviations

$$\begin{aligned} t_{z1} &= iLe^{-i\varphi-s_1}[(m-x_0)e^{-i\varphi} + (m'-x_1)e^{-s_1}], \\ t_{z2} &= iLe^{-i\varphi-s_2}[(m-x_0)e^{-i\varphi} + (m'-x_1)e^{-s_2}], \\ t_{z12} &= iLe^{-i\varphi-s_1-s_2}[2(m-x_0)e^{-i\varphi} + (m'-x_1)(e^{-s_1} + e^{-s_2})], \\ d_1 &= (\nu+1)e^{-i\varphi-s_1}, \\ d_2 &= (\nu+1)e^{-i\varphi-s_2}, \\ d_{12} &= \nu(\nu+1)e^{-2i\varphi-s_1-s_2}, \\ t_{a1} &= 4a^2[1 + e^{-i\varphi-s_1}(e^{-2i\varphi} + e^{-2s_1} + e^{-i\varphi-s_1})], \\ t_{a2} &= 4a^2[1 + e^{-i\varphi-s_2}(e^{-2i\varphi} + e^{-2s_2} + e^{-i\varphi-s_2})], \\ t_{a12} &= 4a^2e^{-i2\varphi-s_1-s_2}(3e^{-2i\varphi} + e^{-s_1-s_2} + e^{-2s_1} + e^{-2s_2} + 2e^{-i\varphi-s_1} + 2e^{-i\varphi-s_2}). \end{aligned} \quad (\text{B7})$$

The final result for the generating function is up to an overall constant

$$\begin{aligned}
Z \propto & \int_{-\pi}^{\pi} \frac{d\varphi}{2\pi} \int_{-\infty}^{\infty} ds_1 \int_{-\infty}^{\infty} ds_2 \left| \sinh \frac{s_1 - s_2}{2} \right| e^{(\nu+2)i\varphi - (\nu-2)(s_1+s_2)/2} \exp [2Lm \sin \varphi + iLm'(\sinh s_1 + \sinh s_2)] \\
& \times \exp [-2iLx_0 \cos \varphi + iLx_1(\cosh s_1 + \cosh s_2) + 4a^2 \cos 2\varphi - 2a^2(\cosh 2s_1 + \cosh 2s_2)] \\
& \times [(d_1 - t_{z1} - t_{a1})(d_2 - t_{z2} - t_{a2}) + d_{12} - d_1 d_2 + t_{z12} + t_{a12}].
\end{aligned} \tag{B8}$$

This expression is explicitly shown in Eq. (63) which immediately makes clear that the integral splits into a finite sum and each term factorizes into a compact one-fold integral and a coupled, non-compact two-fold integral.

2. Properties of the Functions $S_{\mu,\alpha}$ and Φ_{μ}

In this appendix we discuss properties of the integrals $S_{\mu,\alpha}$ and Φ_{μ} which were introduced in Eqs. (65) and (64). Their properties are in particular useful for the numerical evaluation of the integrals.

The integrals (64) and (65) satisfy the following recurrence relations

$$\begin{aligned}
0 &= \mu\Phi_{\mu} + (x_0 + m)\Phi_{\mu+1} + (x_0 - m)\Phi_{\mu-1} - 4a^2\Phi_{\mu+2} + 4a^2\Phi_{\mu-2}, \\
0 &= \mu S_{\mu,\alpha} + (x_1 + m')S_{\mu-1,\alpha+1} + (x_1 - m')S_{\mu+1,\alpha+1} - 4a^2(2S_{\mu-2,\alpha+2} - 2S_{\mu+2,\alpha+2} - S_{\mu-2,\alpha} + S_{\mu+2,\alpha}).
\end{aligned} \tag{B9}$$

These relations can be found by acting ∂_{φ} and $(\partial_{s_1} + \partial_{s_2})$ onto the integrands which vanish under the integrals. They are useful to check the quality of the numerical evaluation of the integrals (64) and (65).

Two other useful relations of $S_{\mu,\alpha}$ concern the derivatives which are important to calculate the observables introduced in subsection II B. The derivatives with respect to the quark mass m' and the axial mass x_1 are given by

$$\partial_{m'} S_{\mu,\alpha} = -S_{\mu+1,\alpha+1} - S_{\mu-1,\alpha+1}, \quad \partial_{x_1} S_{\mu,\alpha} = S_{\mu+1,\alpha+1} - S_{\mu-1,\alpha+1}. \tag{B10}$$

Moreover, there are also relations between a negative and positive index μ ,

$$\Phi_{\mu}(m, x_0, a) = (-1)^{\mu} \Phi_{-\mu}(-m, x_0, a) \quad \text{and} \quad S_{\mu,\alpha}(m', x_1, a) = (-1)^{\mu} S_{-\mu,\alpha}(-m', x_1, a). \tag{B11}$$

These relations are helpful when computing these integrals.

3. Real and Imaginary Part of $S_{\mu,\alpha}$

We assume $\mu \geq 0$ because of the relation (B11). This simplifies the computation of the imaginary part of the integral (65). This integral can first of all be written in a more suitable version. For this purpose we introduce a Gaussian integral over an auxiliary variable t to linearize the term $\cosh 2s = 2\sinh^2 s + 1$ to a $\sinh s$ term,

$$\begin{aligned}
S_{\mu,\alpha}(m', x_1, a) &= \frac{(iL)^{\mu}}{\sqrt{8\pi a^2}} \int_{-\infty}^{\infty} ds \int_1^{\infty} dy \int_{-\infty}^{\infty} dt e^{-\mu s} \frac{y^{\alpha+1}}{\sqrt{2y^2 - 1}} \\
&\times \exp \left[-\frac{y^2}{8a^2(2y^2 - 1)}(t - m')^2 + 2iLty \sinh s + 2iLx_1y \cosh s - 4a^2(2y^2 - 1) \right].
\end{aligned} \tag{B12}$$

Hence the variable t acts as an effective quark mass. The integral over s is equal to a modified Bessel function of the second kind,

$$\begin{aligned}
S_{\mu,\alpha}(m', x_1, a) &= \frac{1}{\sqrt{2\pi a^2}} \int_1^{\infty} dy \int_{-\infty}^{\infty} dt \frac{y^{\alpha+1}}{\sqrt{2y^2 - 1}} \frac{1}{(t - x_1)^{\mu}} \left(\sqrt{|t^2 - x_1^2|} e^{i\phi} \right)^{\mu} \\
&\times \exp \left[-\frac{y^2}{8a^2(2y^2 - 1)}(t - m')^2 - 4a^2(2y^2 - 1) \right] K_{\mu} \left(2y\sqrt{|t^2 - x_1^2|} e^{i\phi} \right)
\end{aligned} \tag{B13}$$

with $\phi = -L\text{sign}(x_1)\Theta(x_1^2 - t^2)\pi/2$. The phase is important and reflects the transformation (only a complex shift in the variable s) to bring the integral into the form (A3).

The imaginary part of this integral consists of two contributions. The imaginary part has to be taken either of the term $1/(t-x_1)^\mu$ which results in the $(\mu-1)$ st derivative of the Dirac delta function, $\delta^{(\mu-1)}(t-x_1)$, or of the term $(\sqrt{|t^2-x_1^2|}e^{i\phi})^\mu K_\mu(2y\sqrt{|t^2-x_1^2|}e^{i\phi})$ which can be dealt by relation (A13). Thus, we find,

$$\begin{aligned} \lim_{\varepsilon \rightarrow 0} \text{Im } S_{\mu,\alpha}(m', x_1 + i\varepsilon, a) &= (-1)^{\mu-1} \sqrt{\frac{\pi}{8a^2}} \int_1^\infty dy \int_{-\infty}^\infty dt \frac{y^{\alpha+1}}{\sqrt{2y^2-1}} \exp \left[-\frac{y^2}{8a^2(2y^2-1)}(t-m')^2 - 4a^2(2y^2-1) \right] \\ &\times \left[\frac{1}{y^\mu} \sum_{k=0}^{\mu-1} \frac{(\mu-k-1)!}{(\mu-1)!k!} [y^2(x_1^2-t^2)]^k \delta^{(\mu-1)}(t-x_1) - \text{sign } x_1 J_\mu \left(2y\sqrt{x_1^2-t^2} \right) \left(\frac{x_1+t}{x_1-t} \right)^{\mu/2} \Theta(x_1^2-t^2) \right]. \end{aligned} \quad (\text{B14})$$

The sum in the first term comes from the series representation of K_μ , see Eq. (A14), since the $(\mu-1)$ st derivative of the remaining parts vanish at $t=x_1$.

The real part of the partition function Z is needed to compute the chiral condensate $\Sigma(m)$. The real part of the expression (B13) cannot be easily taken since the integrand has a pole of order μ at $t=0$. Therefore we integrate by parts and symmetrize the integrand with respect to $t \rightarrow -t$. Then the real part is given by

$$\begin{aligned} \text{Re } S_{\mu,\alpha}(m', x_1=0, a) &= S_{\mu,\alpha}(m', x_1=0, a) \\ &= \frac{1}{\sqrt{2\pi a^2}(\mu-1)!} \int_1^\infty dy \int_0^\infty dt \frac{y^{\alpha+1}}{\sqrt{2y^2-1}} \exp[-4a^2(2y^2-1)] \\ &\times \frac{1}{t} \partial_{t'}^{\mu-1} \left[|t'+t|^\mu \exp \left[-\frac{y^2}{8a^2(2y^2-1)}(t'+t-m')^2 \right] K_\mu(2y|t'+t|) - \{t \rightarrow -t\} \right]_{t'=0}. \end{aligned} \quad (\text{B15})$$

Note that $\phi=0$ at $x_1=0$. Despite the modulus in $|t'+t|^\mu K_\mu(2y|t'+t|)$ the function is differentiable at $t'+t=0$ because the pole of the Bessel function is cancelled and the derivative of the logarithm yields a pole which cancels with the zero of the Bessel function I_μ , cf. Eq. (A14).

4. Explicit Expressions for Spectral Observables

In this appendix we give explicit expressions for the spectral observables in terms of the functions $S_{\mu,\alpha}$ and Φ_μ which were introduced in Eqs. (65) and (64), and we use the short-hand notations

$$\Phi_\mu = \Phi_\mu(m, \lambda, a), \quad S_{\mu,\alpha} = S_{\mu,\alpha}(m, \lambda=0, a), \quad \text{and } \mathcal{S}_{\mu,\alpha} = \mathcal{S}_{\mu,\alpha}(m, \lambda, a). \quad (\text{B16})$$

For the spectral density of the Hermitian Wilson Dirac operator we find

$$\begin{aligned} \rho_5(m, \lambda, a) &= \partial_{x_1} \text{Im } Z_\nu(\widehat{M}, \widehat{X}, a) \Big|_{\substack{\widehat{M}=m\mathbf{1}_4 \\ \widehat{X}=(\lambda+i\varepsilon)\mathbf{1}_4 \rightarrow \lambda\mathbf{1}_4}} \\ &= 16a^4 [\Phi_{\nu-4}(\mathcal{S}_{\nu+1,1} - \mathcal{S}_{\nu-1,1}) + 2\Phi_{\nu-3}(\mathcal{S}_{\nu+2,2} - \mathcal{S}_{\nu,2}) + \Phi_{\nu-2}(4\mathcal{S}_{\nu+3,3} - 4\mathcal{S}_{\nu+1,3} - \mathcal{S}_{\nu+3,1} + \mathcal{S}_{\nu+1,1}) \\ &+ 2\Phi_{\nu-1}(\mathcal{S}_{\nu+4,2} - \mathcal{S}_{\nu+2,2} + \mathcal{S}_{\nu,2} - \mathcal{S}_{\nu-2,2}) + \Phi_\nu(\mathcal{S}_{\nu+5,1} - \mathcal{S}_{\nu+3,1} + 4\mathcal{S}_{\nu+1,3} - 4\mathcal{S}_{\nu-1,3} - 2\mathcal{S}_{\nu+1,1} + 2\mathcal{S}_{\nu-1,1}) \\ &+ 2\Phi_{\nu+1}(4\mathcal{S}_{\nu+2,4} - 4\mathcal{S}_{\nu,4} - 3\mathcal{S}_{\nu+2,2} + 3\mathcal{S}_{\nu,2}) + \Phi_{\nu+2}(\mathcal{S}_{\nu-1,1} - \mathcal{S}_{\nu-3,1})] \\ &+ 4a^2 [\Phi_{\nu-2}((2\nu+1)\mathcal{S}_{\nu+1,1} - (2\nu-1)\mathcal{S}_{\nu-1,1}) + 2\Phi_{\nu-1}(\mathcal{S}_{\nu+2,0} + (\nu-1)\mathcal{S}_{\nu+2,2} - (\nu-1)\mathcal{S}_{\nu,2}) \\ &+ \Phi_\nu((2\nu+1)\mathcal{S}_{\nu+1,1} - (2\nu-1)\mathcal{S}_{\nu+3,1} + 4\nu\mathcal{S}_{\nu+3,3} - 4\nu\mathcal{S}_{\nu+1,3}) + 2\Phi_{\nu+1}((\nu+3)\mathcal{S}_{\nu,2} - (\nu+1)\mathcal{S}_{\nu-2,2} - \mathcal{S}_{\nu,0})] \\ &- 8a^2(m-\lambda) [\Phi_{\nu-3}(\mathcal{S}_{\nu+1,1} - \mathcal{S}_{\nu-1,1}) + 2\Phi_{\nu-2}(\mathcal{S}_{\nu+2,2} - \mathcal{S}_{\nu,2}) + 2\Phi_{\nu-1}(\mathcal{S}_{\nu+3,3} - \mathcal{S}_{\nu+1,3}) \\ &+ \Phi_\nu(\mathcal{S}_{\nu,2} - \mathcal{S}_{\nu-2,2} + \mathcal{S}_{\nu+4,2} - \mathcal{S}_{\nu+2,2}) + \Phi_{\nu+1}(2\mathcal{S}_{\nu+1,3} - 2\mathcal{S}_{\nu-1,3} - \mathcal{S}_{\nu+1,1} + \mathcal{S}_{\nu-1,1})] \\ &+ (m-\lambda)^2 [\Phi_{\nu-2}(\mathcal{S}_{\nu+1,1} - \mathcal{S}_{\nu-1,1}) + 2\Phi_{\nu-1}(\mathcal{S}_{\nu+2,2} - \mathcal{S}_{\nu,2}) + \Phi_\nu(\mathcal{S}_{\nu+3,1} - \mathcal{S}_{\nu+1,1})] \\ &- 2(m-\lambda) [\Phi_{\nu-1}((\nu+1)\mathcal{S}_{\nu+1,1} - \nu\mathcal{S}_{\nu-1,1}) + \Phi_\nu(\mathcal{S}_{\nu+2,0} + \nu\mathcal{S}_{\nu+2,2} - \nu\mathcal{S}_{\nu,2})] \\ &+ \nu\Phi_\nu((\nu+3)\mathcal{S}_{\nu+1,1} - (\nu+1)\mathcal{S}_{\nu-1,1}). \end{aligned} \quad (\text{B17})$$

The analytical result for the chiral condensate for the quenched theory is given by

$$\begin{aligned}
\Sigma(m, a) &= \partial_{m'} \text{Re} Z_\nu(\widehat{M}, \widehat{X}, a) \Big|_{\substack{\widehat{M}=m\mathbf{1}_4 \\ \widehat{X}=i\varepsilon\mathbf{1}_4 \rightarrow 0}} \\
&= 16a^4 [\Phi_{\nu-4}(S_{\nu+1,1} + S_{\nu-1,1}) + 2\Phi_{\nu-3}(S_{\nu+2,2} + S_{\nu,2}) + \Phi_{\nu-2}(4S_{\nu+3,3} + 4S_{\nu+1,3} - S_{\nu+3,1} - S_{\nu+1,1}) \\
&+ 2\Phi_{\nu-1}(S_{\nu+4,2} + S_{\nu+2,2} + S_{\nu,2} + S_{\nu-2,2}) + \Phi_\nu(S_{\nu+5,1} + S_{\nu+3,1} + 4S_{\nu+1,3} + 4S_{\nu-1,3} - 2S_{\nu+1,1} - 2S_{\nu-1,1}) \\
&+ 2\Phi_{\nu+1}(4S_{\nu+2,4} + 4S_{\nu,4} - 3S_{\nu+2,2} - 3S_{\nu,2}) + \Phi_{\nu+2}(S_{\nu-1,1} + S_{\nu-3,1})] \\
&\quad + 4a^2 [\Phi_{\nu-2}((2\nu+1)S_{\nu+1,1} + (2\nu-1)S_{\nu-1,1}) + 2\Phi_{\nu-1}(S_{\nu+2,0} + (\nu-1)S_{\nu+2,2} + (\nu-1)S_{\nu,2}) \\
&+ \Phi_\nu(4\nu S_{\nu+3,3} + 4\nu S_{\nu+1,3} - (2\nu-1)S_{\nu+3,1} - (2\nu+1)S_{\nu+1,1}) + 2\Phi_{\nu+1}((\nu+3)S_{\nu,2} + (\nu+1)S_{\nu-2,2} - S_{\nu,0})] \\
&\quad - 8a^2 m [\Phi_{\nu-3}(S_{\nu+1,1} + S_{\nu-1,1}) + 2\Phi_{\nu-2}(S_{\nu+2,2} + S_{\nu,2}) + 2\Phi_{\nu-1}(S_{\nu+3,3} + S_{\nu+1,3}) \\
&+ \Phi_\nu(S_{\nu,2} + S_{\nu-2,2} + S_{\nu+4,2} + S_{\nu+2,2}) + \Phi_{\nu+1}(2S_{\nu+1,3} + 2S_{\nu-1,3} - S_{\nu+1,1} - S_{\nu-1,1})] \\
&\quad + m^2 [\Phi_{\nu-2}(S_{\nu+1,1} + S_{\nu-1,1}) + 2\Phi_{\nu-1}(S_{\nu+2,2} + S_{\nu,2}) + \Phi_\nu(S_{\nu+3,1} + S_{\nu+1,1})] \\
&\quad - 2m [\Phi_{\nu-1}((\nu+1)S_{\nu+1,1} + \nu S_{\nu-1,1}) + \Phi_\nu(S_{\nu+2,0} + \nu S_{\nu+2,2} + \nu S_{\nu,2})] \\
&\quad + \nu \Phi_\nu((\nu+3)S_{\nu+1,1} + (\nu+1)S_{\nu-1,1}). \tag{B18}
\end{aligned}$$

The distribution of chirality over the real eigenvalues can be written as

$$\begin{aligned}
\rho_\chi(m, a) &= -\frac{1}{\pi} \partial_m \text{Im} Z_\nu(\widehat{M}, \widehat{X}, a) \Big|_{\substack{\widehat{M}=m\mathbf{1}_4 \\ \widehat{X}=(\lambda+i\varepsilon)\mathbf{1}_4 \rightarrow \lambda\mathbf{1}_4}} \\
&= 16a^4 [\Phi_{\nu-4}(\mathcal{S}_{\nu+1,1} + \mathcal{S}_{\nu-1,1}) + 2\Phi_{\nu-3}(\mathcal{S}_{\nu+2,2} + \mathcal{S}_{\nu,2}) + \Phi_{\nu-2}(4\mathcal{S}_{\nu+3,3} + 4\mathcal{S}_{\nu+1,3} - \mathcal{S}_{\nu+3,1} - \mathcal{S}_{\nu+1,1}) \\
&+ 2\Phi_{\nu-1}(\mathcal{S}_{\nu+4,2} + \mathcal{S}_{\nu+2,2} + \mathcal{S}_{\nu,2} + \mathcal{S}_{\nu-2,2}) + \Phi_\nu(\mathcal{S}_{\nu+5,1} + \mathcal{S}_{\nu+3,1} + 4\mathcal{S}_{\nu+1,3} + 4\mathcal{S}_{\nu-1,3} - 2\mathcal{S}_{\nu+1,1} - 2\mathcal{S}_{\nu-1,1}) \\
&+ 2\Phi_{\nu+1}(4\mathcal{S}_{\nu+2,4} + 4\mathcal{S}_{\nu,4} - 3\mathcal{S}_{\nu+2,2} - 3\mathcal{S}_{\nu,2}) + \Phi_{\nu+2}(\mathcal{S}_{\nu-1,1} + \mathcal{S}_{\nu-3,1})] \\
&\quad + 4a^2 [\Phi_{\nu-2}((2\nu+1)\mathcal{S}_{\nu+1,1} + (2\nu-1)\mathcal{S}_{\nu-1,1}) + 2\Phi_{\nu-1}(\mathcal{S}_{\nu+2,0} + (\nu-1)\mathcal{S}_{\nu+2,2} + (\nu-1)\mathcal{S}_{\nu,2}) \\
&+ \Phi_\nu(4\nu\mathcal{S}_{\nu+3,3} + 4\nu\mathcal{S}_{\nu+1,3} - (2\nu-1)\mathcal{S}_{\nu+3,1} - (2\nu+1)\mathcal{S}_{\nu+1,1}) + 2\Phi_{\nu+1}((\nu+3)\mathcal{S}_{\nu,2} + (\nu+1)\mathcal{S}_{\nu-2,2} - \mathcal{S}_{\nu,0})] \\
&\quad - 8a^2 m [\Phi_{\nu-3}(\mathcal{S}_{\nu+1,1} + \mathcal{S}_{\nu-1,1}) + 2\Phi_{\nu-2}(\mathcal{S}_{\nu+2,2} + \mathcal{S}_{\nu,2}) + 2\Phi_{\nu-1}(\mathcal{S}_{\nu+3,3} + \mathcal{S}_{\nu+1,3}) \\
&+ \Phi_\nu(\mathcal{S}_{\nu,2} + \mathcal{S}_{\nu-2,2} + \mathcal{S}_{\nu+4,2} + \mathcal{S}_{\nu+2,2}) + \Phi_{\nu+1}(2\mathcal{S}_{\nu+1,3} + 2\mathcal{S}_{\nu-1,3} - \mathcal{S}_{\nu+1,1} - \mathcal{S}_{\nu-1,1})] \\
&\quad + m^2 [\Phi_{\nu-2}(\mathcal{S}_{\nu+1,1} + \mathcal{S}_{\nu-1,1}) + 2\Phi_{\nu-1}(\mathcal{S}_{\nu+2,2} + \mathcal{S}_{\nu,2}) + \Phi_\nu(\mathcal{S}_{\nu+3,1} + \mathcal{S}_{\nu+1,1})] \\
&\quad - 2m [\Phi_{\nu-1}((\nu+1)\mathcal{S}_{\nu+1,1} + \nu\mathcal{S}_{\nu-1,1}) + \Phi_\nu(\mathcal{S}_{\nu+2,0} + \nu\mathcal{S}_{\nu+2,2} + \nu\mathcal{S}_{\nu,2})] \\
&\quad + \nu \Phi_\nu((\nu+3)\mathcal{S}_{\nu+1,1} + (\nu+1)\mathcal{S}_{\nu-1,1}). \tag{B19}
\end{aligned}$$

Though all three expressions look quite complicated they are a finite sum of two kinds of integrals, only. This simplifies the numerical evaluation a lot.

Appendix C: The Continuum Limit $a \rightarrow 0$

To be self-consistent we briefly review the exact continuum limit (see subsection C 1) and the Gaussian orthogonal random matrix ensemble of finite matrix size (see subsection C 2) which should describe the spectral broadening of the former zero modes into the real axis quite well at small lattice spacing $|a| \ll 1$. In particular we wish to show how to extract the known results for the spectral observables from our calculations.

1. Exact limit $a \rightarrow 0$

In the continuum limit $a \rightarrow 0$ the partition function takes the form

$$\begin{aligned}
Z_\nu(\widehat{M}, \widehat{X}, a=0) &= (m-x_0)^2 \Phi_{\nu-2} S_{\nu,0} + 2(m-x_0)(m'-x_1) \Phi_{\nu-1} S_{\nu+1,1} - 2\nu(m-x_0) \Phi_{\nu-1} S_{\nu,0} \\
&\quad + (m'-x_1)^2 \Phi_\nu S_{\nu+2,0} - 2\nu(m'-x_1) \Phi_\nu S_{\nu+1,1} + (\nu+1)\nu \Phi_\nu S_{\nu,0}. \tag{C1}
\end{aligned}$$

with

$$\Phi_\mu(m, x_0, a) = \left(\frac{m-x_0}{m+x_0} \right)^{\mu/2} I_\mu \left(2\sqrt{m^2 - x_0^2} \right) \tag{C2}$$

and

$$S_{\mu,\alpha}(m', x_1, a) = 2 \frac{1}{(m' - x_1)^\mu} \int_1^\infty dy y^\alpha \left(\sqrt{|m'^2 - x_1^2|} e^{i\phi} \right)^\mu K_\mu \left(2y \sqrt{|m'^2 - x_1^2|} e^{i\phi} \right) \quad (C3)$$

with $\phi = -L \text{sign}(x_1) \Theta(x_1^2 - m'^2) \pi/2$. We have to be careful about the phase $e^{i\phi}$ since it may change the sign of the result while it is unimportant for the phase of $\sqrt{m^2 - x_0^2}$ in the compact, analytic integral. The reason is the cut along the negative real line of K_μ . The index α only takes the values $\alpha = 0, 1$ which simplifies the calculation a lot.

In the first step we simplify the partition function by employing the relations

$$\begin{aligned} \mu \Phi_\mu + (x_0 + m) \Phi_{\mu+1} + (x_0 - m) \Phi_{\mu-1} &= 0, \\ z K_{\mu+1}(z) + (z \partial_z - \mu) K_\mu(z) &= 0, \\ K_{\mu+1}(z) + K_{\mu-1}(z) + 2 \partial_z K_\mu(z) &= 0. \end{aligned} \quad (C4)$$

The second and third relation is needed for expressing $S_{\nu+1,1}$ and $S_{\nu+2,0}$ in terms of $S_{\nu,0}$ and K_ν respectively,

$$\begin{aligned} (m' - x_1) S_{\nu+1,1}(m', x_1, a = 0) &= \frac{\nu + 1}{2} S_{\nu,0}(m', x_1, a = 0) + \frac{\left(\sqrt{|m'^2 - x_1^2|} e^{i\phi} \right)^\nu}{(m' - x_1)^\nu} K_\nu \left(2 \sqrt{|m'^2 - x_1^2|} e^{i\phi} \right), \\ (m' - x_1)^2 S_{\nu+2,0}(m', x_1, a = 0) &= -(m'^2 - x_1^2) S_{\nu,0}(m', x_1, a = 0) \\ &\quad + 2 \frac{\left(\sqrt{|m'^2 - x_1^2|} e^{i\phi} \right)^{\nu+1}}{(m' - x_1)^\nu} K_{\nu+1} \left(2 \sqrt{|m'^2 - x_1^2|} e^{i\phi} \right) \end{aligned} \quad (C5)$$

resulting from integration by parts. Then the quenched partition function reads

$$\begin{aligned} Z_\nu(\widehat{M}, \widehat{X}, a = 0) &= 2 \frac{\left(\sqrt{|m'^2 - x_1^2|} e^{i\phi} \right)^\nu (m - x_0)^{\nu/2}}{(m' - x_1)^\nu (m + x_0)^{\nu/2}} \left[[(m^2 - x_0^2) - (m'^2 - x_1^2)] I_\nu \left(2 \sqrt{m^2 - x_0^2} \right) \right. \\ &\quad \times \int_1^\infty dy K_\nu \left(2y \sqrt{|m'^2 - x_1^2|} e^{i\phi} \right) + \sqrt{m^2 - x_0^2} I_{\nu+1} \left(2 \sqrt{m^2 - x_0^2} \right) K_\nu \left(2 \sqrt{|m'^2 - x_1^2|} e^{i\phi} \right) \\ &\quad \left. + \sqrt{|m'^2 - x_1^2|} e^{i\phi} I_\nu \left(2 \sqrt{m^2 - x_0^2} \right) K_{\nu+1} \left(2 \sqrt{|m'^2 - x_1^2|} e^{i\phi} \right) \right]. \end{aligned} \quad (C6)$$

The last two terms also appear in QCD with three colors. In this way one can easily check the normalization $Z_\nu(m \mathbf{1}_4, x \mathbf{1}_4, a = 0) = 1$.

In the second step we take the derivative with respect to m' or x_1 and set $m = m'$ and $x_0 = x_1 = x$, yielding

$$\begin{aligned} \partial_{m'} Z_\nu(\widehat{M}, \widehat{X}, a = 0) \Big|_{\substack{\widehat{M}=m \mathbf{1}_4 \\ \widehat{X}=x \mathbf{1}_4}} &= -\frac{\nu x}{m^2 - x^2} - 4m I_\nu \left(2 \sqrt{|m^2 - x^2|} e^{i\phi} \right) \int_1^\infty dy K_\nu \left(2y \sqrt{|m^2 - x^2|} e^{i\phi} \right) \\ &+ \frac{2m}{\sqrt{|m^2 - x^2|} e^{i\phi}} \partial_y \left[2 \sqrt{|m^2 - x^2|} e^{i\phi} I_{\nu+1} \left(2 \sqrt{|m^2 - x^2|} e^{i\phi} \right) K_\nu(y) + y I_\nu \left(2 \sqrt{|m^2 - x^2|} e^{i\phi} \right) K_{\nu+1}(y) \right]_{y=2 \sqrt{|m^2 - x^2|} e^{i\phi}} \\ &= \frac{\nu}{x - m} - 4m I_\nu \left(2 \sqrt{|m^2 - x^2|} e^{i\phi} \right) \int_1^\infty dy K_\nu \left(2y \sqrt{|m^2 - x^2|} e^{i\phi} \right) \\ &- 4m \left[I_{\nu+1} \left(2 \sqrt{|m^2 - x^2|} e^{i\phi} \right) K_{\nu-1} \left(2 \sqrt{|m^2 - x^2|} e^{i\phi} \right) + I_\nu \left(2 \sqrt{|m^2 - x^2|} e^{i\phi} \right) K_\nu \left(2 \sqrt{|m^2 - x^2|} e^{i\phi} \right) \right] \end{aligned} \quad (C7)$$

and

$$\begin{aligned} \partial_{x_1} Z_\nu(\widehat{M}, \widehat{X}, a = 0) \Big|_{\substack{\widehat{M}=m \mathbf{1}_4 \\ \widehat{X}=x \mathbf{1}_4}} &= \frac{\nu m}{m^2 - x^2} + 4x I_\nu \left(2 \sqrt{|m^2 - x^2|} e^{i\phi} \right) \int_1^\infty dy K_\nu \left(2y \sqrt{|m^2 - x^2|} e^{i\phi} \right) \\ &- \frac{2x}{\sqrt{|m^2 - x^2|} e^{i\phi}} \partial_y \left[2 \sqrt{|m^2 - x^2|} e^{i\phi} I_{\nu+1} \left(2 \sqrt{|m^2 - x^2|} e^{i\phi} \right) K_\nu(y) + y I_\nu \left(2 \sqrt{|m^2 - x^2|} e^{i\phi} \right) K_{\nu+1}(y) \right]_{y=2 \sqrt{|m^2 - x^2|} e^{i\phi}} \\ &= \frac{\nu}{m - x} + 4x I_\nu \left(2 \sqrt{|m^2 - x^2|} e^{i\phi} \right) \int_1^\infty dy K_\nu \left(2y \sqrt{|m^2 - x^2|} e^{i\phi} \right) \\ &+ 4x \left[I_{\nu+1} \left(2 \sqrt{|m^2 - x^2|} e^{i\phi} \right) K_{\nu-1} \left(2 \sqrt{|m^2 - x^2|} e^{i\phi} \right) + I_\nu \left(2 \sqrt{|m^2 - x^2|} e^{i\phi} \right) K_\nu \left(2 \sqrt{|m^2 - x^2|} e^{i\phi} \right) \right]. \end{aligned} \quad (C8)$$

Up to an overall sign, Equation (C7) is equal to the chiral condensate Σ when setting $x = 0$ (implying $\phi = 0$), i.e. the chiral condensate without zero modes is

$$\Sigma_{\text{chGOE}}^{(\nu)}(m) = 4m \left[I_{\nu+1}(2|m|) K_{\nu-1}(2|m|) + I_{\nu}(2|m|) K_{\nu}(2|m|) + I_{\nu}(2|m|) \int_1^{\infty} dy K_{\nu}(2y|m|) \right]. \quad (\text{C9})$$

This result is in agreement with the expression in [66], but has the advantage that there is no need to distinguish even and odd ν . For odd ν the Bessel function K_{ν} can be written as a total derivative allowing us to evaluate the integral exactly,

$$K_{2k+1}(x) = -2 \frac{d}{dx} [K_{2k}(x) - K_{2k-2}(x) + \dots + (-1)^k K_2(x) + (-1)^{k+1} \frac{1}{2} K_0(x)]. \quad (\text{C10})$$

For $\nu = 2k + 1$, this results in the condensate

$$\begin{aligned} \Sigma(m) &= -\frac{\nu}{m} + 4I_{\nu}(2m)[K_{2k}(2m) - K_{2k-2}(2m) + \dots + (-1)^k K_2(2m)] + (-1)^{k+1} I_{\nu}(2m) K_0(2m) \\ &\quad - 4m I_{\nu+1}(2m) K_{\nu-1}(2m) - 4m I_{\nu+1}(2m) K_{\nu-1}(2m), \end{aligned} \quad (\text{C11})$$

which up to a rescaling $m \rightarrow 2m$ and $\Sigma \rightarrow \Sigma/2$ agrees with the result in [66]. For even ν we can also use the recursion relation for Bessel functions but we are left with an integral over K_0 .

$$K_{2k}(x) = 2(-1)^{\nu/2} \frac{d}{dx} \left[\sum_{k=0}^{\nu/2-1} (-1)^k K_{2k+1}(x) \right] + (-1)^{\nu/2} K_0(x). \quad (\text{C12})$$

This results in

$$\begin{aligned} \Sigma(m) &= -\frac{\nu}{m} - 4m I_{\nu+1}(2m) K_{\nu-1}(2m) - 4m I_{\nu+1}(2m) K_{\nu-1}(2m) \\ &\quad + 4(-1)^{\nu/2} I_{\nu}(2m) \sum_{k=0}^{\nu/2-1} (-1)^k K_{2k+1}(x) - 2m(-1)^{\nu/2} I_{\nu}(2m) \int_1^{\infty} dy K_0(2my). \end{aligned} \quad (\text{C13})$$

The integral over K_0 can be expressed into modified Struve functions, and it can be numerically shown that it agrees with Eq. (8) of [66].

Let us underline that the valence quark mass dependence of the chiral condensate for chGSE is also derived in [66]. The authors again obtain separate expressions for even and odd ν which can be simplified to $-2x K_{N_f+2\nu}(2x) \int_0^1 dy I_{N_f+2\nu}(2xy)$ up to rescaling.

From the result (C7) we can immediately deduce the well-known result for the distribution of the chiralities over the real eigenvalues which is a Dirac delta function in the continuum limit,

$$\rho_{\chi}(m, a = 0) = \frac{1}{\pi} \text{Im} \partial_{m'} Z_{\nu}(\widehat{M}, \widehat{X}, a = 0) \Big|_{\substack{\widehat{M}=m\mathbf{1}_4 \\ \widehat{X}=-i\varepsilon\mathbf{1}_4 \rightarrow 0}} = \nu \delta(m). \quad (\text{C14})$$

Only the first term of Eq. (C7) contributes to this results since the remaining parts are real for $m > x = 0$.

The spectral density of the Hermitian Dirac operator D_5 can be obtained by setting $x = \lambda + i\varepsilon$ and taking the imaginary part of Eq. (C8) in the limit $\varepsilon \rightarrow 0$. We have to distinguish two cases, $|m| > |\lambda|$ or $|m| < |\lambda|$. In the first case all terms are real and vanish while in the latter case we have to apply the relations (A8), (A13), and (A19) yielding,

$$\begin{aligned} \rho_5(\lambda, m, a = 0) &= \frac{1}{\pi} \text{Im} \partial_{x_1} Z_{\nu}(\widehat{M}, \widehat{X}, a = 0) \Big|_{\substack{\widehat{M}=m\mathbf{1}_4 \\ \widehat{X}=(\lambda+i\varepsilon)\mathbf{1}_4 \rightarrow \lambda\mathbf{1}_4}} \\ &= \nu \delta(m - \lambda) + \frac{|\lambda|}{\sqrt{\lambda^2 - m^2}} J_{\nu}(2\sqrt{\lambda^2 - m^2}) \left[1 - \int_0^{2\sqrt{\lambda^2 - m^2}} dy J_{\nu}(y) \right] \Theta(|\lambda| - |m|) \\ &\quad + 2|\lambda| \left[J_{\nu}^2(2\sqrt{\lambda^2 - m^2}) - J_{\nu+1}(2\sqrt{\lambda^2 - m^2}) J_{\nu-1}(2\sqrt{\lambda^2 - m^2}) \right] \Theta(|\lambda| - |m|), \end{aligned} \quad (\text{C15})$$

cf. [65]. Note that Eqs. (A13) and (A19) are multiplied with $n = -\text{sign}(\lambda)$ because of the phase $\phi = -\text{sign}(x_1)\Theta(x_1^2 - m'^2)\pi/2$ for $L = 1$.

2. Spectral Observables of the Gaussian Orthogonal Ensemble

We choose the abbreviation $\widehat{Y} = (\widehat{M} - \widehat{X})/(4a) = \text{diag}(y_0, y_0, y_1, y_1)$. The partition function (62) is equal to a partition function of $\nu \times \nu$ real symmetric random matrices distributed by a Gaussian. Let $\text{Sym}(\nu)$ be the set of these real symmetric matrices. In terms of these matrices, the partition function reads,

$$Z_{\text{GOE}}^{(\nu)}(\widehat{Y}) = \frac{1}{(2\pi)^{\nu(\nu-1)/4} \pi^{\nu/2}} \int_{\text{Sym}(\nu)} dH \exp[-\text{tr} H^2] \frac{\det(H - y_0 \mathbf{1}_\nu)}{\det(H - y_1 \mathbf{1}_\nu)}. \quad (\text{C16})$$

For the cases $\nu = 0, 1$ they take particular simple forms,

$$Z_{\text{GOE}}^{(0)}(\widehat{Y}) = 1 \quad (\text{C17})$$

and

$$Z_{\text{GOE}}^{(1)}(\widehat{Y}) = \frac{1}{\sqrt{\pi}} \int_{-\infty}^{\infty} dE \frac{E - y_0}{E - y_1} e^{-E^2} = 1 + \sqrt{\pi}(y_0 - y_1) \frac{\text{erf}(iy_1)}{i} e^{-y_1^2} - iL\sqrt{\pi}(y_1 - y_0) e^{-y_1^2}. \quad (\text{C18})$$

In the latter equation we assumed that the imaginary part of $x_1 = \text{Re} x_1 + iL\varepsilon$ ($L = \pm 1$) is infinitesimal small, $\varepsilon \rightarrow 0$. The error function $\text{erf}(z) = 2 \int_0^z dz' e^{-z'^2} / \sqrt{\pi}$ is real despite the imaginary unit.

For $\nu > 1$ the result directly following from the representation (C16) are not that trivial as the ones in Eqs. (C17) and (C18). Therefore we start for those cases from the supersymmetric representation (62) which, in the parametrization (59), reads as

$$Z_{\text{GOE}}^{(\nu)}(\widehat{Y}) = \frac{1}{\pi} \int_{-\infty}^{\infty} du \int_{-\infty}^{\infty} dv_1 \int_{-\infty}^{\infty} dv_2 |v_1 - v_2| e^{-(2u^2 + v_1^2 + v_2^2)} \frac{(y_0 - iu)^\nu}{(y_1 - v_1)^{\nu/2} (y_1 - v_2)^{\nu/2}} \times \left[1 - \frac{\nu}{4} \frac{2y_1 - v_1 - v_2}{(y_0 - iu)(y_1 - v_1)(y_1 - v_2)} + \frac{\nu(\nu - 1)}{16} \frac{1}{(y_0 - iu)^2 (y_1 - v_1)(y_1 - v_2)} \right]. \quad (\text{C19})$$

We have already integrated over the orthogonal matrix \widetilde{O} and the four Grassmann variables $\eta, \eta^*, \chi, \chi^*$. Moreover, we rescaled the remaining variables $(u, v_1, v_2) \rightarrow 4a(u, v_1, v_2)$. The normalization constant is fixed by $y_0 = y_1 = i\varepsilon \rightarrow \infty$.

The integral over u is equal to Hermite polynomials,

$$\int_{-\infty}^{\infty} du e^{-2u^2} (y_0 - iu)^\mu = \sqrt{\frac{\pi}{2}} 2^{-\mu} H_\mu(2y_0), \quad (\text{C20})$$

where we have chosen the monic normalization $H_\mu(z) = z^\mu + \dots$. Then the partition function is equal to

$$Z_{\text{GOE}}^{(\nu)}(\widehat{Y}) = H_\nu(2y_0) \mathcal{I}_{\nu,0}(y_1) + H_{\nu-1}(2y_0) \mathcal{I}_{\nu,1}(y_1) + \nu(\nu - 1) H_{\nu-2}(2y_0) \mathcal{I}_{\nu+2,0}(y_1) \quad (\text{C21})$$

with

$$\mathcal{I}_{\mu,\alpha}(y_1) = \frac{2^{-\mu}}{\sqrt{2\pi}} \partial_{y_1}^\alpha \int_{-\infty}^{\infty} dv_1 \int_{-\infty}^{\infty} dv_2 |v_1 - v_2| e^{-(v_1^2 + v_2^2)} \frac{1}{(y_1 - v_1)^{\mu/2} (y_1 - v_2)^{\mu/2}}. \quad (\text{C22})$$

The latter twofold integral exits due to the non-vanishing imaginary part of $y_1 = m - \text{Re} x_1 - iL\varepsilon$. This integral can be brought into a form which is easily integrable, and the spectral observables we are interested in can be readily extracted. To find such a representation it is suitable to understand the integral (C22) in terms of an integral over a 2×2 real symmetric matrix H ,

$$\mathcal{I}_{\mu,\alpha}(y_1) \propto \partial_{y_1}^\alpha \int_{\text{Sym}(2)} \frac{dH e^{-\text{tr} H^2}}{\det^{\mu/2}(y_1 \mathbf{1}_2 - H)}, \quad (\text{C23})$$

where v_1 and v_2 are the eigenvalues of H . The determinant in Eq. (C23) can be written as an integral over 2×2 positive definite real symmetric matrix H'

$$\frac{1}{\det^{\mu/2}(y_1 \mathbf{1}_2 - H)} \propto e^{iL\pi\mu/2} \int_{\text{Sym}_+(2)} dH' \exp[-2iL\text{tr} H'(y_1 \mathbf{1}_2 - H)] \det^{(\mu-3)/2} H'. \quad (\text{C24})$$

The index μ has to be larger than 1 and thus $\nu \geq 2$ which is okay since we know explicit results for $\nu = 0, 1$. The phase in front of this integral is important as well. The integral over H yields a Gaussian integral in H' . After diagonalizing $H' = O' \text{diag}(E_1, E_2) O'^T$ with $O' \in O(2)$ and $E_1, E_2 > 0$ we find

$$\mathcal{I}_{\mu,\alpha}(y_1) = \frac{2^{\mu+\alpha-3} e^{iL\pi(\mu-\alpha)/2}}{(\mu-2)!} \int_0^\infty dE_1 \int_0^\infty dE_2 |E_1 - E_2| (E_1 E_2)^{(\mu-3)/2} (E_1 + E_2)^\alpha \exp[-(E_1^2 + E_2^2) - 2iLy_1(E_1 + E_2)]. \quad (\text{C25})$$

Already at this point we can set the imaginary part of y_1 exactly to zero. We order the eigenvalues $E_1 > E_2$ and change to polar coordinates $E_1 = r \cos \varphi$ and $E_2 = r \sin \varphi$ with $r > 0$ and $0 \leq \varphi \leq \pi/4$,

$$\begin{aligned} \mathcal{I}_{\mu,\alpha}(y_1) &= \frac{2^{(\mu+3\alpha)/2} e^{iL\pi(\mu-\alpha)/2}}{(\mu-2)!} \int_0^\infty dR \int_0^{\pi/4} d\varphi R^{\mu+\alpha-1} \sin^{(\mu-3)/2}(2\varphi) \cos\left(\varphi + \frac{\pi}{4}\right) \cos^\alpha\left(\varphi - \frac{\pi}{4}\right) \\ &\quad \times \exp\left[-R^2 - \sqrt{8}iLy_1 R \cos\left(\varphi - \frac{\pi}{4}\right)\right] \\ &= \frac{2^{(\mu+3\alpha-2)/2}}{(\mu-2)!} \int_0^{\pi/4} d\varphi \sin^{(\mu-3)/2}(2\varphi) \cos\left(\varphi + \frac{\pi}{4}\right) \cos^\alpha\left(\varphi - \frac{\pi}{4}\right) \\ &\quad \times \left[\Gamma\left(\frac{\mu+\alpha}{2}\right) e^{iL\pi(\mu-\alpha)/2} M\left(\frac{\mu+\alpha}{2}, \frac{1}{2}; -2y_1^2 \cos^2\left(\varphi - \frac{\pi}{4}\right)\right) \right. \\ &\quad \left. + \sqrt{8}\Gamma\left(\frac{\mu+\alpha+1}{2}\right) e^{iL\pi(\mu-\alpha-1)/2} y_1 \cos\left(\varphi - \frac{\pi}{4}\right) M\left(\frac{\mu+\alpha+1}{2}, \frac{3}{2}; -2y_1^2 \cos^2\left(\varphi - \frac{\pi}{4}\right)\right) \right]. \quad (\text{C26}) \end{aligned}$$

We have employed Kummer's confluent hypergeometric function [68]

$$M(a, b; z) = \sum_{j=0}^{\infty} \frac{\Gamma[a+j]\Gamma[b] z^j}{\Gamma[a]\Gamma[b+j] j!}. \quad (\text{C27})$$

We underline that only one of the two terms in Eq. (C26) is real and the other one imaginary depending on the parity of μ . In random matrix theory this subtle difference between even and odd matrix dimension for real matrices is well known [61].

Let us define the abbreviations

$$\mathcal{I}_{\mu,\alpha}^{(1)}(y_1) = \int_0^{\pi/4} d\varphi \sin^{(\mu-3)/2}(2\varphi) \cos\left(\varphi + \frac{\pi}{4}\right) \cos^\alpha\left(\varphi - \frac{\pi}{4}\right) M\left(\frac{\mu+\alpha}{2}, \frac{1}{2}; -2y_1^2 \cos^2\left(\varphi - \frac{\pi}{4}\right)\right), \quad (\text{C28})$$

and

$$\mathcal{I}_{\mu,\alpha}^{(2)}(y_1) = y_1 \int_0^{\pi/4} d\varphi \sin^{(\mu-3)/2}(2\varphi) \cos\left(\varphi + \frac{\pi}{4}\right) \cos^{\alpha+1}\left(\varphi - \frac{\pi}{4}\right) M\left(\frac{\mu+\alpha+1}{2}, \frac{3}{2}; -2y_1^2 \cos^2\left(\varphi - \frac{\pi}{4}\right)\right). \quad (\text{C29})$$

Then the real part of the first derivative in y_1 and setting $y_1 \rightarrow m/4a$ yields the contribution of the chiral condensate which results from this finite dimensional Gaussian orthogonal ensemble, i.e.

$$\begin{aligned} \Sigma_{\text{GOE}}^{(\nu>1)}\left(\frac{m}{4a}\right) &= -\partial_{m'} \text{Re} Z_{\text{GOE}}^{(\nu)}(\widehat{Y}) \Big|_{\widehat{Y}=(m/4a)\mathbf{1}_4} \quad (\text{C30}) \\ &= \frac{2^{\nu/2} \Gamma[(\nu+2)/2]}{(\nu-2)! a} \cos\left(\frac{\pi\nu}{2}\right) \left[H_\nu\left(\frac{m}{2a}\right) \mathcal{I}_{\nu,1}^{(2)}\left(\frac{m}{4a}\right) + H_{\nu-1}\left(\frac{m}{2a}\right) \mathcal{I}_{\nu,2}^{(1)}\left(\frac{m}{4a}\right) - (\nu+2) H_{\nu-2}\left(\frac{m}{2a}\right) \mathcal{I}_{\nu+2,1}^{(2)}\left(\frac{m}{4a}\right) \right] \\ &\quad - \frac{2^{(\nu-1)/2} \Gamma[(\nu+3)/2]}{(\nu-2)! a} \sin\left(\frac{\pi\nu}{2}\right) \left[\frac{1}{\nu+1} H_\nu\left(\frac{m}{2a}\right) \mathcal{I}_{\nu,1}^{(1)}\left(\frac{m}{4a}\right) - 4H_{\nu-1}\left(\frac{m}{2a}\right) \mathcal{I}_{\nu,2}^{(2)}\left(\frac{m}{4a}\right) - H_{\nu-2}\left(\frac{m}{2a}\right) \mathcal{I}_{\nu+2,1}^{(1)}\left(\frac{m}{4a}\right) \right]. \end{aligned}$$

Note that only one of the two terms contribute because either $\cos(\pi\nu/2)$ or $\sin(\pi\nu/2)$ does not vanish depending on the parity of ν . The ‘‘chiral condensate’’ for the case $\nu = 0$ vanishes,

$$\Sigma_{\text{GOE}}^{(\nu=0)}\left(\frac{m}{4a}\right) = 0, \quad (\text{C31})$$

while the one for $\nu = 1$ can be read off from Eq. (C18),

$$\Sigma_{\text{GOE}}^{(\nu=1)}\left(\frac{m}{4a}\right) = \sqrt{\frac{\pi}{16a^2}} \frac{\text{erf}(im/4a)}{i} \exp\left(-\frac{m^2}{16a^2}\right). \quad (\text{C32})$$

Other representations of the partition function and the chiral condensate in terms of Hermite polynomials and its Cauchy transform exist in the literature [61]. However we chose the representation Eq. (C30) which can be easily evaluated numerically and the cases even and odd ν can be discussed on the same footing.

The level density is obtained from the imaginary part of the first derivative in y_1 ,

$$\begin{aligned} \rho_{\text{GOE}}^{(\nu>1)}\left(\frac{m}{4a}\right) &= -\frac{1}{\pi} \partial_{m'} \text{Im} Z_{\text{GOE}}^{(\nu)}(\widehat{Y}) \Big|_{\widehat{Y}=(m/4a)\mathbf{1}_4} \\ &= \frac{2^{\nu/2} \Gamma[(\nu+2)/2]}{(\nu-2)!a} \sin\left(\frac{\pi\nu}{2}\right) \left[H_\nu\left(\frac{m}{2a}\right) \mathcal{I}_{\nu,1}^{(2)}\left(\frac{m}{4a}\right) + H_{\nu-1}\left(\frac{m}{2a}\right) \mathcal{I}_{\nu,2}^{(1)}\left(\frac{m}{4a}\right) - (\nu+2) H_{\nu-2}\left(\frac{m}{2a}\right) \mathcal{I}_{\nu+2,1}^{(2)}\left(\frac{m}{4a}\right) \right] \\ &\quad + \frac{2^{(\nu-1)/2} \Gamma[(\nu+3)/2]}{(\nu-2)!a} \cos\left(\frac{\pi\nu}{2}\right) \left[\frac{1}{\nu+1} H_\nu\left(\frac{m}{2a}\right) \mathcal{I}_{\nu,1}^{(1)}\left(\frac{m}{4a}\right) - 4 H_{\nu-1}\left(\frac{m}{2a}\right) \mathcal{I}_{\nu,2}^{(2)}\left(\frac{m}{4a}\right) - H_{\nu-2}\left(\frac{m}{2a}\right) \mathcal{I}_{\nu+2,1}^{(1)}\left(\frac{m}{4a}\right) \right]. \end{aligned} \quad (\text{C33})$$

The exceptional cases for $\nu = 0, 1$ are

$$\rho_{\text{GOE}}^{(\nu=0)}\left(\frac{m}{4a}\right) = 0, \quad (\text{C34})$$

and

$$\rho_{\text{GOE}}^{(\nu=1)}\left(\frac{m}{4a}\right) = \frac{1}{\sqrt{16\pi a^2}} \exp\left(-\frac{m^2}{16a^2}\right). \quad (\text{C35})$$

These expressions are a good approximation for the level density of the real eigenvalues of the non-Hermitian Wilson Dirac operator at very small lattice spacing $|a| \ll 1$ which are the former zero modes of the continuum QCD Dirac operator.

Appendix D: Computation of the Saddle Point Solutions (82) and (84)

We have to solve the rational equation

$$p(V) = \frac{m}{2}(V - V^{-1}) + \frac{\lambda}{2}(V + V^{-1}) - 2a^2(V^2 - V^{-2}) = 0. \quad (\text{D1})$$

with real coefficients. In particular each eigenvalue z of V satisfies exactly the same equation. Because the rational function $p(z)$ has real coefficients it has either no, two or four real zero points satisfying Eq. (D1). All other zero points are complex conjugate pairs. Since $p(z \rightarrow 0) \rightarrow 2a^2 z^{-2} \rightarrow +\infty$ while $p(z \rightarrow \pm\infty) \rightarrow -2a^2 z^2 \rightarrow -\infty$ we have at least two real zero points. The question is: What happens with the other two zero points? We are in particular interested the complex solutions since they are important for the level density ρ_5 when we have the general situation with $\lambda \neq 0$.

Splitting the eigenvalue z of V into a radial and angular part, i.e. $z = r e^{i\varphi}$ with $r \geq 0$ and $\varphi \in]-\pi, \pi[$, we obtain two equations,

$$\begin{aligned} \left(\frac{m+\lambda}{2} r \cos \varphi - \frac{m-\lambda}{2} r^{-1} \cos \varphi - 2a^2(r^2 - r^{-2})(2 \cos^2 \varphi - 1) \right) &= 0, \\ \left(\frac{m+\lambda}{2} r + \frac{m-\lambda}{2} r^{-1} - 4a^2(r^2 + r^{-2}) \cos \varphi \right) \sin \varphi &= 0, \end{aligned} \quad (\text{D2})$$

corresponding to the real and imaginary part of the saddle point equation, respectively. The second equality is either solved by $\sin \varphi = 0$ implying a real solution or the cosine can be expressed in terms of the radius $r > 0$.

Let us assume $\sin \varphi \neq 0$. Then the equation solved by the radius is

$$\sinh^3 2\vartheta + \left(1 - \frac{m^2 - \lambda^2}{(8a^2)^2}\right) \sinh 2\vartheta + \frac{2m\lambda}{(8a^2)^2} = 0 \quad (\text{D3})$$

with $r = e^\vartheta$. This equation has always one real solution which is

$$\sinh 2\vartheta = - \left(\frac{m\lambda}{(8a^2)^2} + \sqrt{\frac{m^2\lambda^2}{(8a^2)^4} - \frac{1}{27} \left(\frac{m^2 - \lambda^2}{(8a^2)^2} - 1 \right)^3} \right)^{1/3} - \left(\frac{m\lambda}{(8a^2)^2} - \sqrt{\frac{m^2\lambda^2}{(8a^2)^4} - \frac{1}{27} \left(\frac{m^2 - \lambda^2}{(8a^2)^2} - 1 \right)^3} \right)^{1/3}, \quad (\text{D4})$$

where we have to take the following root $x^{1/3} = \text{sign}(x)|x|^{1/3}$ if x is real. There are two additional real solutions in the region with

$$\frac{m^2\lambda^2}{(8a^2)^4} < \frac{1}{27} \left(\frac{m^2 - \lambda^2}{(8a^2)^2} - 1 \right)^3 \Leftrightarrow \frac{\lambda^2}{8a^2} < \left[\left(\frac{m}{8a^2} \right)^{2/3} - 1 \right]^3 \quad (\text{D5})$$

which implies $\lambda^2 < m^2 - (8a^2)^2$ and can only appear if the quark mass satisfies $|m| > 8a^2$. However in this region the cosine of the angle φ has to be larger than 1 implying that it has to be complex which should not be the case. This can be seen in the following short computation.

The other two solutions are given by

$$\begin{aligned} \sinh 2\vartheta_n = -\text{sign}(m\lambda) & \left[e^{i2n\pi/3} \left(\frac{|m\lambda|}{(8a^2)^2} + i \text{sign}(m\lambda) \sqrt{\frac{1}{27} \left(\frac{m^2 - \lambda^2}{(8a^2)^2} - 1 \right)^3 - \frac{m^2\lambda^2}{(8a^2)^4}} \right)^{1/3} \right. \\ & \left. + e^{-i2n\pi/3} \left(\frac{|m\lambda|}{(8a^2)^2} - i \text{sign}(m\lambda) \sqrt{\frac{1}{27} \left(\frac{m^2 - \lambda^2}{(8a^2)^2} - 1 \right)^3 - \frac{m^2\lambda^2}{(8a^2)^4}} \right)^{1/3} \right] \end{aligned} \quad (\text{D6})$$

with $n = 1, 2$. Hence each solution is bounded as

$$\begin{aligned} \frac{1}{\sqrt{3}} \sqrt{\frac{m^2 - \lambda^2}{(8a^2)^2} - 1} \leq \text{sign}(m\lambda) \sinh 2\vartheta_1 \leq \sqrt{\frac{m^2 - \lambda^2}{(8a^2)^2} - 1} \Rightarrow \frac{1}{\sqrt{3}} \sqrt{\frac{m^2 - \lambda^2}{(8a^2)^2} + 2} \leq \cosh 2\vartheta_1 \leq \sqrt{\frac{m^2 - \lambda^2}{(8a^2)^2}}, \\ 0 \leq \text{sign}(m\lambda) \sinh 2\vartheta_2 \leq \frac{1}{\sqrt{3}} \sqrt{\frac{m^2 - \lambda^2}{(8a^2)^2} - 1} \Rightarrow 1 \leq \cosh 2\vartheta_0 \leq \frac{1}{\sqrt{3}} \sqrt{\frac{m^2 - \lambda^2}{(8a^2)^2} + 2}. \end{aligned} \quad (\text{D7})$$

We combine the two equalities in Eq. (D2) such that we have for the angle

$$|\cos 2\varphi| = \left| \frac{(m + \lambda)^2 r^2 - (m - \lambda)^2 r^{-2}}{32a^4(r^4 - r^{-4})} \right| = \frac{m^2 + \lambda^2}{(8a^2)^2 \cosh 2\vartheta_n} + \frac{2|m\lambda|}{(8a^2)^2 |\sinh 2\vartheta_n|}. \quad (\text{D8})$$

This allows us to make the following estimations

$$\begin{aligned} n = 1 : |\cos 2\varphi| & \geq \frac{m^2 + \lambda^2}{8a^2 \sqrt{m^2 - \lambda^2}} + \frac{2|m\lambda|}{8a^2 \sqrt{m^2 - \lambda^2} - (8a^2)^2} \geq \frac{(|m| + |\lambda|)^2}{8a^2 \sqrt{m^2 - \lambda^2}}, \\ n = 2 : |\cos 2\varphi| & \geq \frac{\sqrt{3}(m^2 + \lambda^2)}{8a^2 \sqrt{m^2 - \lambda^2} + 2(8a^2)^2} + \frac{\sqrt{12}|m\lambda|}{8a^2 \sqrt{m^2 - \lambda^2} - (8a^2)^2} \geq \frac{\sqrt{3}(|m| + |\lambda|)^2}{8a^2 \sqrt{m^2 - \lambda^2} + 2(8a^2)^2}, \end{aligned} \quad (\text{D9})$$

In both cases the right hand side is a function which is monotonously increasing in $|\lambda|$ implying that $|\lambda| = 0$ is the minimum. The remaining function in $|m|$ is also monotonously increasing such that we have a minimum at the values at $|m| = 8a^2$ which results in

$$|\cos 2\varphi| \geq 1 \quad (\text{D10})$$

meaning that those solutions for $\sinh 2\vartheta$ are forbidden.

Hence we have only a complex solution if

$$\frac{|\lambda|}{8a^2} > \left[\left(\frac{|m|}{8a^2} \right)^{2/3} - 1 \right]^{3/2} \quad (\text{D11})$$

which is

$$U_0 = iL e^{\vartheta + Li\varphi} \mathbf{1}_4 \text{ with } \varphi = \arccos \left[\frac{m \cosh \vartheta + \lambda \sinh \vartheta}{8a^2 \cosh 2\vartheta} \right] \quad (\text{D12})$$

and ϑ is given by Eq. (D4). The sign L is fixed because of the non-compact double integral over s_1 and s_2 . The infinitesimal imaginary shift $iL\epsilon$ in λ and the singularity at $e^{s_1}, e^{s_2} = 0$ prevents to shift the contour to the solution $z = e^{\vartheta - Li\varphi}$ in the thermodynamic limit.

The region (D11) implies a spectral gap of D_5 in the interval

$$\lambda \in \left[- \left(|m|^{2/3} - (8a^2)^{2/3} \right)^{3/2}, \left(|m|^{2/3} - (8a^2)^{2/3} \right)^{3/2} \right], \quad (\text{D13})$$

cf. Fig. 2.a). It is closed if $|m| \leq 8a^2$ such that we enter a new phase which is the Aoki phase for lattice QCD with two colors.

The situation of the spectrum looks slightly different at $\lambda = 0$. In this case the saddle point equation takes the simple form $p(z) = 2a^2(z - z^{-1})(z + z^{-1} - m/(4a^2)) = 0$ where we can readily read off the solutions. Plugging these solutions into the exponent (80) we have to choose the maximum which is

$$U_0 = \begin{cases} iL \frac{m}{8a^2} + \sqrt{1 - \left(\frac{m}{8a^2} \right)^2}, & |m| < 8a^2, \\ iL \operatorname{sign} m \mathbf{1}_4, & |m| > 8a^2. \end{cases} \quad (\text{D14})$$

Again we would obtain always two solutions but only one is accessible in the thermodynamic limit due to the infinitesimal increment $iL\varepsilon$.

Appendix E: Density of $\rho_5(m-1, \lambda=0, a \rightarrow 0)$

In this appendix we consider the continuum limit of $\rho_5(m=0, \lambda=0, a)$ and show that the convergence to the continuum limit is non-uniform. The level density reduces in this situation to

$$\begin{aligned} \rho_5(m=0, \lambda=0, a) = & 16a^4 [2\Phi_4 \mathcal{S}_{1,1} - 2\Phi_3 (\mathcal{S}_{2,2} - \mathcal{S}_{0,2}) + 4\Phi_2 (\mathcal{S}_{3,3} - \mathcal{S}_{1,3}) \\ & + 2\Phi_1 (4\mathcal{S}_{2,4} - 4\mathcal{S}_{0,4} - \mathcal{S}_{2,2} + 2\mathcal{S}_{0,2} - \mathcal{S}_{4,2}) + \Phi_0 (\mathcal{S}_{5,1} - \mathcal{S}_{3,1} + 8\mathcal{S}_{1,3} - 4\mathcal{S}_{1,1})] \\ & + 4a^2 [2\Phi_1 (2\mathcal{S}_{0,2} - \mathcal{S}_{0,0} - \mathcal{S}_{2,0}) + \Phi_0 (\mathcal{S}_{1,1} + \mathcal{S}_{3,1})]. \end{aligned} \quad (\text{E1})$$

Thereby we used the relations (B11) between positive and negative indices. Considering Eq. (64), the compact integrals Φ_μ vanish for μ an odd integer if the quark mass and the axial mass are zero. Hence we have

$$\rho_5(m=0, \lambda=0, a) = 16a^4 [2\Phi_4 \mathcal{S}_{1,1} + 4\Phi_2 (\mathcal{S}_{3,3} - \mathcal{S}_{1,3}) + \Phi_0 (\mathcal{S}_{5,1} - \mathcal{S}_{3,1} + 8\mathcal{S}_{1,3} - 4\mathcal{S}_{1,1})] + 4a^2 \Phi_0 (\mathcal{S}_{1,1} + \mathcal{S}_{3,1}). \quad (\text{E2})$$

Thus we have only non-compact integrals $\mathcal{S}_{\mu,\alpha}$ with the index $\alpha = 1, 3$ and μ odd and positive. The integral over y , see Eq. (65), can be integrated for both indices $\alpha = 1, 3$,

$$\mathcal{S}_{\mu,1} = \frac{(-1)^{(\mu-1)/2}}{2\pi(8a^2)} \int_{-\infty}^{\infty} ds \frac{e^{-\mu s}}{\cosh 2s} \exp[-4a^2 \cosh 2s], \quad (\text{E3})$$

and

$$\mathcal{S}_{\mu,3} - \mathcal{S}_{\mu,1} = \frac{(-1)^{(\mu-1)/2}}{2\pi(8a^2)^2} \int_{-\infty}^{\infty} ds \frac{e^{-\mu s}}{\cosh^2 2s} \exp[-4a^2 \cosh 2s]. \quad (\text{E4})$$

We can omit the exponential in the limit $a \rightarrow 0$ if μ is small enough, i.e.

$$\mathcal{S}_{\mu,1} \stackrel{|a| \ll 1}{\approx} \frac{(-1)^{(\mu-1)/2}}{2\pi(8a^2)} \int_{-\infty}^{\infty} ds \frac{e^{-\mu s}}{\cosh 2s} = \frac{(-1)^{(\mu-1)/2}}{32a^2 \cos(\mu\pi/4)}, \quad \text{for } |\mu| < 2, \quad (\text{E5})$$

and

$$\mathcal{S}_{\mu,3} - \mathcal{S}_{\mu,1} \stackrel{|a| \ll 1}{\approx} \frac{(-1)^{(\mu-1)/2}}{2\pi(8a^2)^2} \int_{-\infty}^{\infty} ds \frac{e^{-\mu s}}{\cosh^2 2s} = \frac{(-1)^{(\mu-1)/2} \mu}{8(8a^2)^2 \sin(\mu\pi/4)}, \quad \text{for } |\mu| < 4. \quad (\text{E6})$$

For larger μ the exponential becomes crucial since it guarantees the integrability. Before performing the other integrals let us see what remains to be calculated,

$$\rho_5(m=0, \lambda=0, a) \stackrel{|a| \ll 1}{\approx} 16a^4 \left(\mathcal{S}_{5,1} - \mathcal{S}_{3,1} + \frac{1}{2^{11/2} a^4} \right) + 4a^2 \left(\frac{1}{2^{9/2} a^2} + \mathcal{S}_{3,1} \right). \quad (\text{E7})$$

Here we used the fact that $\Phi_\mu \propto |a|^\mu$ and $\Phi_0 \approx 1$ for $|a| \ll 1$. Thus we have still to calculate the asymptotics of $\mathcal{S}_{3,1}$ and $\mathcal{S}_{5,1}$ which can be done by splitting the integrals,

$$\begin{aligned}
\mathcal{S}_{3,1} &= -\frac{1}{2\pi(8a^2)} \int_{-\infty}^{\infty} ds \frac{e^{-3s}}{\cosh 2s} \exp[-4a^2 \cosh 2s] \\
&= \frac{1}{2\pi(8a^2)} \int_{-\infty}^{\infty} ds \frac{e^s}{\cosh 2s} \exp[-4a^2 \cosh 2s] - \frac{1}{\pi(8a^2)} \int_{-\infty}^{\infty} ds e^{-s} \exp[-4a^2 \cosh 2s] \\
&\stackrel{|a| \ll 1}{\approx} \frac{1}{2^{9/2} a^2} - \frac{K_{1/2}(4a^2)}{\pi(8a^2)} \\
&\stackrel{|a| \ll 1}{\approx} \frac{1}{2^{9/2} a^2} - \frac{1}{2^{9/2} \sqrt{\pi} a^3} + \mathcal{O}(a^{-1})
\end{aligned} \tag{E8}$$

and

$$\begin{aligned}
\mathcal{S}_{5,1} &= \frac{1}{2\pi(8a^2)} \int_{-\infty}^{\infty} ds \frac{e^{-5s}}{\cosh 2s} \exp[-4a^2 \cosh 2s] \\
&= -\frac{1}{2\pi(8a^2)} \int_{-\infty}^{\infty} ds \frac{e^{-s}}{\cosh 2s} \exp[-4a^2 \cosh 2s] + \frac{1}{\pi(8a^2)} \int_{-\infty}^{\infty} ds e^{-3s} \exp[-4a^2 \cosh 2s] \\
&\stackrel{|a| \ll 1}{\approx} -\frac{1}{2^{9/2} a^2} + \frac{K_{3/2}(4a^2)}{\pi(8a^2)} \\
&\stackrel{|a| \ll 1}{\approx} \frac{1}{2^{9/2} a^2} + \frac{1}{2^{9/2} \sqrt{\pi} a^3} + \frac{1}{2^{13/2} \sqrt{\pi} a^5} + \mathcal{O}(a^{-1})
\end{aligned} \tag{E9}$$

which yields the limit (104).

-
- [1] S. Itoh, Y. Iwasaki, and T. Yoshie, Phys. Rev. D **36**, 527 (1987).
 - [2] P. Hasenfratz, V. Laliena and F. Niedermayer, Phys. Lett. B **427**, 125 (1998) [arXiv: hep-lat/9801021].
 - [3] L. Giusti and M. Lüscher, JHEP **0903**, 013 (2009) [arXiv: 0812.3638 [hep-lat]].
 - [4] M. Lüscher and F. Palombi, JHEP **1009**, 110 (2010) [arXiv: 1008.0732 [hep-lat]].
 - [5] M. Lüscher, JHEP **1008**, 071 (2010) [arXiv:1006.4518 [hep-lat]].
 - [6] B. Berg, Phys. Lett. B **104**, 475 (1981).
 - [7] Y. Iwasaki and T. Yoshie, Phys. Lett. B **131**, 159 (1983).
 - [8] M. Teper, Phys. Lett. B **162**, 357 (1985).
 - [9] E. M. Ilgenfritz, M. L. Laursen, G. Schierholz, M. Müller-Preussker, and H. Schiller, Nucl. Phys. B **268**, 693 (1986).
 - [10] M. Albanese *et al.* [APE Collaboration], Phys. Lett. B **192**, 163 (1987).
 - [11] A. Hasenfratz and F. Knechtli, Phys. Rev. D **64**, 034504 (2001) [arXiv: hep-lat/0103029].
 - [12] K. Cichy, A. Dromard, E. Garcia-Ramos, K. Ottnad, C. Urbach, M. Wagner, U. Wenger, and F. Zimmermann, PoS LATTICE **2014**, 075 (2014) [arXiv: 1411.1205 [hep-lat]].
 - [13] P. H. Damgaard, K. Splittorff, and J. J. M. Verbaarschot, Phys. Rev. Lett. **105**, 162002 (2010) [arXiv: 1001.2937 [hep-th]].
 - [14] G. Akemann, P. H. Damgaard, K. Splittorff, and J. J. M. Verbaarschot, PoS LATTICE2010, 079 (2010) [arXiv: 1011.5121 [hep-lat]]; PoS LATTICE2010, 092 (2010) [arXiv: 1011.5118 [hep-lat]] Phys. Rev. D **83**, 085014 (2011) [arXiv: 1012.0752 [hep-lat]].
 - [15] G. Akemann and T. Nagao, JHEP **10**, 060 (2011) [arXiv: 1108.3035 [math-ph]].
 - [16] M. Kieburg, J. Phys. A **45**, 205203 (2012), some minor amendments where done in a newer version at [arXiv: 1202.1768v3 [math-ph]].
 - [17] L. Del Debbio, L. Giusti, M. Lüscher, R. Petronzio, and N. Tantalo, JHEP **0602**, 011 (2006) [arXiv: hep-lat/0512021]; JHEP **0702**, 056 (2007) [arXiv: hep-lat/0610059].
 - [18] S. R. Sharpe and R. L. Singleton, Phys. Rev. D **58**, 074501 (1998) [arXiv: hep-lat/9804028].
 - [19] M. Kieburg, K. Splittorff, and J. J. M. Verbaarschot, Phys. Rev. D **85**, 094011 (2012) [arXiv: 1202.0620 [hep-lat]].
 - [20] M. Kieburg, J. J. M. Verbaarschot, and S. Zafeiropoulos, PoS LATTICE2011, 312 (2011) [arXiv: 1110.2690 [hep-lat]]; Phys. Rev. Lett. **108**, 022001 (2012) [arXiv: 1109.0656 [hep-lat]]; Phys. Rev. D **88**, 094502 (2013) [arXiv: 1307.7251 [hep-lat]]; PoS LATTICE2013, 117 (2013) [arXiv: 1310.7009 [hep-lat]]; Acta Phys. Polon. Supp. **7**, 625 (2014).
 - [21] D. D. Dietrich and F. Sannino, Phys. Rev. D **75**, 085018 (2007) [arXiv: hep-ph/0611341].
 - [22] H. Ohki, T. Aoyama, E. Itou, M. Kurachi, C. -J. D. Lin, H. Matsufuru, T. Onogi, and E. Shintani *et al.*, PoS LATTICE **2010**, 066 (2010) [arXiv: 1011.0373 [hep-lat]].
 - [23] K. Rummukainen, AIP Conf. Proc. **1343**, 51 (2011) [arXiv: 1101.5875 [hep-lat]].
 - [24] J. Kuti, PoS LATTICE **2013**, 004 (2013).

- [25] A. M. Halasz and J. J. M. Verbaarschot, Phys. Rev. D **52**, 2563 (1995) [arXiv: hep-th/9502096].
- [26] J. B. Kogut, M. A. Stephanov, D. Toublan, J. J. M. Verbaarschot, and A. Zhitnitsky, Nucl. Phys. B **582**, 477 (2000) [arXiv: hep-ph/0001171].
- [27] S. Hands, S. Kim, and J. I. Skullerud, Phys. Rev. D **81**, 091502 (2010) [arXiv: 1001.1682 [hep-lat]].
- [28] J. O. Andersen and T. Brauner, Phys. Rev. D **81**, 096004 (2010) [arXiv: 1001.5168 [hep-ph]].
- [29] L. Del Debbio, M. T. Frandsen, H. Panagopoulos, and F. Sannino, JHEP **0806**, 007 (2008) [arXiv: 0802.0891 [hep-lat]].
- [30] M. Kieburg, J. J. M. Verbaarschot, and S. Zafeiropoulos, PoS LATTICE **2012**, 209 (2012) [arXiv: 1303.3242 [hep-lat]].
- [31] J. J. M. Verbaarschot, Phys. Rev. Lett. **72**, 2531 (1994) [arXiv: hep-th/9401059]; Nucl. Phys. B **426**, 559 (1994) [arXiv: hep-th/9401092].
- [32] M. E. Peskin, Nucl. Phys. B **175**, 197 (1980).
- [33] M. Vysotskii, Y. Kogan, and M. Shifman, Sov. J. Nucl. Phys. **42**, 318 (1985).
- [34] K. G. Wilson; *New Phenomena In Subnuclear Physics*, edited by A. Zichichi, Plenum Press: New York, 69 (1977)
- [35] O. Bar, S. Necco and S. Schaefer, JHEP **0903**, 006 (2009) [arXiv:0812.2403 [hep-lat]].
- [36] O. Bar, S. Necco and A. Shindler, JHEP **1004**, 053 (2010) [arXiv:1002.1582 [hep-lat]].
- [37] J. Gasser and H. Leutwyler, Phys. Lett. B **188**, 477 (1987).
- [38] L. Giusti, C. Hoelbling, M. Luscher, and H. Wittig, Comput. Phys. Commun. **153**, 31 (2003) [arXiv: hep-lat/0212012].
- [39] L. Giusti, P. Hernandez, M. Laine, P. Weisz, and H. Wittig, JHEP **0404**, 013 (2004) [arXiv: hep-lat/0402002].
- [40] H. Fukaya *et al.* [JLQCD Collaboration], Phys. Rev. Lett. **98**, 172001 (2007) [arXiv: hep-lat/0702003].
- [41] R. Kaiser and H. Leutwyler, Eur. Phys. J. C **17**, 623 (2000) [arXiv: hep-ph/0007101].
- [42] D. Dalmazi and J. J. M. Verbaarschot, Phys. Rev. D **64**, 054002 (2001) [arXiv: hep-th/0101035].
- [43] U. Magnea, Phys. Rev. D **61**, 056005 (2000) [arXiv: hep-th/9907096].
- [44] F. J. Dyson, J. Math. Phys. **3**, 140 (1962); J. Math. Phys. **3**, 1199 (1962).
- [45] L. Hua, *Harmonic Analysis of Functions of Several Complex Variables in the Classical Domains*, Am. Math. Soc. (1963).
- [46] K. Splittorff and J. J. M. Verbaarschot, Phys. Rev. D **84**, 065031 (2011) [arXiv: 1105.6229 [hep-lat]].
- [47] F. Berezin, *Introduction to Superanalysis*, 1st ed, Reidel, Dordrecht (1987).
- [48] K. Efetov, *Supersymmetry in Disorder and Chaos*, 1st ed., Cambridge University Press: Cambridge (1997).
- [49] H-J. Sommers, Act. Phys. Pol. B **38**, 4105 (2007) [arXiv: 0710.5375 [cond-mat.stat-mech]].
- [50] P. Littellmann, H-J. Sommers, and M. R. Zirnbauer, Comm. Math. Phys. **283**, 343 (2008) [arXiv: 0707.2929 [math-ph]].
- [51] M. Kieburg, H-J. Sommers, and T. Guhr, J. Phys. A **42**, 275206 (2009) [arXiv: 0905.3256 [math-ph]].
- [52] V. Kaymak, M. Kieburg, and T. Guhr, J. Phys. A **47**, 295201 (2014) [arXiv: 1402.3458 [math-ph]].
- [53] T. Guhr, Ann. Phys. **250**, 145 (1996) [arXiv: cond-mat/9510052].
- [54] G. Parisi and N. Sourlas, Phys. Rev. Lett. **43**, 744 (1979).
- [55] K. Efetov, Adv. Phys. **32**, 53 (1983).
- [56] F. Constantinescu, J. Stat. Phys. **50**, 1167 (1988).
- [57] F. Constantinescu and H. de Groote, J. Math. Phys. **30**, 981 (1989).
- [58] M. Kieburg, H. Kohler, and T. Guhr, J. Math. Phys. **50**, 013528 (2009) [arXiv: 0809.2674 [math-ph]].
- [59] F. Wegner, unpublished notes (1983).
- [60] U. Magnea, J. Phys. A **41**, 045203 (2008) [arXiv: 0707.0418 [math-ph]].
- [61] M. L. Mehta, *Random Matrices*, Academic Press Inc., New York, 3rd ed. (2004).
- [62] P. H. Damgaard, U. M. Heller, and K. Splittorff, Phys. Rev. D **85**, 014505 (2012) [arXiv: 1110.2851 [hep-lat]]; Phys. Rev. D **86**, 094502 (2012) [arXiv: 1206.4786 [hep-lat]].
- [63] N. G. de Bruijn, J. Indian Math. Soc. **19**, 133 (1955).
- [64] A. V. Smilga and J. J. M. Verbaarschot, Phys. Rev. D **51**, 829 (1995) [arXiv: hep-th/9404031].
- [65] P.J. Forrester, T. Nagao, G. Honner, Nucl. Phys. B **553**, 601 (1999) [arXiv: cond-mat/9811142].
- [66] P. H. Damgaard, R. G. Edwards, U. M. Heller, and R. Narayanan, Phys. Rev. D **61**, 094503 (2000) [arXiv: hep-lat/9907016].
- [67] M. Hanada, C. Hoyos, A. Karch and L. G. Yaffe, JHEP **1208**, 081 (2012) [arXiv:1201.3718 [hep-th]].
- [68] M. Abramowitz and I. A. Stegun, *Handbook of Mathematical Functions with Formulas, Graphs, and Mathematical Tables*, New York: Dover Books on Mathematics (1965).